MUSCARINIC CHOLINERGIC RECEPTORS IN THE DEVELOPING AND MATURE BASAL GANGLIA

by

Mary Alden Nastuk

B.A., Biology, Wesleyan University

SUBMITTED TO THE DEPARTMENT OF BRAIN AND COGNITIVE SCIENCES IN PARTIAL FULFILLMENT OF THE REQUIREMENTS FOR THE DEGREE OF

DOCTOR OF PHILOSOPHY

at the

MASSACHUSETTS INSTITUTE OF TECHNOLOGY

May 1988

Signature of Author _____

Department of Brain and Cognitive Sciences
May 12, 1988

Certified by _____

Dr. Ann M. Graybiel
Thesis Supervisor

Accepted by _____

Dr. Emilio Bizzi
Head, Department of Brain and Cognitive Sciences

Muscarinic Cholinergic Receptors
in the Developing and Mature
Basal Ganglia

by

Mary Alden Nastuk

Submitted to the Department of Brain and Cognitive Science on May 12, 1988 in partial fulfillment of the requirements for the degree of Ph.D..

Abstract

It is now known that the cytochemical heterogeneity of the mammalian striatum (the caudate nucleus and putamen) is reflected in the distributions of a number of neurotransmitter-related substances found in this key element of the basal ganglia. At the histochemical level, striatal compartmentalization was first defined by virtue of the patterns seen in sections stained for acetylcholinesterase (AChE). In these sections, macroscopic patches of weak staining ("striosomes") were seen scattered upon a darkly stained matrix. The finding that AChE, the degradative enzyme for the neurotransmitter acetylcholine, has a modular distribution in the caudate nucleus and putamen suggests that other components of the striatum's cholinergic system might be spatially ordered in accord with the overarching principle of compartmentalization. If so, it is almost certain that functional consequences exist.

Although the cholinergic interneurons of the striatum predominate only moderately in the matrix, their terminal fields may be more markedly heterogeneous. With the reasoning that a suitable marker for such heterogeneity would be the autoradiographically labeled muscarinic cholinergic receptor, a series of investigations was undertaken to determine whether these receptors have distributions relating to striosomal compartmentalization either at adulthood or during pre- and postnatal development when this compartmentalization is established and matures. Also included was a consideration of muscarinic receptor distributions in the closely allied substantia nigra.

For the first set of experiments, binding sites in fetal and mature striatal tissue sections from several species were labeled with the muscarinic antagonist [^{3}H]-propylbenzilylcholine mustard, and comparisons were made among binding site distributions, catecholamine histofluorescence, AChE staining, Nissl staining and

cell labeling with [^{3}H]-thymidine. At immaturity, muscarinic binding sites were concentrated in patches that corresponded to dopamine islands, AChE-rich patches and clusters of [^{3}H]-thymidine-positive neurons. In the adult striatum, muscarinic binding was nearly uniform except for a very few patches of particularly heavy binding that matched striosomes. Thus, striatal muscarinic binding sites have compartmentalized distributions that are associated with nigrostriatal afferents during development and to a lesser extent with striosomes at maturity.

It remained unclear whether the apparent maturational diminution in striatal muscarinic binding heterogeneity was real or was a consequence of the choice of ligand (*i.e.*, a nonspecific antagonist). Accordingly, a second study was pursued with a newly developed muscarinic antagonist, pirenzepine, that had been found to bind differentially to two subtypes of muscarinic receptor (termed M1 and M2). The distributions of radiolabeled M1 and M2 sites were mapped in the developing and mature striatum, and were compared to patterns of AChE staining and tyrosine hydroxylase-like immunoreactivity to assess the degree of compartmentalization present. Tissue sections from the substantia nigra were also studied in this way.

In the fetal striatum M1 and M2 binding sites initially had heterogeneous distributions, with patches of dense binding corresponding to AChE-rich patches. During development overall binding increased, but more so in the matrix than in the patches, and more so for non-patch M2 than for non-patch M1 sites. By maturity M2 binding was virtually uniform but M1 binding was still slightly concentrated in patches corresponding to striosomes. These findings suggest that the ontogenetic regulation of muscarinic binding sites is influenced by location relative to striatal compartments, that expression of M1 and M2 binding sites is differentially regulated, and that the distinct distributions of the two subtypes of muscarinic binding sites may provide a mechanism for the spatial segregation of striatal cholinergic function.

M1 and M2 binding sites were also present in the substantia nigra at all ages studied. For M1 sites in particular, the embryonic pars reticulata of the substantia nigra was more prominently labeled than the pars compacta. At adulthood both nigral subdivisions contained M1 and M2 sites, and there was heterogeneity of binding within the pars compacta. These findings provide evidence that the substantia nigra is a site of cholinergic transmission and indicate that aspects of the functional balance between acetylcholine and dopamine in the basal ganglia occur here as well as in the striatum.

Thesis Supervisor: Dr. Ann M. Graybiel
Title: Professor of Neuroanatomy

Acknowledgements

I take great pleasure in thanking all those who provided me with assistance and support as I worked my way through the investigations reported here.

My parents, Dr. William L. and Ruth A.L. Nastuk, instilled in me a love of learning and supplied the means and the encouragement to pursue it. My father did not see the completion of this work, but his spirit permeates its pages. I am proud to be following in his footsteps. My mother, through her intelligence, generosity and strength, continues to provide an example that I aspire to follow. Her tireless help has been crucial to the writing of this thesis.

The time and guidance given to me by the members of my thesis committee, Dr. Bernard W. Agranoff, Dr. Walle J.H. Nauta and Dr. Richard J. Wurtman, is much appreciated. Dr. Ann M. Graybiel, my thesis advisor, allowed me the privilege of great freedom as I worked within the highly stimulating environment that is her laboratory. My graduate years have been filled with unique and rewarding experiences thanks to Ann's consideration and guidance. During difficult times, she also has given me emotional support that will be long remembered.

I received first-class technical advice and aid from Dianne S. Boghossian, Lisa M. Dunning, Henry F. Hall, Diane Major and Carol J. Watkins. Jan Ellertsen saw to it that I had funding during the all-important last term. Thanks go to Dr. Jan K. Blusztajn for insightful discussions and counsel about phosphatidylinositol, and for the accompanying cheer and encouragement. The latter also came from Laura A. Feigenbaum, who in addition generously offered me the use of her computer terminal and the home around it. Dr. Helen Newman-Gage never hesitated to lend

valued input concerning the enigmas of striatal development. Far beyond that, she is a treasured friend.

The deepest respect and appreciation of all go to my husband, Dr. Michael J. Zackin. Mike never fails as a boundless source of strength and stability. His self-discipline is my model and his sense of humor is my salvation.

Funding during the course of this work was provided by N.I.H. training grants in the Department of Brain and Cognitive Science, and by a Whitaker Health Sciences Fund Fellowship.

Table of Contents

Chapter 1

Introduction

The striatum, made up of the caudate nucleus and putamen, is a central component of the basal ganglia. Once widely thought of as a homogeneous structure, the striatum is now known to possess an internal compartmentalization that is well-ordered though not readily belied by cytoarchitecture. Evidence to support this notion began to accrue in the 1970s.

One principal set of findings about striatal provincialization concerns patterns of afferent innervation from various sources in the brain. In 1975, Kunzle showed with anterograde tract tracing methods that corticostriate fibers (from motor cortex) in monkeys had patchy terminal fields. Shortly thereafter it was demonstrated that fibers arising in the somatosensory cortex (Kunzle, 1977; Jones et al., 1977) as well as the prefrontal cortex (Goldman and Nauta, 1977) of monkeys also had heterogeneous distributions of termination in the striatum. Another projection system to the striatum, that from the intralaminar complex of the thalamus, was reported to terminate in patches in the monkey (Kalil, 1978) and the cat (Royce, 1978). Clustering of terminations from a third source of striatal afferentation, the substantia nigra, was inferred from studies of catecholamine histofluorescence in the developing rat (Olson et al., 1972), rabbit (Tennyson et al., 1972) and human (Nobin and Bjorklund, 1973). These studies documented the presence of intensely fluorescent striatal patches (termed "dopamine islands" by the first group), presumably composed of dopaminergic nigrostriatal fibers.

Other instances of neurochemical heterogeneity were also found to characterize the striatum: in 1976, Pert et al. discovered that opiate receptors were

concentrated in patches in the rat's caudoputamen. By contrast, staining for acetylcholinesterase (AChE, the degradative enzyme of acetylcholine) in the striatum of the cat, monkey and human demonstrated pale patches ("striosomes") upon a dark matrix (Graybiel and Ragsdale, 1978). During the past ten years, not only has it been shown that opiate receptor-rich patches, AChE-poor striosomes, and heterogeneous afferentation mark the same system of striatal compartmentalization (see Graybiel and Ragsdale, 1983), but also that the vast majority of neurotransmitter-related compounds in the striatum have macroscopic distributions reflecting striosomal organization. Among these are enkephalin-like immunoreactivity (Graybiel et al., 1981a), neurotensin-like immunoreactivity and neurotensin receptors (Goedert et al., 1984), substance P-like immunoreactivity (Graybiel et al., 1981b; Beach and McGeer, 1984), benzodiazepine receptors (Faull and Villiger, 1986), and D1 and D2 dopamine receptors (Joyce et al., 1986; Loopuijt et al., 1987; Beckstead et al., 1988; Besson et al., 1988).

Of the many neurotransmitter systems in the striatum, one that has been the subject of particularly intense study is the cholinergic system. Much of this attention is rooted in clinical findings suggesting that striatal acetylcholine and nigrostriatal dopamine function in mutual balance (see Lloyd et al., 1975; Weiner and Klawans, 1978)). For example, when neuroleptics (which block dopamine receptors) are given as therapy for schizophrenia, Parkinsonian side effects can be ameliorated by administering centrally acting cholinergic receptor blockers. It is likely that this neurochemical balance is anything but straightforward in nature, occurring as it does against a highly complex backdrop. Nonetheless, our understanding of neurotransmitter interactions in the striatum will be furthered by the study of each participating neurotransmitter system.

The striatal cholinergic system is immediately notable because, although only

about one percent of the total neuron population is estimated to consist of cholinergic interneurons (Phelps et al., 1985) and there are probably no extrinsic cholinergic inputs to the caudate nucleus or putamen, (see Graybiel et al., 1987a) levels of acetylcholine and almost all of its related enzymes and receptors are exceptionally high in the striatum (see Graybiel and Ragsdale, 1983). Despite the fact that the cholinergic interneurons are only slightly more concentrated in matrix than in striosomes (Graybiel et al., 1983; Graybiel et al., 1987a), most of their associated neurochemical markers are quite clearly arranged in accord with the compartmental organization of the striatum whether at maturity or during development. These include AChE (Graybiel and Ragsdale, 1978; Graybiel and Ragsdale, 1980), choline acetyltransferase immunoreactivity for neuropil (Graybiel et al., 1987a), high affinity choline uptake sites (Lowenstein et al., 1987) and muscarinic cholinergic receptors (Nastuk and Graybiel, 1985), the subject of the present work.

This series of investigations is aimed at studying the macroscopic distributions of autoradiographically localized muscarinic binding sites in the developing and mature striatum and substantia nigra. The advantage of such an approach lies in the potential to draw connections between anatomy, physiology and biochemistry. At one level, populations of cholinergic binding sites can be mapped relative to a host of other anatomically defined striatal and nigral landmarks ranging from distributions of other neurotransmitter-associated molecules to patterns of neuronal connectivity. At quite another level, conclusions about the possible function of these binding sites can be made with the aid of a considerable and growing literature on cholinergic receptors as molecules mediating intercellular communication.

Chapter 2

Patterns of Muscarinic Cholinergic Binding in the Striatum and Their Relation to Dopamine Islands and Striosomes

ABSTRACT

The distribution of muscarinic cholinergic binding sites in the striatum was investigated in relation to the locations of other neurochemical markers in the developing rat, ferret, cat and human. In addition, striatal patterns of muscarinic binding were studied in the adult cat. Receptor binding autoradiography was carried out with tritiated propylbenzilylcholine mustard ([^{3}H]-PrBCM), the irreversible muscarinic antagonist, and subsequent serial section analyses involved comparisons among patterns of muscarinic binding, catecholamine histofluorescence, acetylcholinesterase (AChE) staining, Nissl staining, and cell labeling with [^{3}H]-thymidine.

Muscarinic binding in the immature striatum was characterized by local patchiness as well as regional density gradients in all species, with the most complex patterns appearing in the human. Patches of dense muscarinic binding were shown to lie in register with fluorescent dopamine islands (rat, cat, ferret), with AChE-positive patches (all species), and with clusters of neurons pulse-labeled by exposure to [^{3}H]-thymidine on embryonic day E27 (ferret). At the developmental stages examined, the [^{3}H]-PrBCM-positive patches were roughly complementary to zones of heavy Nissl staining (cat, human).

Striatal [^{3}H]-PrBCM binding in the adult cat was dense, and though it usually appeared nearly homogeneous, in some sections patches of elevated binding

were present. These had as counterparts, in neighboring sections, AChE-poor striosomes. It is concluded that during development, muscarinic cholinergic function is compartmentalized in the striatum in association with dopamine-containing afferents, and that this compartmentalization may persist to some degree in the adult.

INTRODUCTION

The interactions between striatal acetylcholine and dopamine have been subjects of intensive pharmacological and clinical study for over 20 years. It is thought that either of these two neurotransmitters may be capable of modulating the release of the other in the striatum though it is still not clear what mechanisms might underlie such mutual effects (see Lehmann and Langer, 1983; Chesselet, 1984). There is now also evidence that the interplay between cholinergic and dopaminergic mechanisms in the striatum occurs within the context of a rich repertoire of other neurotransmitter systems (Graybiel and Ragsdale, 1983). Both excitatory and inhibitory amino acids and many neuropeptides have been localized to striatal neurons and afferent fibers, and the anatomical distribution of many of these other neurotransmitter systems is governed by a compartmental architecture. For example, several neuropeptides and peptide ligand binding sites in the striatum are preferentially distributed in discrete macroscopic patches and these biochemically defined compartments are related to inhomogeneities in the distribution of striatal afferent and efferent connections (see Graybiel and Ragsdale, 1983; Graybiel, 1984b).

Pharmacological studies of acetylcholine and dopamine-containing elements have not yet taken this heterogeneity into account, despite the fact that many

markers related to dopamine and acetylcholine in adult striatal tissue have nonuniform distributions (Olson et al., 1972; Graybiel et al., 1983; Meininger et al., 1983; Graybiel et al., 1987a; Graybiel et al., 1987b; Besson et al., 1988). Furthermore, there is evidence in the developing brain for nonuniformity both of dopamine-containing afferents and of muscarinic cholinergic binding sites in the striatum. For many species, catecholamine-induced fluorescence and tyrosine hydroxylase-like immunoreactivity (largely attributable to dopamine-containing afferents) are concentrated in patches called "dopamine islands" (Olson et al., 1972; Olson et al., 1973; Tennyson et al., 1972; Nobin and Bjorklund, 1973; Graybiel et al., 1981b) and in the caudoputamen of the newborn rat the muscarinic antagonist [^{3}H]-propylbenzilylcholine mustard ([^{3}H]-PrBCM) binds in a patchy fashion (Rotter et al., 1979a).

For the study reported here and briefly elsewhere (Nastuk and Graybiel, 1983) striatal [^{3}H]-PrBCM binding was examined in a number of mammalian species in an effort to characterize better the regional distribution of such a cholinergic marker, both alone and in relation to the striatal dopamine system. The findings demonstrate that distinct zones of dense striatal muscarinic binding are present across species at immaturity and are in register with intensely fluorescent dopamine islands. Furthermore, this congruence can be demonstrated with additional anatomical markers. Evidence is also presented that there is a residual though sharply diminished patchiness of striatal [^{3}H]-PrBCM binding at maturity and that such patchiness bears a relation to the locations of AChE-poor striosomes. These results suggest an intimate relationship between cholinergic and dopamine-containing elements in the striatum during its development, and suggest also that a compartmentalized association may characterize at least some functional interactions of striatal acetylcholine and dopamine-containing systems beyond the period of their maturation.

METHODS

Striatal tissue was obtained from 2 neonatal rats at postnatal day 1 (P1); from 2 infant ferrets P1 and P6; from 9 fetal cats at estimated embryonic days 50-59 (E50-E59); from 4 kittens at PO to P1; and from 2 adult cats. One of the ferrets had been exposed to 0.3 mCi [^{3}H]-thymidine at E27 by intrauterine injection following laparotomy (see Graybiel & Hickey, 1982). In addition, samples of striatal tissue were obtained 2 to 4 hrs. postmortem from the brains of 2 human fetuses aborted at 20.5 and 22 weeks of gestation. Eleven of the animals (5 cat fetuses, 5 kittens and 1 adult cat) were perfused under deep barbiturate anaesthesia with 0.1M PO4 buffer at 2-4° C. Tissue from the remaining animals was obtained under conditions of deep anaesthesia without perfusion. The brains were quickly removed, trimmed and frozen on pulverized dry ice. Blocks containing the striatum were sectioned coronally in a cryostat at -12°C to -14°C; the thickness of the sections ranged from 5μm to 20μm, with optimal results at 15μm. Sections were thaw-mounted onto gelatin coated ("subbed") slides and processed in spaced or serial series for muscarinic ligand binding by the method of Rotter et al. ('79a), for acetylcholinesterase (AChE) staining by a modified Geneser-Jensen and Blackstad protocol (1971), for catecholamine fluorescence by de la Torre's (1980) modification of the glyoxylic acid method, or for Nissl staining with cresylecht violet.

The ligand used for the muscarinic receptor binding autoradiography, [^{3}H]-PrBCM, is a muscarinic antagonist which has been reported to exhibit atropine-sensitive, irreversible binding to tissue from the guinea pig's ileum (Young et al., 1972; Burgen et al., 1974a) and the rat's brain (Burgen et al., 1974b; Birdsall et al., 1976; Rotter et al., 1979b). For the procedure, mounted sections were

postfixed at 4°C for 15 minutes with 0.1% glutaraldehyde in 0.1M PO4 buffer (pH 7.4), rinsed briefly in 0.1M PO4 buffer at room temperature, and preincubated at 30°C in 0.1M PO4 buffer or, if they were control sections, in 0.1M PO4 buffer containing 10^{-6}M atropine. All sections (with controls kept separate) were then incubated in a solution of 2.4nM or 1.2nM [^{3}H]-PrBCM (New England Nuclear) which was added to the preincubation solution. Following the incubation, sections soaked in Carnoy's fluid to terminate binding, and washed in five changes of absolute ethanol. The preincubation, incubation and wash steps were each carried out at 30°C for 15 minutes with constant agitation. Sections were allowed to air-dry and were stored at -20°C in light tight boxes for up to 5 days. (For most of the later cases, slides were taken directly from the cryostat after thaw mounting, kept temporarily in racks at about 4°C, then maintained under vacuum at 0°C for 2 hours in a vacuum desiccator buried in crushed ice and containing Drierite (Dr. M.E.Lewis, personal communication and Lewis et al., 1982). Racks were then stored at -20°C in sealed boxes with Drierite for up to 5 days before further processing, which was the same as that described above.) Sections were defatted, for all cases except some sections from one kitten, air dried, dipped in Kodak NTB-2 nuclear track emulsion and placed in opaque boxes for 4-62 days at -20°C. They were developed in Kodak D19, fixed in Kodak rapidfix, and some sections were lightly counterstained with cresylecht violet. Darkfield photographs of selected sections were taken for comparison with serially adjoining sections stained for AChE or cresylecht violet or processed for glyoxylic acid induced fluorescence.

Figure 2-1: Darkfield photomicrographs illustrating [^{3}H]-PrBCM binding in neighboring experimental (A) and blank (B) sections from the striatum of a P1 kitten. The section shown in B was incubated in 2.4nM [^{3}H]-PrBCM with 10^{-6}M atropine; the section shown in A was incubated in 2.4nM [^{3}H]-PrBCM alone. In the blank section, [^{3}H]-PrBCM binding in the caudate nucleus is reduced nearly to the background levels of binding present in the adjacent internal capsule. CN: caudate nucleus, IC: internal capsule. Scale bar = 0.5mm.

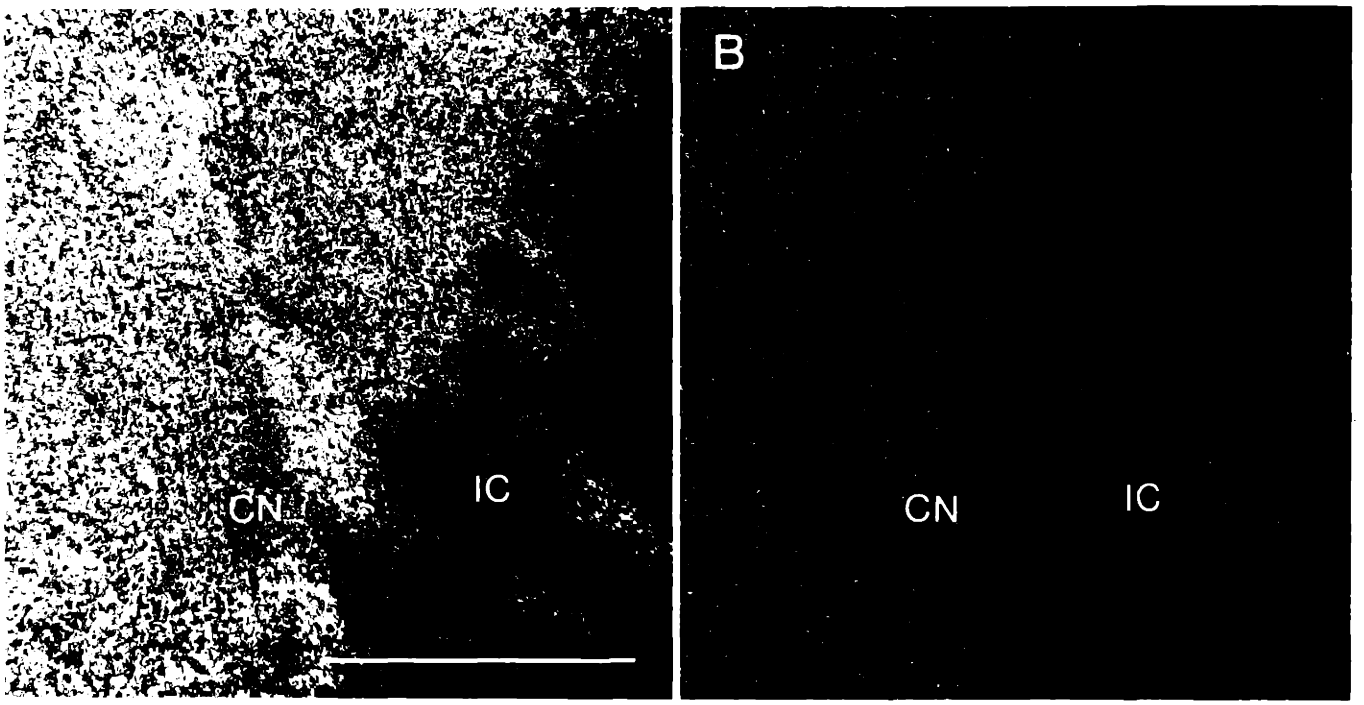
CN
IC
B
CN
IC

RESULTS

Displacement of [^{3}H]-PrBCM binding by atropine. Atropine-treated sections (blanks) were prepared for each case. Figure 1A and 1B illustrate high magnification views of an atropine-treated section (B) through the striatum of a P1 kitten, and a serially adjacent section (A) treated with [^{3}H]-PrBCM alone. The figure shows that striatal radioligand binding was reduced nearly to background levels in the atropine-treated preparation. This low level of labeling was seen in all blanks, and constituted evidence that a major component of [^{3}H]-PrBCM binding was atropine-displaceable, and thus specific for muscarinic cholinergic binding sites.

To test whether a significant amount of bound [^{3}H]-PrBCM was being washed out in the defatting steps, some sections from one kitten were processed for ligand binding without subsequently being defatted. For sections that had not been defatted, the autoradiographic appearance of the striatal [^{3}H]-PrBCM binding was qualitatively the same as it was for sections that had been defatted. This suggests that the defatting steps did not cause appreciable loss of bound ligand.

Ligand binding patterns. There was dense [^{3}H]-PrBCM binding in the striatum of each species studied, and in each species there were striking nonuniformities in the distribution of binding sites during development. The inhomogeneities were present in the form of local patchiness of binding and also in the form of density gradients spanning the entire striatum. There was no appreciable accumulation of silver grains over the ganglionic eminence in immature brains, or over the fibers of the internal capsule. Also, silver grains were not notably dense over the substantia nigra (results not shown).

Figure 2 illustrates the binding patterns at mid-rostral levels of the striatum in a P1 rat (Fig. 2A), an E50 cat fetus (Fig. 2B) and a human fetus at 22 weeks of

Figure 2-2: Darkfield photographs of coronal tissue sections processed for autoradiography illustrating the striatal distribution of [^{3}H]-PrBCM binding sits as seen in (A) a neonatal (P1) rat, (B) an embryonic day 50 (E50) cat fetus and (C) a human fetus at 22 weeks of gestation. Areas rich in binding sites appear as light zones in the photographs. Note that patches of sparse as well as dense binding are visible. Line marked by asterisk points out the medial edge of the ganglionic eminence in B and C. S: septum, C-P: caudoputamen, GE: ganglionic eminence, CN: caudate nucleus, P: putamen, IC: internal capsule. A and B are at same magnification; scale bars (see A,C)=1.0mm.

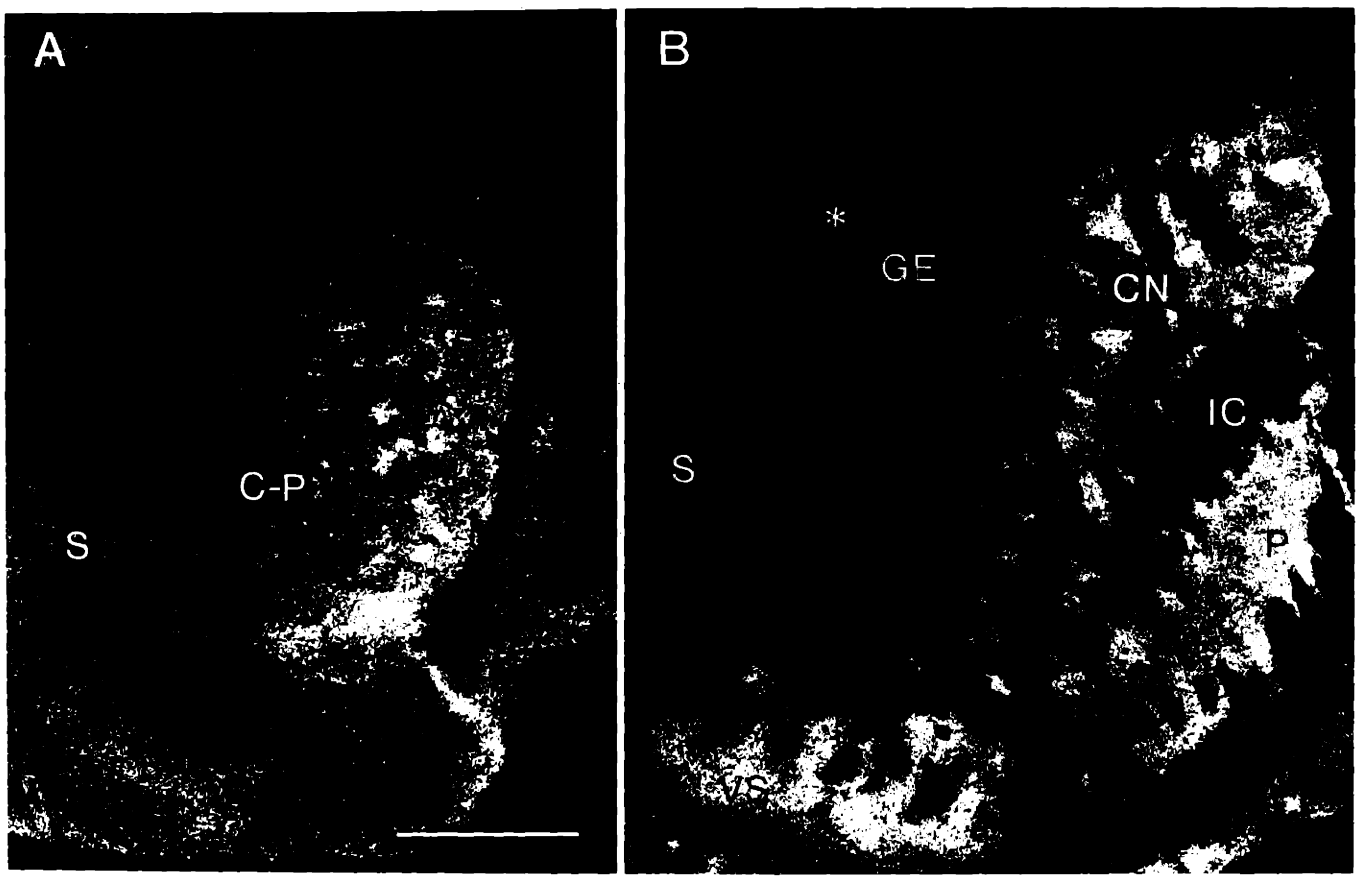
A
C-P
S
B
*
GE
CN
IC
S
P
VS

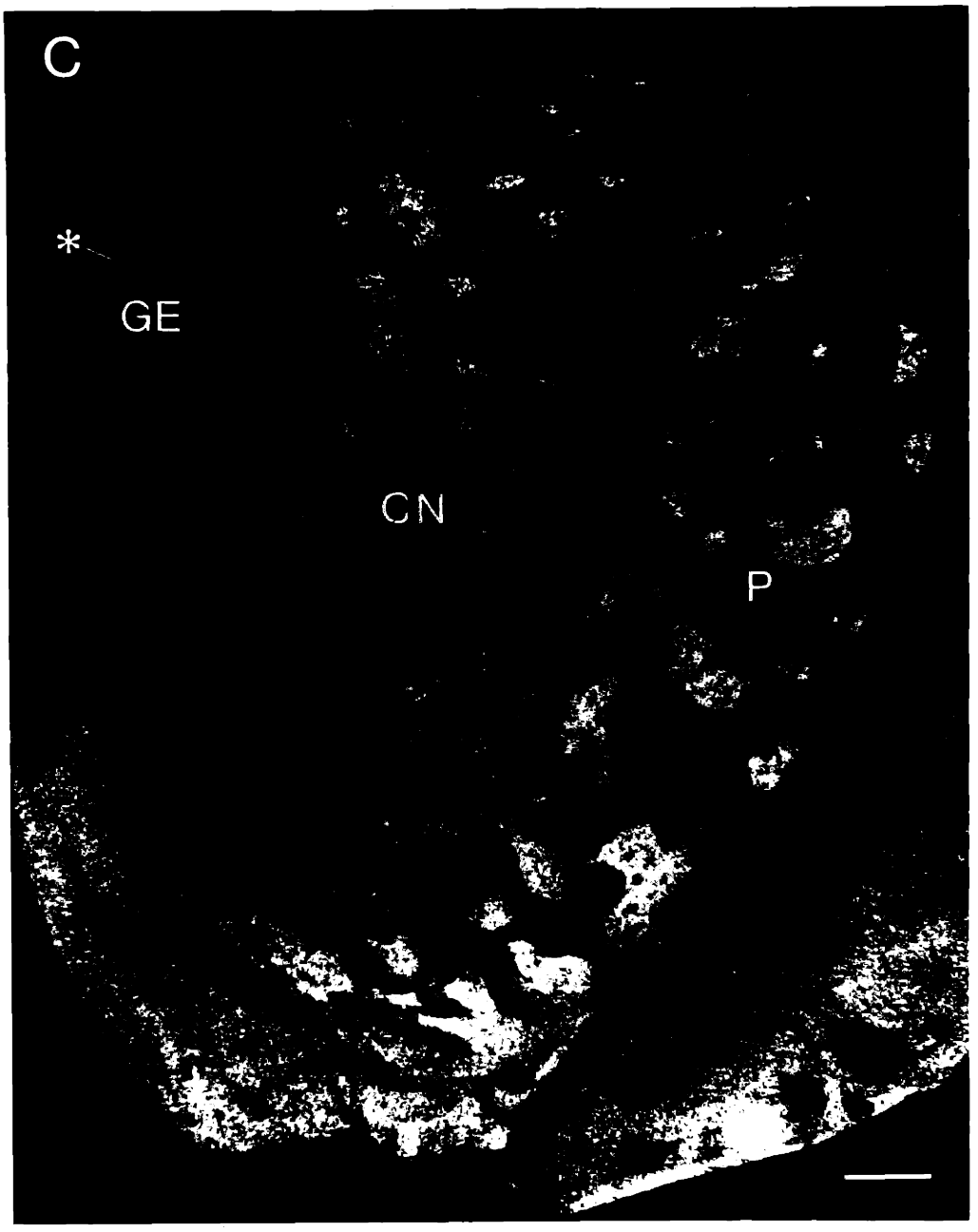
C
*
GE
CN
P

gestation (Fig. 2C). In the caudoputamen of the newborn rat, ca. 0.1 mm wide patches of dense ligand binding were scattered through a field of weaker binding, much as already noted by Rotter et al ('79c). A mediolateral gradient in labeling intensity was present both for the patches and the field in which they lay: the diffusely distributed binding was at its densest laterally, where the patches were most numerous and most densely labeled. A thin strip of heavy binding formed a rim along the extreme lateral edge of the striatum, and ventrally this band extended into a larger zone of dense binding at the foot of the caudoputamen.

In the E50 fetal cat (Fig. 2B), discrete zones of dense [^{3}H]-PrBCM binding were present throughout the caudate nucleus and in the olfactory tubercle-nucleus accumbens region. In the caudate nucleus, the most crisply delineated patches were usually located dorsally. In addition, there were zones in which the labeling intensity was less than that in the surrounding tissue; these were most prominent ventrally. Thus, there often appeared to be more than one set of patches present in the same section, one type being [^{3}H]-PrBCM-rich and another [^{3}H]-PrBCM-poor. Both types of patches appeared against a backdrop of intermediate-level binding which itself displayed a mediolateral density gradient, denser binding being lateral. In contrast to this complex pattern in the caudate nucleus, [^{3}H]-PrBCM binding in the putamen tended to be only faintly patchy and moderately dense throughout, as shown in Figure 2B. However, occasional fingers of dense binding extended across the width of the putamen, sometimes joining dense zones in the lateral part of the caudate nucleus, and there was usually a broad rim of heavy binding at the medial and especially at the lateral edge of the putamen.

The most complicated distribution of muscarinic binding sites appeared in the human fetal striatum (Fig. 2C). Zones of heavy and sparse binding alike took

on a variety of forms, some many-faceted, and the character of the binding array ranged from starkly delineated dense patches in the putamen and dorsolateral caudate nucleus to a less distinct pattern of generally more weakly labeled patches in the ventral part of the caudate nucleus. Both the grain-rich and grain-poor patches in the dorsal part of the caudate nucleus tended to be smaller than those found elsewhere in the striatum, and grain-poor zones were more numerous in the ventral part of the caudate nucleus. There was a mediolateral gradient in the density of striatal binding, both for the patches and for the tissue around them, so that the general level of binding was higher in the putamen than in most of the caudate nucleus. At some rostrocaudal levels this difference was quite marked.

Heterogeneity of striatal [^{3}H]-PrBCM binding was observed at all rostrocaudal levels, and Figure 3 illustrates a series of coronal sections extending from the anterior to the posterior poles of the caudate nucleus in a fetal cat at E58. In general, a medial to lateral density gradient persisted throughout the extent of the caudate nucleus. With respect to clarity of patterning, however, differences were evident at various rostrocaudal levels. Patches of dense binding appeared to gain crispness and become relatively smaller with antero-posterior progression, being most distinct at levels of maximal striatal cross sectional area. At these same levels, areas of sparse binding seemed most complex in shape, particularly mid-dorsally. Farther rostral, grain-poor zones more often took the form of bands extending diagonally downward from the medial to the lateral limits of the caudate nucleus.

Correspondence of [^{3}H]-PrBCM patches and dopamine islands. In the cats, ferrets and rats, direct comparisons were made between the autoradiographic patterns of striatal muscarinic binding and the dopamine islands visible in serially adjoining sections prepared for catecholamine histofluorescence.

Figure 2-3: [^{3}H]-PrBCM binding in a rostro-caudal series of coronal sections through the striatum of an E58 cat fetus. Heterogeneity of binding is present at all levels, but pattern clarity and patch size change with rostro-caudal progression. CN: caudate nucleus, P: putamen, GP: globus pallidus. Scale bar=1.0mm.

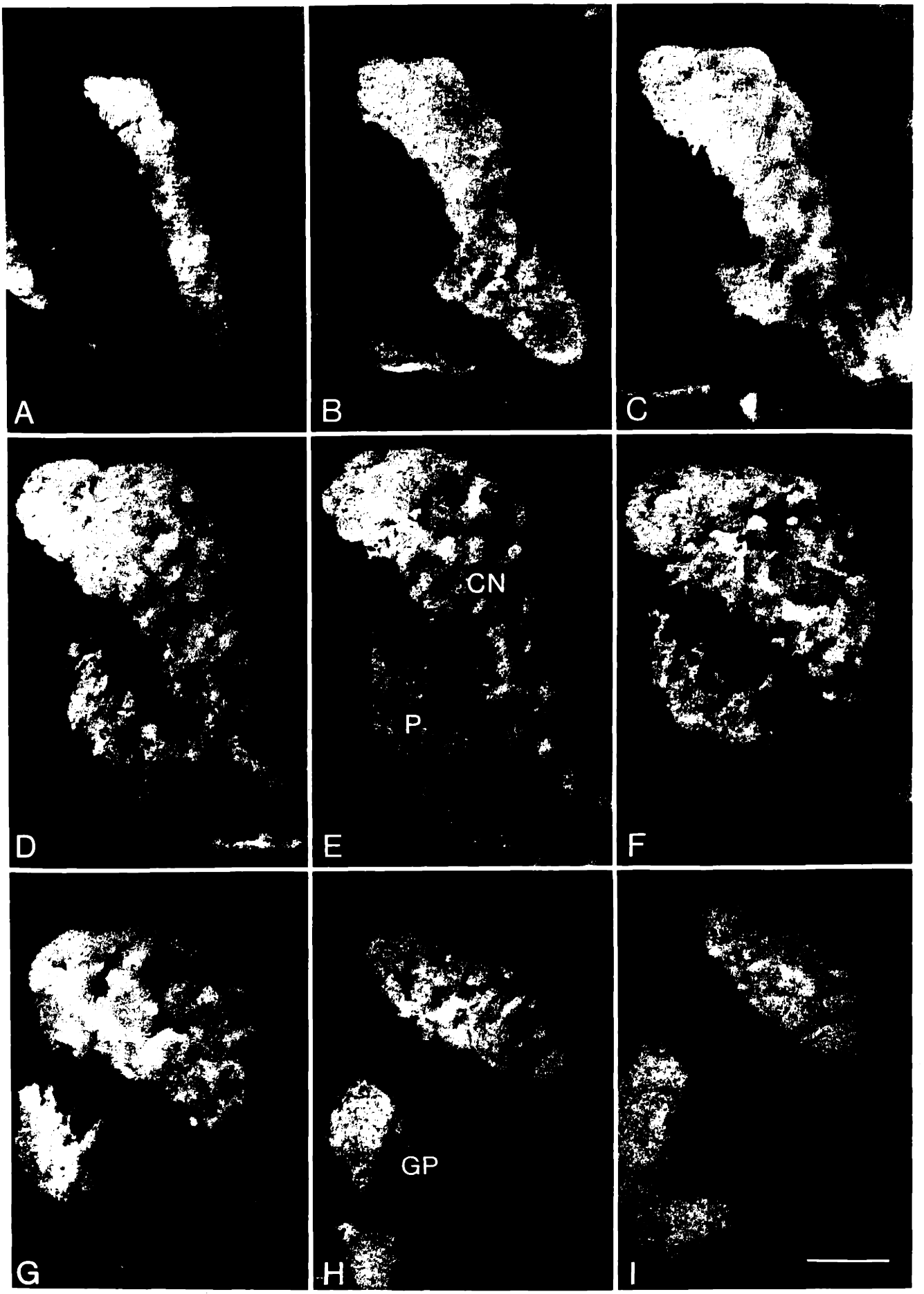
A
B
C
D
CN
P
E
F
GP
G
H
I

Figure 2-4: [^{3}H]-PrBCM binding (A) and catecholamine histofluorescence (B) present in serial sections through the striatum of an E50 cat fetus. Correspondence of patch forms visible with the two markers is particularly distinct in the mid-dorsal caudate nucleus, but is present throughout the striatum. Line marked by asterisk points out the medial edge of the ganglionic eminence. IC: internal capsule, GE: ganglionic eminence, CN: caudate nucleus, P: putamen. Scale bar=1.0mm.

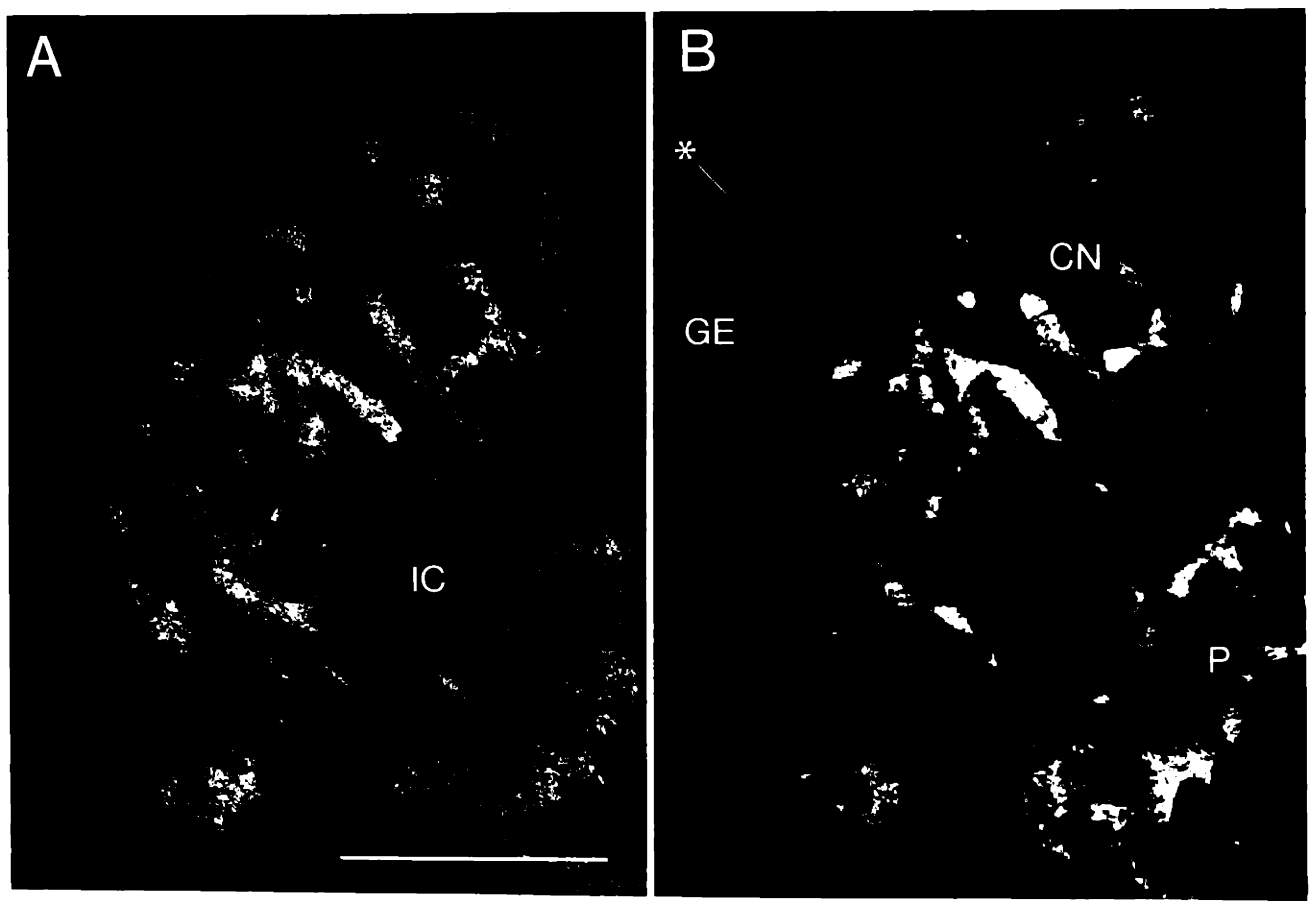
A
IC
B
*
CN
GE
P

The results were similar for each species: crisp patches of dense [^{3}H]-PrBCM binding were in nearly every instance matched by islands of bright fluorescence. Figure 4 illustrates this congruence of the two markers for the cat fetus at E50. Each figure prominent in the caudate nucleus or putamen as a zone of dense binding in the autoradiogram (Fig. 4A) corresponds to a highly fluorescent patch in the adjoining glyoxylic-acid-processed section (Fig. 4B) . Regions of low binding similarly correspond to zones of especially weak fluorescence.

Comparisons of the absolute intensities of muscarinic labeling and catecholamine-induced fluorescence could not be made, and would not be easily interpretable because of inherent variations in histological processing. Nonetheless, there were similarities in many of the subtle gradients observed with each method. In Figure 4, for example, lateral patches show denser ligand binding and brighter fluorescence than medial patches, and mid-dorsal patches are more prominently marked than ventral patches. Whether the gradients in non-patch labeling were also matched in the fluorescence could not be determined because the fluorescence was not sufficiently intense.

A second example of such spatial congruence between the zones of dense [^{3}H]-PrBCM binding and dopamine islands is shown in Figure 5 for the caudoputamen of a newborn rat. As in the E50 cat fetus, zones rich in binding sites in Figure 5B (including the strip along the lateral edge of the caudoputamen) corresponded to zones showing relatively intense fluorescence (Fig. 5C).

Distribution of striatal [^{3}H]-PrBCM binding in relation to AChE activity. Because the patterns of fluorescence visible in the glyoxylic acid preparations were difficult to reconstruct accurately at low magnification, and because catecholamine-induced fluorescence was not obtained in the human material, another marker for the dopamine island system was essential. The

Figure 2-5: Photomicrographs illustrating [^{3}H]-PrBCM binding (B), catecholamine histofluorescence (C) and acetylcholinesterase staining (D) present in neighboring sections in the dorsolateral caudoputamen of a neonatal rat. The rectangle in A delineates the region of the caudoputamen shown in B, C and D. Similar patch forms appear in all three marker patterns although there are differences in the amount of each marker seen in patch and non-patch regions. CC: corpus callosum, S: septum, AC: anterior commissure, C-P: caudoputamen. B, C and D are at same magnification; scale bar (see C)=0.5mm.

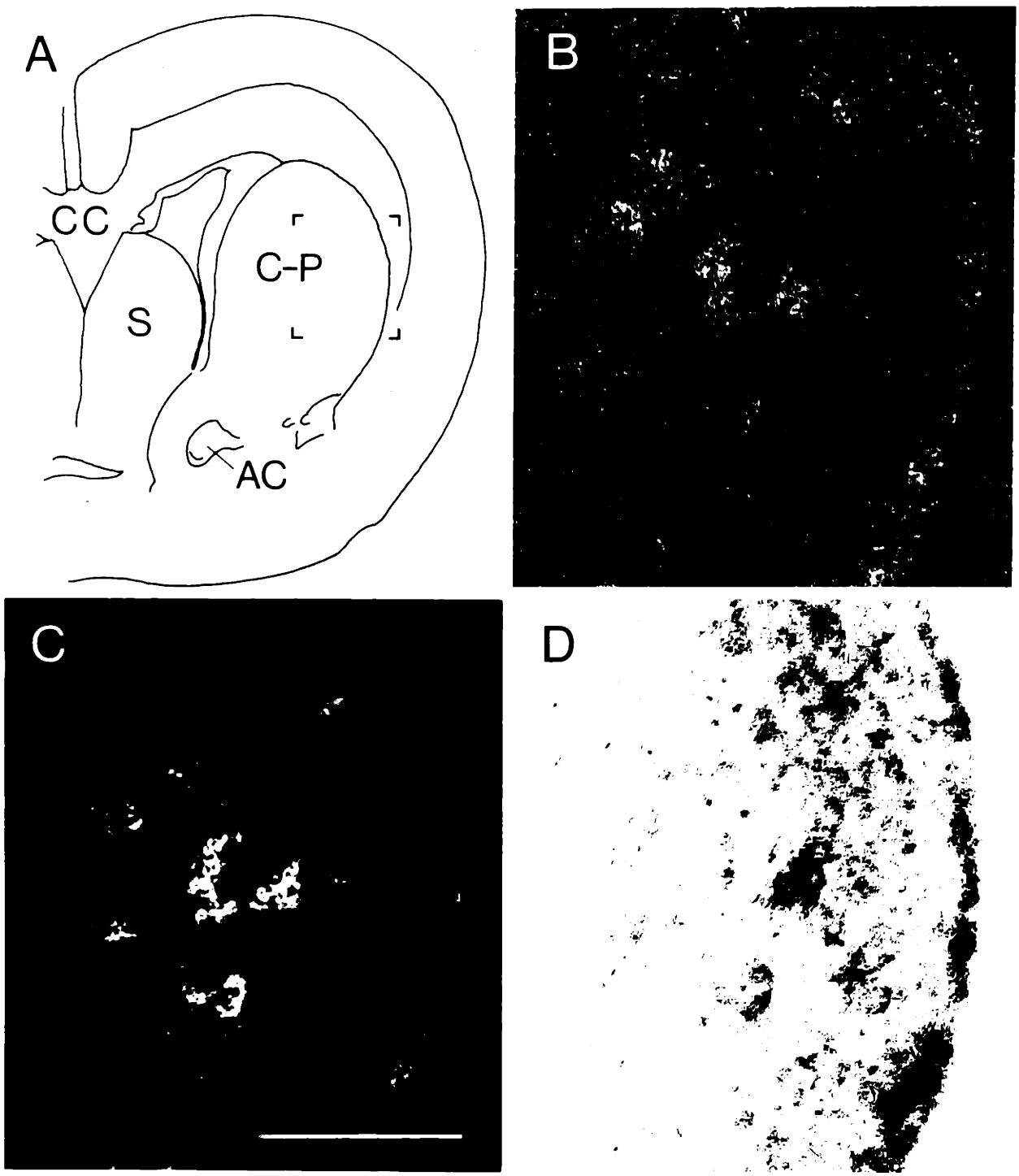
A
CC
C-P
S
AC
B
C
D

patterns visible in sections prepared for AChE histochemistry were practical as substitutes, because it is known that during fetal development in the cat, AChE-positive patches in the striatum line up precisely with intensely fluorescent dopamine islands (Graybiel et al., 1981b). This macroscopic congruence of AChE-positive patches and dopamine islands was confirmed here for the cat and shown also for the rat and ferret. As an example, Figure 5 shows several fluorescent islands in the mid-dorsal caudoputamen of the rat (Fig. 5C) which proved to have higher AChE activity than the surround when the tissue section was restained (Fig. 5D). There was not an exact match of contour between these two markers for every patch. Whether these differences reflect a disparity in tissue content of the two markers (for example, different mediolateral gradients) or simply different degrees of processing by the two methods, could not be determined in the histochemically treated material.

As shown in Figure 5 for the rat, and in Figure 6 for the young ferret, there were matches between zones of dense [^{3}H]-PrBCM binding and the AChE-positive patches seen in serial sections. This was also true in the striatum of the fetal cat. In these AChE preparations of young tissue, AChE-positive neurons were routinely visible in the striatum without pretreatment with diisopropylflurophosphate (DFP), the esterase inactivator ordinarily required for visualization of these neurons in the adult (Lynch et al., 1972; Butcher and Bilezikjian, 1975). The ready staining of these AChE-positive neurons meant that their location could be studied in relation to the patches of dense muscarinic cholinergic binding. As shown in Figure 6 for the P6 ferret, there was no apparent clustering of the AChE-positive neurons in patches of dense [^{3}H]-PrBCM binding, just as AChE positive perikarya are not all aligned with the AChE-positive patches visible in the neuropil (Butcher and Hodge, 1976; Graybiel et al., 1981b); see Fig. 6B and C).

Figure 2-6: Darkfield photograph of [^{3}H]-PrBCM binding (A) in the striatum of a P6 ferret and matching drawing (B) showing the locations of intensely AChE-positive neurons (dots) and of AChE-positive patches (outlined forms) visible in a serially adjacent section. In B, the borders of AChE-rich patches are limited by solid lines where they appear most crisp; dotted lines indicate approximate borders of less sharply delimited patches. In the putamen, the two patches marked with 'p' are AChE-poor relative to the surrounding tissue. Brackets in B indicate the region of the AChE-stained section shown at higher magnification in C in a lightfield photomicrograph. Note that darkly stained AChE-positive cell bodies are present both in and out of AChE-rich patches of neuropil (see arrowheads in C), but that the AChE-patches themselves are strictly aligned with patches of dense [^{3}H]-PrBCM binding. IC: internal capsule. Scale bar in A=1.0mm; in C=0.5mm.

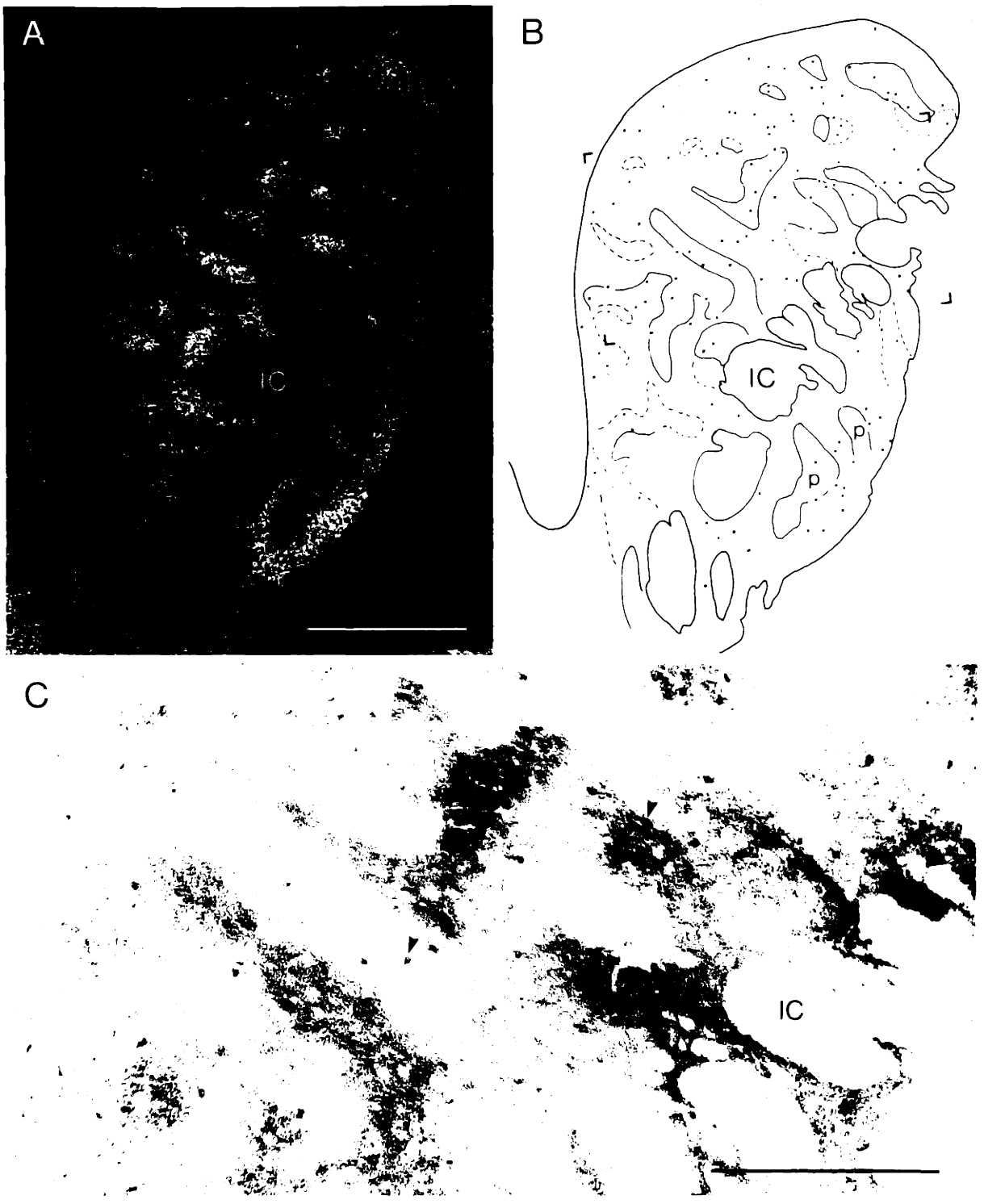
A
IC
B
IC
p
p
C
IC

The most valuable application of the AChE histochemistry was in studying the human striatal tissue, where, presumably because of postmortem delay before freezing, fluorescence was not detected with the glyoxylic acid method. In the 22-week-old fetus (Fig. 7) patchy distributions of striatal muscarinic binding sites and AChE staining showed striking spatial alignments much as in the rats, ferrets and cat fetuses. However, the equivalence did not extend to the general intensity with which the two patch systems were marked, nor to the details of substructure visible within individual patches.

As a first difference, the two labeling patterns were nearly reciprocal in terms of the topography of the most sharply delineated patchworks. In the caudate nucleus, the AChE-positive patches were stained much more intensely relative to the surrounding tissue than were the [^{3}H]-PrBCM patches. In the putamen, the patches were faint in the AChE stain but were vividly labeled in the ligand binding preparations. This difference between the intensity of AChE staining and muscarinic binding in the caudate nucleus and the putamen is illustrated in Figure 7 for a single pair of sections. Throughout the rostrocaudal extent of the striatum, the caudate nucleus was the site of the heaviest average enzyme staining, whereas the putamen was notable for particularly dense levels of [^{3}H]-PrBCM binding.

A second point of contrast between the two systems of patches was that some of the AChE-positive patches, especially those in the dorsal parts of the caudate nucleus and putamen, were not uniformly stained but consisted of a dark staining annulus at the center of which was a disk of weaker tint (cf Graybiel and Ragsdale, 1980). Such complex "ring-and-hollow" forms were not observed in the [^{3}H]-PrBCM binding.

Third, a distinct dorsolateral-to-ventromedial gradient in intensity was a prominent feature of the AChE staining in most sections. No comparable gradient was visible in the [^{3}H]-PrBCM-processed material.

Figure 2-7: Photographs of serial sections through the striatum of a 22-week-old human fetus showing the [^{3}H]-PrBCM binding distribution (A, darkfield) and AChE staining (B, lightfield). Note that there is a spatial correspondence in the locations of marker-rich and marker-poor (see asterisks) patches in the two sections, but that gradients of labeling intensity across the striatum are nearly reciprocal for [^{3}H]-PrBCM binding and AChE staining. Crisp "ring-and-hollow" patch forms seen in AChE staining in the dorsal caudate nucleus are matched by solid patches of heavy ligand binding (see arrowheads). VS: ventral striatum, IC: internal capsule, GE: ganglionic eminence, CN: caudate nucleus, P: putamen. Scale bar=1.0mm (A and B at same magnification).

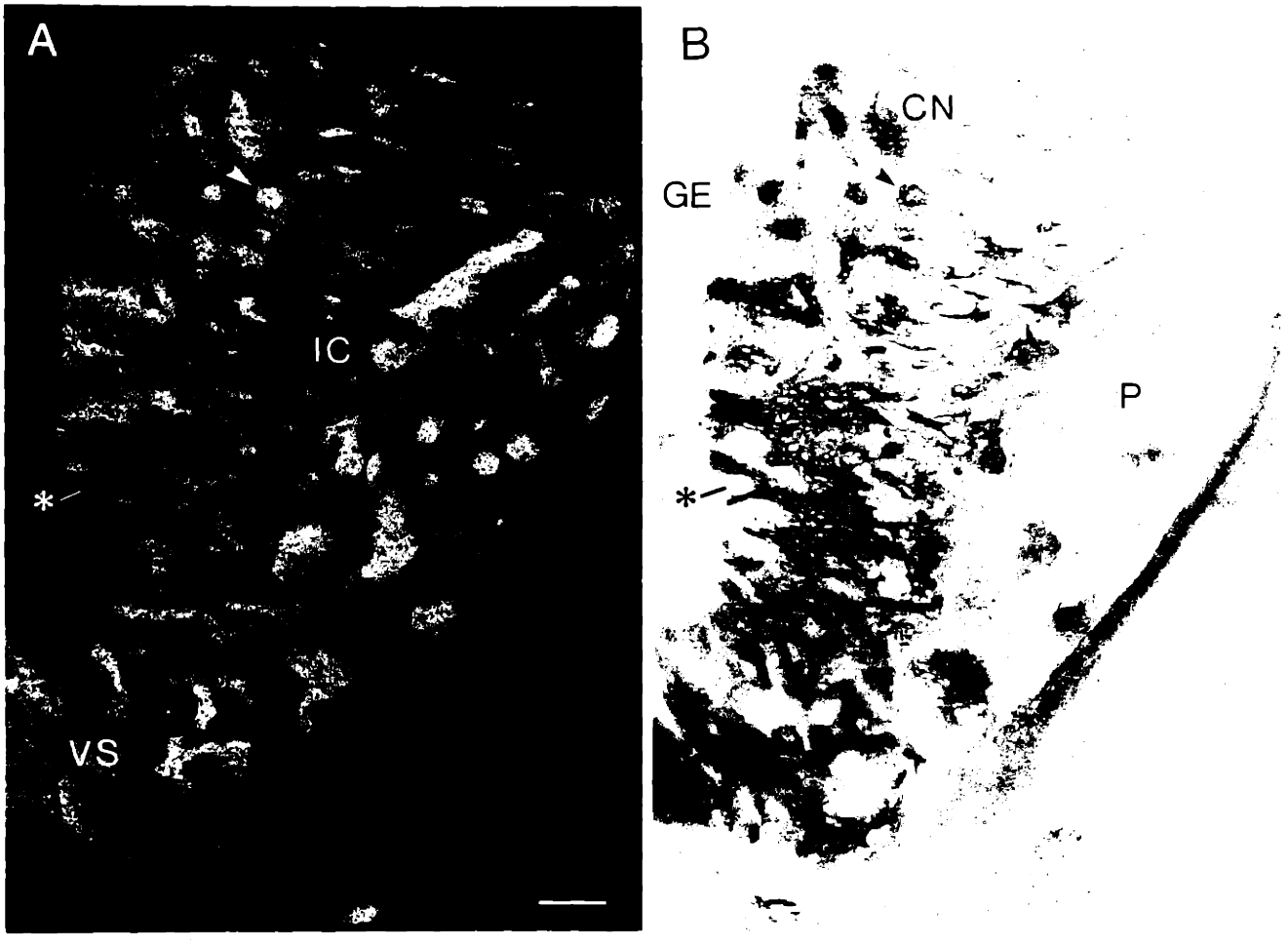
A
IC
VS
*
B
CN
GE
P
*

Despite these differences in relative intensity and degree of internal patterning, there were coordinated variations in the appearance of the two markers in different sectors of the striatum. As shown in Figure 7, both the [^{3}H]-PrBCM binding and AChE staining were characterized by a crisp patch-work in the ventral part of the putamen that extended into a ventral striatal field characterized by interlacing of heavily and lightly labeled zones of generally similar size. In the ventromedial part of the caudate nucleus, there was a prominent set of zones in which both [^{3}H]-PrBCM binding and AChE staining were weak. In some sections these zones alternated quite regularly with patches of heavy labeling and staining. Finally, both the patches of heightened ligand binding and the AChE-positive patches became progressively smaller toward the dorsal part of the caudate nucleus, and both were faint in its dorsolateral quadrant.

Alignment of [^{3}H]-PrBCM-rich patches with clusters of cogenerated striatal neurons. Another indirect method applied to indicate the location of the dopamine island system was the [^{3}H]-thymidine technique, in which the daughters of cells undergoing their final division at the time of injection of the isotope become heavily labeled (and successive generations of dividing cells become progressively more lightly labeled). Pulse labeling of the brains of developing fetal cats with [^{3}H]-thymidine at E23-E30 leads to the appearance later in fetal and postnatal life of clusters of labeled neurons in the striatum. These clusters of [^{3}H]-thymidine-labeled neurons are aligned with dopamine islands and AChE-rich patches in fetal and neonatal cats (Graybiel, 1984b) and with AChE-poor striosomes in adult cats (Graybiel and Hickey, 1982).

In the present study, a ferret brain pulse-labeled at E27 was processed at P6 in order to determine the relationship of such [^{3}H]-thymidine labeled cell-clusters to the distribution of [^{3}H]-PrBCM binding sites. The prediction was that the two sets

Figure 2-8: A and B show darkfield photographs of autoradiographically processed serial sections through the striatum of a P6 ferret that had been exposed to [^{3}H]-thymidine at E27. The section in A was incubated in [^{3}H]-PrBCM and thus shows both muscarinic binding and [^{3}H]-thymidine labeling patterns. The section in B was not processed for ligand binding and thus depicts only [^{3}H]-thymidine labeling. Arrowheads in A and B mark matching patches. Brackets in A delimit the region of the section shown again at higher magnification in C. Note that most [^{3}H]-thymidine positive cells lie within the patches of dense ligand binding (arrowhead in C marks such a cell). LV: lateral ventricle, CN: caudate nucleus, IC: internal capsule. Scale bar in A=1.0mm (A and B at same magnification). Scale bar in C=0.2mm.

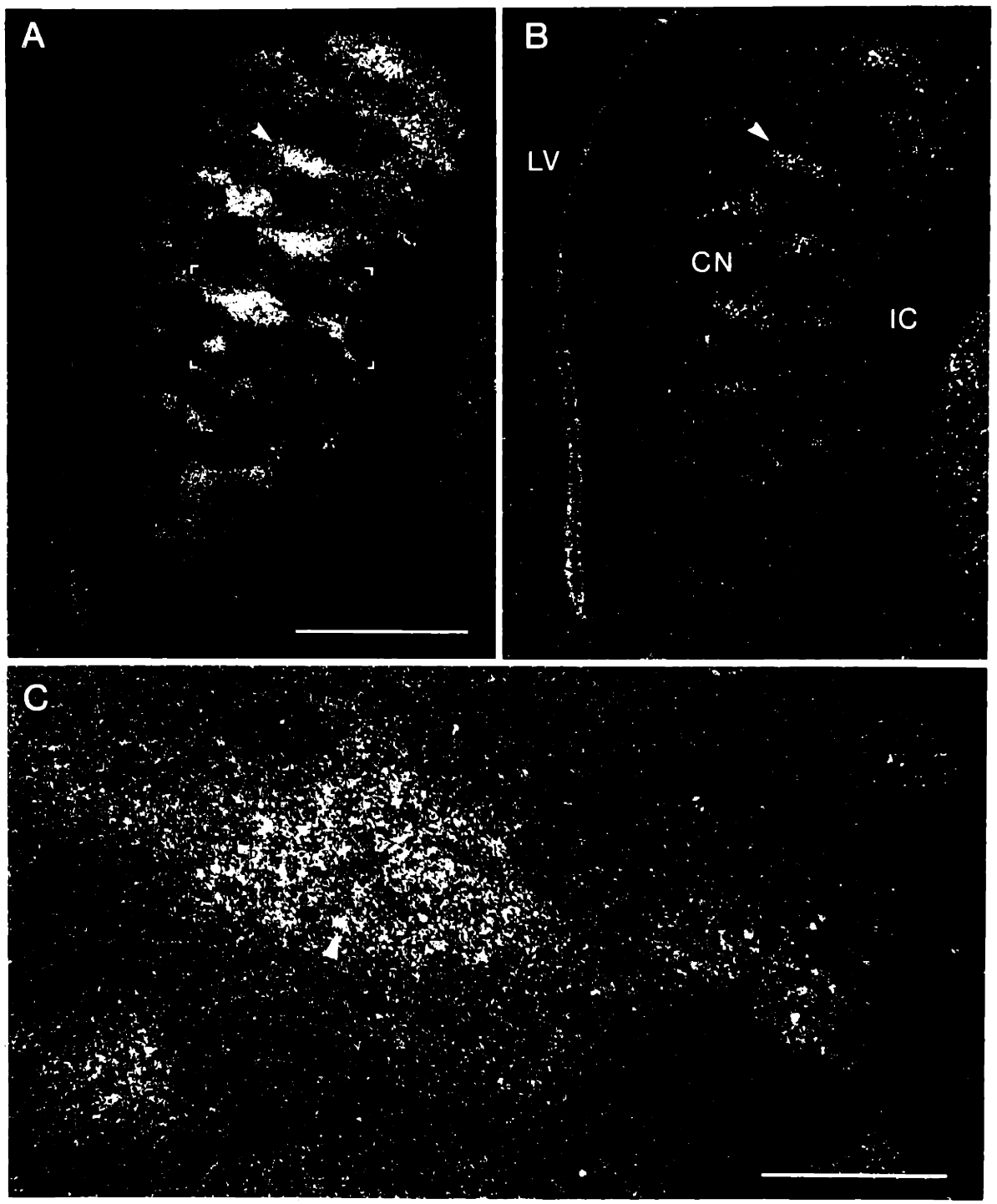
A
B
LV
CN
IC
C

of radioactive patches would be aligned, and the fact that both markers were radioactive meant that it would be possible in a single section to see both the patches of dense and sparse ligand binding and the labeled nuclei of striatal perikarya that had incorporated [^{3}H]-thymidine. This proved to be true. Figure 8A shows a doubly labeled section, and Figure 8B illustrates the [^{3}H]-thymidine pattern alone in a serially adjacent section not processed for [^{3}H]-PrBCM. The [^{3}H]-PrBCM labeling was sufficiently intense in the doubly labeled sections so that at low magnification it often obscured the [^{3}H]-thymidine pattern. But by comparing the macroscopic positions of the [^{3}H]-thymidine patches (Fig. 8B) with the double-labeled pattern (Fig. 8A) it was evident that the [^{3}H]-thymidine patches were in register with the [^{3}H]-PrBCM patches. This was also clear when the autoradiographic labeling was viewed at higher magnifications. As shown for a single patch in Figure 8C, most neurons with [^{3}H]-thymidine labeled nuclei fell within zones of dense [^{3}H]-PrBCM binding. A lateral to medial decrease in labeling was evident for both patch systems, but it was much more pronounced for the thymidine pattern. As a consequence, there were not clear [^{3}H]-thymidine matches for the most medial of the [^{3}H]-PrBCM figures.

[^{3}H]-PrBCM binding in relation to inhomogeneities in Nissl cytoarchitecture. Nissl staining of the caudate nucleus and putamen was remarkable in demonstrating diverse patterns that varied with species and with developmental stage and location within the striatum. Figures 9B and 9D give an indication of the range of complexity presented by Nissl staining in the series of animals studied. Near the end of the middle third of gestation in the cat (Fig. 9B), the Nissl staining patterns were relatively simple: there were patches that were stained darkly relative to their surround, and these were found throughout most of the caudate nucleus. There were very few examples of patches delimited by cell-

Figure 2-9: A comparison of striatal [^{3}H]-PrBCM binding site distribution and Nissl staining in the late-fetal cat (A,B) and in the fetal human at age 22 weeks (C,D). For the fetal cat, the same section was processed for muscarinic ligand binding (visible in A in darkfield illumination) and counterstained for Nissl substance (visible in B in lightfield photograph). For the human fetus, [^{3}H]-PrBCM processing (C, darkfield) and Nissl staining (D, lightfield) were carried out on serially adjacent sections through the striatum. Patterns of labeling are more complex in the human than in the cat but in both species regions that stain darkly for Nissl substance tend to be aligned with zones of sparse muscarinic ligand binding (see asterisks). S: septum, CN: caudate nucleus, IC: internal capsule, P: putamen. Scale bars=1.0mm.

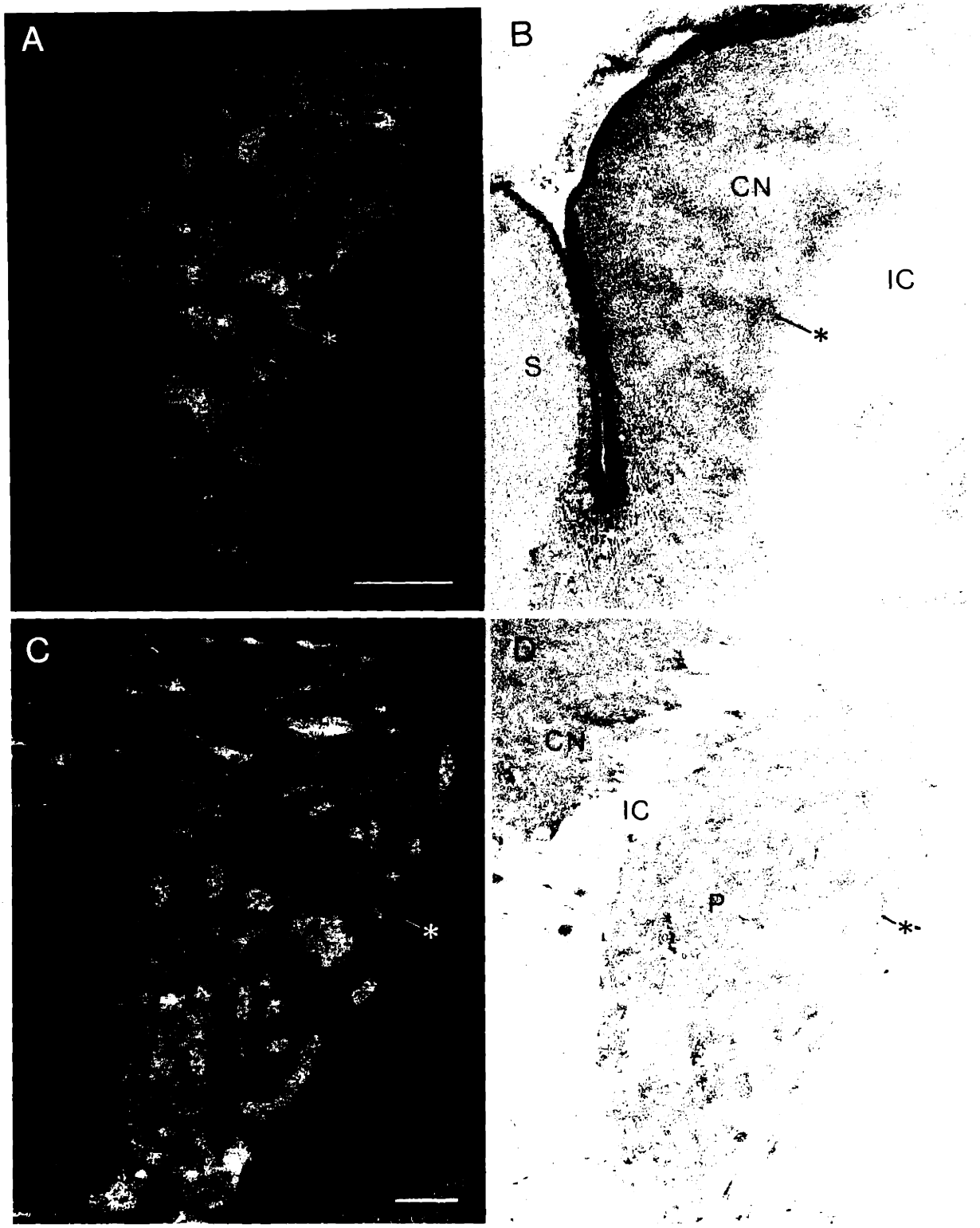
A
B
CN
IC
S
C
D
CN
IC
P

poor capsules; those that were present appeared dorsolaterally. As in the cat, the Nissl staining in the striatum of the infant ferrets and newborn rats was also not highly patterned. By contrast, near the end of the middle third of gestation in the human, the striatum had an ornate appearance when stained for Nissl substance. As shown for the putamen in Figure 9D, there were several different intensities of patchy Nissl staining, and many instances of cell-sparse capsules partially or completely surrounding patches that appeared either more darkly or more lightly stained than the surround. The patchiness of Nissl staining observed in the infant ferrets and newborn rats resembled that in the E50 fetal cat far more than that in the E22-week human.

Despite the difference in the complexity of striatal Nissl staining in the cat and human, a possibly unifying observation became evident from making serial-pair comparisons of the Nissl patterns and [^{3}H]-PrBCM binding distributions. In both the cat and human fetus, darkly staining Nissl patches were in approximate register with zones of sparse [^{3}H]-PrBCM binding. Conversely, patches of lighter Nissl staining could usually be aligned with [^{3}H]-PrBCM-dense areas. Accordingly, a rough complementarity between the two patch patterns was often discernible even when, as in the human, this might not have been predicted at first glance because of the complicated appearance of the Nissl staining. Whether this relationship is consistent throughout development or throughout the striatum is unclear.

[^{3}H]-PrBCM binding in the ventral striatum. The olfactory tubercle and nucleus accumbens region, together comprising the ventral striatum (Heimer and Wilson, 1975), also were characterized by local variations in [^{3}H]-PrBCM binding site density in each species studied. In the olfactory tubercle these inhomogeneities often took the form of radially oriented strips of dense binding

Figure 2-10: [^{3}H]-PrBCM binding (A) in the olfactory tubercle and nucleus accumbens of an E50 cat fetus and Nissl staining (B), catecholamine histofluorescence (C) and AChE staining (D) in serially adjacent sections (the same section is shown in C and D). Zones of dense binding in A are aligned with clusters of darkly staining cells in B (see arrowheads). C shows a patch of catecholamine histofluorescence corresponding to the hook-shaped [^{3}H]-PrBCM-dense zone indicated by the right-hand arrowhead in A. The same patch form was visible as an AChE-positive patch when the section was counterstained for AChE activity. NA: nucleus accumbens, IC: internal capsule, P: putamen, Olf. T: olfactory tubercle. Scale bar in A=1.0mm.

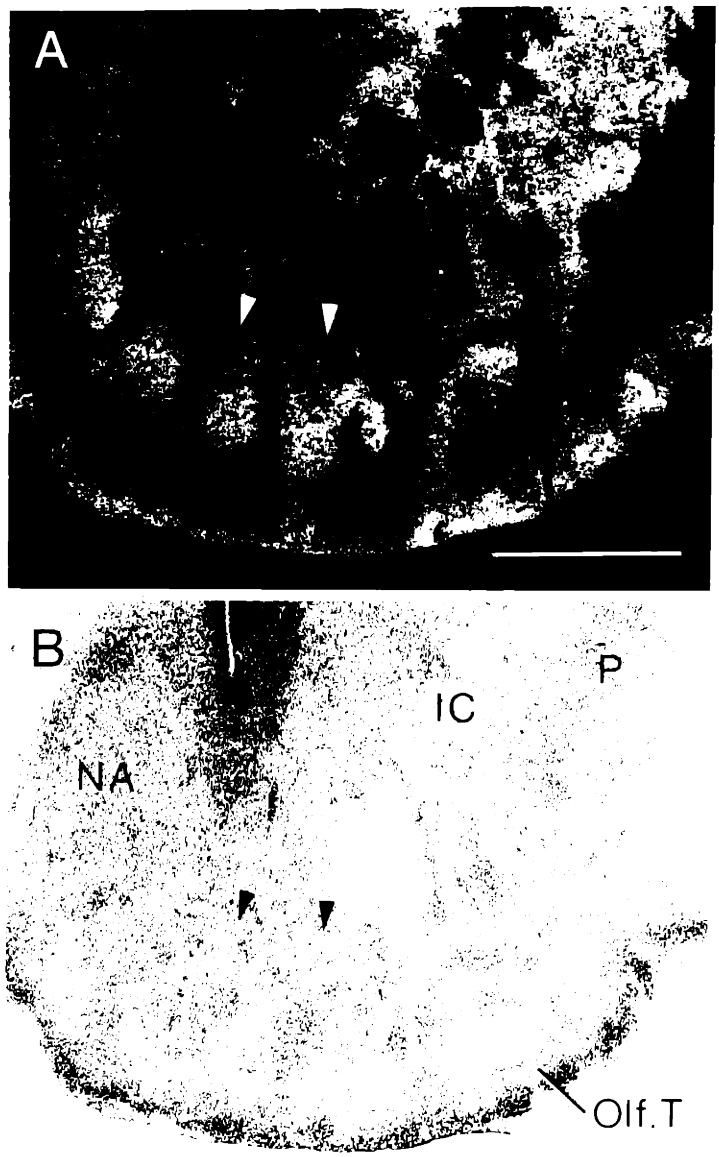
A
B
P
IC
NA
Olf.T
C
D

that alternated with strips of sparse binding and that matched darkly and lightly stained zones seen in Nissl staining. These patterns are shown in Figure 10A and B for a fetal cat at E50. In the nucleus accumbens, labeling was generally weaker than that in the olfactory tubercle, and nonuniformities were present but indistinct.

To allow comparison of the [^{3}H]-PrBCM binding to the histochemical compartmentalization of the ventral striatum, sections adjacent to [^{3}H]-PrBCM prepartions were processed for dopamine fluorescence and then restained for AChE. In the olfactory tubercle, there was a pattern of periodic strips in the fluorescence similar to that seen in the autoradiogram, and the positive and negative zones in the two preparations were closely enough aligned and similar enough in shape so that matching pairs could be recognized at a glance. One example is shown in Figure 10, where the [^{3}H]-PrBCM positive form marked by the right-hand arrowhead in Figure 10A has a match in the fluorescent figure shown in Figure 10C and also in the AChE-positive patch shown in Figure 10D. In the nucleus accumbens, fluorescence was relatively intense despite weak [^{3}H]-PrBCM binding in the adjacent autoradiographic preparation.

Striatal [^{3}H]-PrBCM binding in the adult cat. Muscarinic ligand binding in the mature striatum was studied in the adult cat and was found to be sharply different from that observed in the fetal cat both quantitatively and qualitatively. First, the general density of binding sites increased greatly with age, to judge from the conditions needed to generate satisfactory autoradiographs: whereas 25-30 day exposure times ordinarily were needed for the cat fetuses, 15-20 day exposures following incubation in half-strength [^{3}H]-PrBCM were adequate for the adult. Second, there were few local variations in the distributions of binding sites visible in most of the striatal sections from the adults, though there were perceptible gradients in general binding density.

There were exceptions to this apparent lack of local inhomogeneity in binding site distribution in that there were occasional patches in which the density of binding was greater than that present in the surround. As shown in Figure 11A, such patches were mostly found in the mid-dorsal part of the caudate nucleus. Laterally, where the general intensity of binding was very high, the patches were discriminable mainly by virtue of having rims almost free of binding. Some appeared to have more intense binding inside the rim than outside, but this was difficult to judge by visual inspection. Medially, rims were not prominent but the labeling in the area around the patches was sufficiently low so that the [^{3}H]-PrBCM-rich zones could be identified by the hightened intensity of ligand binding. Figure 11A illustrates examples of these [^{3}H]-PrBCM patches, and Figure 11B shows that part of the district in which the [^{3}H]-PrBCM patches were most readily identifiable was also the region in which patches of AChE-poor neuropil ("striosomes") were clearest in neighboring sections. In fact, this was a help in identifying the [^{3}H]-PrBCM-dense figures, because nearly every patch of heavier binding corresponded to a striosome even though the reverse was not always true.

Figure 2-11: [^{3}H]-PrBCM binding (A, darkfield) and AChE staining (B, lightfield) present in neighboring sections through the striatum of an adult cat. Both sections show a distinct mediolateral gradient of marker intensity in the caudate nucleus, with heaviest labeling and staining appearing laterally. In the mid-dorsal part of the caudate nucleus, particularly in the region where AChE-poor striosomes are most prominent, there are patches of heightened muscarinic binding that are aligned with striosomes (see asterisks). NA: nucleus accumbens, P: putamen, IC: internal capsule. Scale bar=1.0mm.

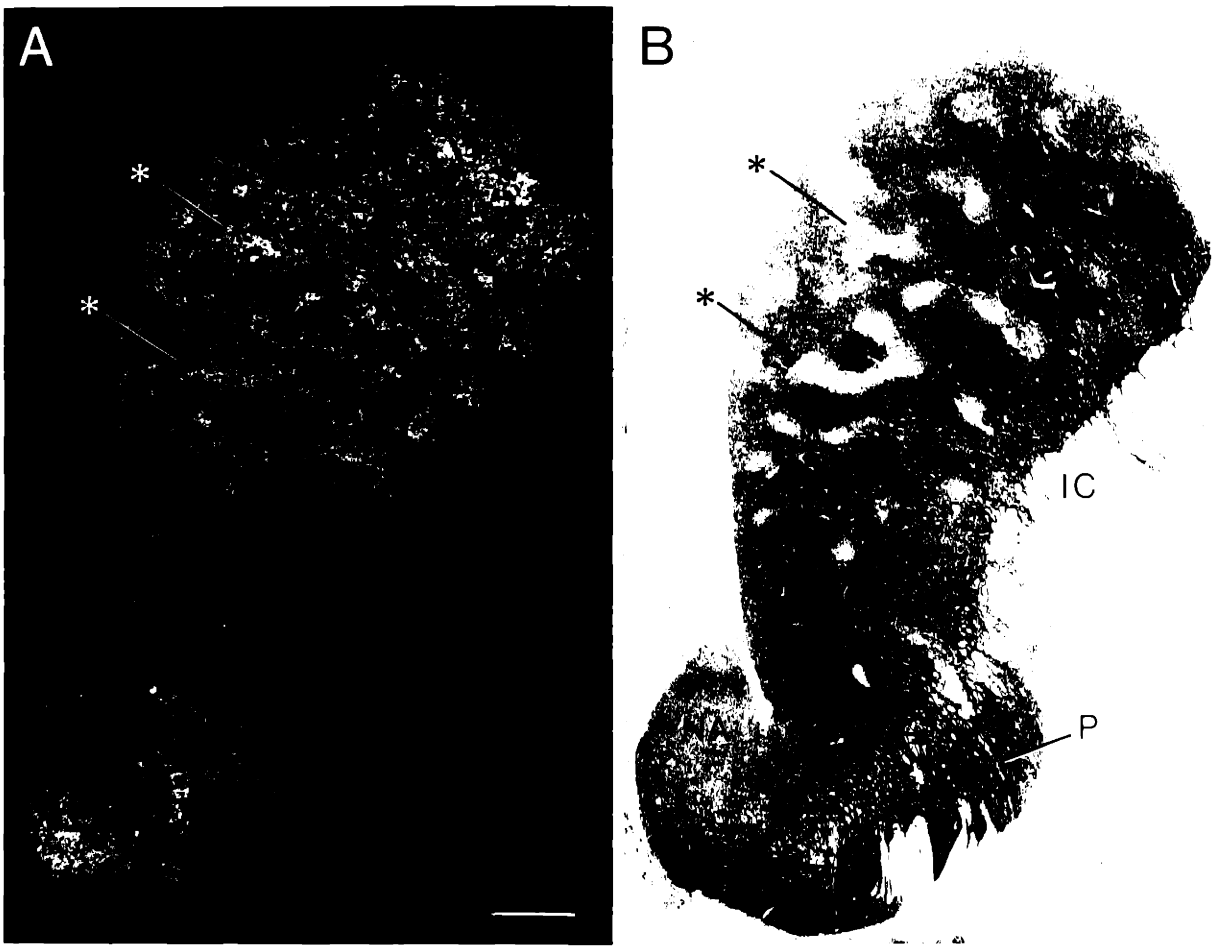
A
*
*
B
*
*
IC
P

DISCUSSION

The key findings of this study are first, that striatal muscarinic cholinergic binding sites have a distribution that for a range of mammalian species is markedly patchy during development. Second, patches of dense muscarinic binding lie in register with the clusters of early arriving dopamine-containing afferents forming dopamine islands. Third, some heterogeneity in muscarinic binding persists into adulthood, at least in the cat, and the patches of heightened binding in the mature striatum are in register with AChE-poor striosomes. Finally, the fields of diffuse muscarinic binding around the patches exhibit density gradients both during maturation and at adulthood, as do the patches themselves. These results suggest that there are both regional and local compartmental aspects to the interplay between acetylcholine and other neurotransmitters in the striatum, and suggest in particular that the muscarinic patch and dopamine island systems may reflect selective channels by which certain dopaminergic and cholinergic elements are brought into proximity.

Striatal Muscarinic Binding Sites During Development

The evidence for compartmentalization of binding sites in the immature striatum was remarkably consistent from rat to human despite topographic variations in the binding in different species and despite the fact that only one or a few gestational ages were sampled for each species. Much the same consistency characterized matches between the patches of high muscarinic binding and the dopamine islands in these species. The ubiquity of the congruences suggests that ontogenetic interactions between striatal cholinergic and dopaminergic elements may occur in the maturing striatum. Catecholamine-containing pathways characteristically appear early in development and may exert ontogenetic influences on other neural components (see Molliver, 1982). There is already evidence that

early interactions between opioid binding sites and a dopaminergic mechanism may occur in the rat's caudoputamen (Kent et al., 1982; Moon Edley, 1983; Murrin and Ferrer, 1984; van der Kooy, 1984).

It is unclear whether muscarinic receptors expressed during development subserve any of the functions which have been ascribed to them at maturity; such a question is technically difficult to address, especially in fetal animals. Electrophysiological recordings and anatomical observations in young kittens and monkeys suggest that the striatum is functionally immature at birth (Hull et al., 1981; Morris et al., 1979; DiFiglia et al., 1980) and information about other neurotransmitter systems in the striatum indicates this also (Coyle and Yamamura, 1976; Nomura et al., 1981). If in fact the early-forming muscarinic binding sites are functional in some way then the present observations strongly suggest that they function in coordination with incoming dopaminergic fibers. It seems highly probable that the eventual functional interactions between the cholinergic and dopaminergic systems of the mature striatum would be influenced as a result.

Though the muscarinic-dopaminergic matches described here were usually readily apparent, it was also clear that these correspondences occur within a complex developmental framework in which striatal components mature at differing rates and with different spatial gradients. First, there were sharply different intensities of AChE staining and muscarinic binding in the human caudate nucleus and putamen at 22 weeks of gestation, with the enzyme staining densest in the caudate nucleus and the binding densest in the putamen (Fig. 7). Nobin and Bjorklund's description (1973) of particularly intense catecholamine histofluorescence fluorescence in the putamen of 3 to 4 month old human fetuses suggests that gradients in the expression of striatal dopamine and muscarinic receptors may be yoked in some way, but that expression of AChE may be

temporally separate though spatially congruent. There was a suggestion of this also in the P1 rat, where there seemed to be relatively more intense non-patch AChE staining than [^{3}H]-PrBCM binding or fluorescence in the lateral part of the caudoputamen (Fig. 5).

A second gradient was noted in the [^{3}H]-thymidine labeled ferret brain where there were no clusters of [^{3}H]-thymidine labeled neurons to match the most medial of the [^{3}H]-PrBCM patches (themselves weakly labeled; Fig. 8). The most complex patterns were seen in the Nissl stained material where there were both cell-dense and cell-sparse zones. There was a consistent lack of alignment, but not a strict complementarity, between the [^{3}H]-PrBCM patches and the clumps of relatively darkly Nissl-stained cell bodies. This observation (made in fetal material from the cat and human) directly parallels the previously reported lack of alignment between darkly staining cell clusters and clusters of E27 [^{3}H]-thymidine labeling in the caudate nucleus of the cat fetus (Graybiel, 1984b), and the finding by van der Kooy (1984) that in the young rat, striatal opiate receptor patches lie in cell-sparse zones. The interpretation of such observations is unclear. It is not known whether the clumps of darkly staining cells represent developmentally transient compartments; moreover, in other work in cat (Graybiel, 1982) and primate (Nastuk and Graybiel, unpublished observations) certain well-encapsulated clusters of cells dark with Nissl stain have been shown to lie in register with the same markers as the [^{3}H]-PrBCM binding patches. Another unknown is the relationship between the darkly staining cell clusters illustrated here and the cellular islands described by Goldman-Rakic (1981, 1982) in the striatum of the monkey.

[^{3}H]-PrBCM Binding in the Mature Striatum

Though most of the information obtained in this study concerns the arrangement of striatal [^{3}H]-PrBCM binding sites during development, observations

on the distribution of cholinergic markers in the mature striatum are of particular importance because almost all physiological and pharmacological data on the cholinergic system have been culled from studies of mature tissue. Furthermore, most clinical work concerning interactions between striatal acetylcholine and dopamine has focused on mature tissue (see Weiner and Klawans, 1978). The evidence presented here indicates that, at least in the adult cat, muscarinic binding sites have a striatal distribution that is generally very dense compared with that in the developing striatum, but that is nevertheless not strictly uniform. The patches of [^{3}H]-PrBCM binding observed in the adults were in the dorsal part of the caudate nucleus and were visible because their binding density was slightly greater than that of the surrounding tissue. Under the conditions of our experiments, these patches were rare. However, the fact that any patches were observed at all indicates that there is at least some heterogeneity of muscarinic binding in the mature striatum. Technical factors may account for the fact that this patchiness was not identified in previous studies with the reversible muscarinic antagonist [^{3}H]3-quinuclidinyl benzilate ([^{3}H]-QNB) in mature rats (Kuhar and Yamamura, 1975; Kuhar and Yamamura, 1976; Rotter et al., 1979b) and cats (Brand, 1980).

The significance of the few patches of especially dense muscarinic binding seen at maturity is increased by the observation that most of these patches were aligned with AChE-poor striosomes visible in neighboring sections. Thus, the distribution of striatal muscarinic binding sites apparently is subject to the striosomal compartmentalization that was initially defined by the landmark of differential AChE content (Graybiel and Ragsdale, 1978). The matches were confined to dorsally situated striosomes, which are known to represent sites at which the early forming dopamine islands appear during development and are most intensely fluorescent and express the highest levels of tyrosine hydroxylase-like

immunoreactivity (Graybiel, 1984b). This suggests that the relationship between the dopamine islands and the muscarinic binding patches evident in the young brains is maintained in some form into adulthood, particularly in the region innervated by the pronounced "dorsal island system".

Such a compartmental relationship between dopaminergic and cholinergic elements is not readily seen with all markers: both [^{3}H]PrBCM binding and dopamine fluorescence appear nearly uniform in the adult striatum. It is possible that neither the muscarinic binding nor the dopamine fluorescence has more than an occasional residuum of the compartmentalization characterizing them during development. Alternatively, the island and patch systems may still be present in adulthood but may be obscured by additional dopaminergic and cholinergic systems which appear late in development. Olson et al. (1972) have provided evidence that this latter hypothesis may be true for the dopamine-containing afferents: pretreatment of adult rats with the tyrosine hydroxylase inhibitor α-methylparatyrosine (α-MPT) led to the "unmasking" of dopamine islands in the caudoputamen, perhaps because of their differentially lower rate of dopamine turnover. In fact, the application of tract tracing techniques has shown that both nigrostriatal and striatonigral projections are distributed in a patchy manner in adult rats (Wright and Arbuthnott, 1981; Gerfen, 1984; Gerfen, 1985) and cats (Moon Edley and Graybiel, 1983; Jiminez-Castellanos and Graybiel, 1985; Jiminez-Castellanos and Graybiel, 1986; Jiminez-Castellanos and Graybiel, 1987a). Furthermore, tyrosine hydroxylase-like immunoreactivity is lower in striosomes than in the extrastriosomal matrix (Graybiel et al., 1987b) of the adult cat, monkey and human, suggesting again that dopamine metabolism and availability may vary for different striatal compartments. As for muscarinic receptors, the possibility that heterogeneity of one subtype persists into adulthood but is masked by the distribution of another subtypes is shown to be true in the following two chapters.

Though the presence of patches of striatal muscarinic binding is a major focus of this report, the potential functional importance of the non-patch regions of binding should not be underestimated. Binding sites found outside the patches are densely distributed themselves, and the non-patch regions occupy a large part of the caudate nucleus and putamen, even in sections in which the patches are quite prominent. In addition, there are mediolateral gradients of muscarinic binding density for non-patch zones in the mature striatum: as in development, the heaviest binding occurs laterally. It is notable that immunoassay shows the highest levels of choline acetyltransferase (CAT) to be lateral (Guyenet et al., 1977). Interactions between cholinergic neurons and other elements - including dopamine-containing fibers - may accordingly be regionally specific quite aside from being compartmentalized into units as small as striosomes.

Localization of Striatal [^{3}H]-PrBCM Binding Sites in Relation to Cholinergic Markers

The striatal cholinergic system is thought to be mainly, and possibly exclusively, intrinsic (see Fibiger, 1982; Lehmann and Langer, 1983; but see Saelens et al., 1979; Saper and Loewy, 1982; Parent et al., 1983; Arikuni and Kubota, 1984) and to consist of the large striatal neurons whose cell bodies stain positively both for immunoreactive CAT and (in young animals and animals pretreated with DFP) for AChE (Wainer et al., 1984a). In the present study we found no obvious compartmental organization of AChE-positive cell bodies in relation to the patches of muscarinic binding visualized in the immature brains: the cell bodies appeared both in and out of the patches. A quantitative study of the relative distributions of muscarinic binding sites and AChE-positive cell bodies was not undertaken, but in the adult cat, when CAT- and AChE-positive cell bodies also appear in and out of striosomes, there is a slight tendency for the cell bodies to be concentrated at the boundaries of striosomes (Graybiel et al., 1983).

From the pronounced patchiness in [^{3}H]-PrBCM binding found during development, it seems likely that even if cholinergic cell bodies were not clustered, the processes of the developing cholinergic neurons would be. Though AChE-positive fibers are arranged in macroscopic patches, their AChE content is not considered indicative of cholinergic transmission; in fact, much of this AChE is thought to be present in dopamine-containing afferent fibers (see Butcher and Hodge, 1976; Graybiel et al, 1981a). It has been reported, however, that CAT-immunoreactive fibers form patches in the adult ferret striatum (Meininger et al., 1983). By contrast, a recent study with a different antibody against CAT revealed patches in the feline striatum that were low in CAT-like immunoreactivity and that coincided with striosomes (Graybiel et al., 1987a). The existence of a relationship between the two marker patterns (*i.e.*, muscarinic ligand binding and CAT-like immunoreactivity) strongly supports the present indication that there may be persistent compartmentalization of cholinergic function at maturity, and suggests also that this compartmentalization is related to the original distribution of dopamine islands. The striosomal patterning of AChE staining in the adult striatum may reflect in part this organization as well.

Though the present experiments demonstrate unequivocally that muscarinic receptors are compartmentalized in the striatum at least during development, there is no comparable information about nicotinic sites. In the rat, the concentration of putative nicotinic binding sites in the caudoputamen is reported to be very low (Morley et al., 1977; Speth et al., 1977; Hunt and Schmidt, 1978; Segal et al., 1978) or moderate (Schwartz et al., 1982; Clarke et al., 1985). Amenta et al. (1979) have shown that only a small dorsolateral strip of the rat's caudoputamen is labeled with fluorescein-conjugated α-BTX, but Marchand et al (1979) and Arimatsu et al (1981) report in the mouse that an extensive dorsolateral region of the

caudoputamen has low to moderate levels of ^{125}I-α-bungarotoxin binding seen autoradiographically. Limited results obtained during the course of the present work indicate that [^{3}H]-nicotine binding is relatively sparse but uniform in the striatum of the adult cat.

Implications of the Compartmental Appearance of [^{3}H]-PrBCM Binding Sites for Striatal Cholinergic and Dopaminergic Function

Cellular localization of muscarinic binding sites. Striatal muscarinic receptors are likely to be of two sorts: autoreceptors on cholinergic interneurons, and heterologous receptors on other neuronal and/or non-neuronal elements. There is pharmacological and physiological evidence that muscarinic receptors are present in both of the above capacities in the striatum (Misgeld et al., 1980; Misgeld et al., 1982; James and Cubeddu, 1987). The present finding that muscarinic binding sites are especially concentrated during development at sites of dense nigrostriatal innervation (i.e., at sites of dopamine islands) suggests that preferred localizations for some muscarinic receptors are either on the dopaminergic terminals themselves or on other neural or non-neural elements which are preferentially distributed in register with the dopamine islands. Interactions between the striatal dopaminergic and cholinergic systems occurring within (as well as outside) these regions of congruence are likely to take place within a relatively broad time frame, as both dopaminergic and cholinergic effects are relatively slow in course; some dopaminergic and muscarinic receptors are thought to be functionally linked to adenylate cyclases in the striatum (Olianas et al., 1983a; Olianas et al., 1983b) and other muscarinic receptor subtypes exert their effects by increasing phosphatidylinositol turnover (see Nishizuka, 1984).

Binding site localization on nigrostriatal fibers. The idea that some

muscarinic (and also nicotinic) binding sites in the striatum are on dopamine-containing terminals is supported by studies of cholinergic regulation of dopamine release in the striatum (Westfall, 1974a; Westfall, 1974b; Giorguieff et al., 1976; Giorguieff et al., 1977; Giorguieff-Chesselet et al., 1979; deBelleroche and Bradford, 1978; deBelleroche and Gardiner, 1982; Lehmann and Langer, 1982; Raiteri et al., 1982; Sakurai et al., 1982) and also by experiments entailing the destruction of nigrostriatal afferents followed by measurement of muscarinic ligand binding in striatal tissue (Kato et al., 1978; deBelleroche et al., 1979, 1982; Nomura et al., 1979; Gurwitz et al., 1980; Clarke and Pert, 1985). Most reports state that following destruction of the dopamine-containing terminals with 6-hydroxydopamine (6-OHDA) there is a low to moderate decrease in striatal muscarinic binding levels, presumably due to a loss of presynaptic muscarinic receptors.

Though the above findings suggest that heterologous presynaptic receptors constitute only a small proportion of the total striatal muscarinic receptor population, they could, if present, have a powerful effect on the release (and perhaps synthesis; see Horwitz and Perlman, 1984) of dopamine in the striatum. The above cited studies of cholinergic actions on striatal dopamine release state with near unanimity that muscarinic (and nicotinic) agonists enhance basal and stimulus-induced dopamine release. Though some of the physiological evidence obtained is problematic (given the long time course of the effects measured and the reliance on measurements of newly synthesized transmitters), the possibility of a presynaptic localization for muscarinic receptors is particularly interesting in light of the finding that patches of [^{3}H]-PrBCM binding sites are aligned with islands of early forming nigrostriatal dopaminergic fibers.

One would presume such presynaptic binding sites to be located on the

dopaminergic terminals themselves (although functional receptors could be located at places relatively remote from classical synapses). The idea remains unresolved; there is almost no morphological evidence for the presence of axo-axonic synapses in the striatum (see Lehmann and Langer, 1983), though Bouyer et al (1984) have suggested that juxtapositions of striatal nerve terminals may be difficult to see in ultrathin sections because such appositions go in and out of the plane of section. Furthermore, an uneven macroscopic distribution of presynaptic sites could cause problems in regional sampling of tissue taken for ultrastructural observation.

If such presynaptic muscarinic receptors were to exist, they presumably would undergo transport away from the sites of their production in dopamine-containing cell bodies of the midbrain. Axonal transport of muscarinic receptors has been demonstrated in both the peripheral and central nervous system (Laduron, 1980; Wamsley et al., 1981b; Zarbin et al., 1982; Wamsley, 1983). For the nigrostriatal system in particular, evidence exists for the transport of opiate and dopamine receptors (van der Kooy et al., 1986). In the present study, the substantia nigra was not noteworthy for significant levels of ligand binding. Other investigators (Kuhar and Yamamura, 1975; Kuhar and Yamamura, 1976; Rotter et al., 1979b) also have not observed appreciable levels of endogenous muscarinic binding in the substantia nigra. Ruberg et al (1982) and Cortes et al (1984), however, have noted low levels of nigral muscarinic binding in human postmortem tissue. Furthermore, studies described in the following chapter do indicate the presence of muscarinic receptor subtypes in the substantia nigra. Thus, the possibility remains that nigrostriatal neurons produce muscarinic receptors, at least some of which may be subject to axonal transport.

Binding site locations on neurons intrinsic to the striatum. A considerable proportion of the muscarinic binding sites in the striatum are believed

to be on intrinsic striatal neurons, to judge from the ca. 40% decrease in binding found after injection of the neurotoxin kainic acid into the caudoputamen of adult rats (Hruska et al., 1978). Muscarinic autoreceptors have been identified in striatal tissue and studied with respect to pharmacology and physiology (James and Cubeddu, 1987). Such receptors are thought to mediate the inhibitory effects exerted by acetylcholine on its own release from striatal cholinergic neurons. The alignment of [^{3}H]-PrBCM-dense patches and dopamine islands suggests that a subset of striatal neurons receiving a dopaminergic input may be further characterized as a class by virtue of receiving muscarinic cholinergic input of the particular type predominating in the patches. The subclass of cholinergic neurons in or alongside striosomes might also be singled out as a preferred target for muscarinic autoreceptor effects.

Non-neuronal striatal binding sites: blood vessels and glia. There was no obvious association of the patches of [^{3}H]-PrBCM binding with striatal blood vessels, though the resolution of the autoradiograms may be too low to detect this. However, muscarinic receptors have been shown to mediate vasodilation in the central nervous system (Scremin et al., 1973), and to be present on cerebral blood vessels (Estrada and Krause, 1982; Krause and Estrada, 1982). Furthermore, cerebral blood flow studies show that circulating tracers display patchiness in all brain areas, including the striatum (Pulsinelli and Duffy, 1979; Lear et al., 1982). When McCulloch et al. (1983) injected apomorphine or haloperidol into the striatal parenchyma of the rat, a patchy distribution of uptake of intravenously administered 2-deoxyglucose was produced and was found to be related to inhomogeneities in AChE staining.

The presence of muscarinic binding sites on astroglia has been documented in the bovine caudate nucleus (Henn et al., 1979). It is not known whether such

binding sites are also associated with other types of glial cells, or whether there are patchy distributions of the various glial cell types that could relate to striatal compartmentalization.

Receptor subtypes and their proportional distributions. A reasonable interpretation of the compartmentalized binding distributions described here is that there are differing proportions of muscarinic receptors on neuronal elements found in and out of striosomes and their forerunners, and that the patch and non-patch receptors mature at different rates. However, a second key possibility is that the total density of muscarinic receptors may be nearly equivalent in and out of striosomes, but the relative proportions of receptor subtypes may vary for patch versus non-patch regions. There is evidence that this second mode of distribution characterizes the striatal opioid receptor systems. Opioid binding sites of the μ type occur in dense patches are in register with AChE-poor zones in the caudoputamen of the mature rat (Herkenham and Pert, 1981) and with dopamine islands in the developing rat (Moon Edley, 1983; Murrin and Ferrer, 1984; van der Kooy, 1984), whereas δ opioid binding sites have a uniform or near uniform striatal distribution (Goodman et al., 1980; Moskowitz and Goodman, 1984).

The possibility that muscarinic receptor subtypes have differential distributions was not analyzed in the presently described experiments because [^{3}H]-PrBCM does not distinguish among receptor subtypes, at least in fresh tissue homogenates (Hulme et al., 1978). The present work nevertheless suggests the hypothesis that there is a differential spatial distribution of muscarinic receptor subtypes with certain subtypes occuring in patches (and developing early) and other subtypes being concentrated elsewhere and possibly in the patches as well (and developing later). Of the identified muscarinic binding site subtypes (Birdsall et al., 1976; Birdsall et al., 1978; Hammer et al., 1980), those with low agonist

affinity (or "L" sites) and those with high affinity for the antagonist pirenzepine (or "M1" sites) are reported to predominate in striatal tissue (Birdsall et al., 1980; Wamsley et al., 1980; Potter et al., 1984; Cortes et al., 1986). In fact, findings described in the following two chapters show that subtypes of muscarinic receptors have differing striatal densities and distributions at maturity, and that prenatally the distributions of receptor subtypes appear to be ontogenetically linked.

Patterns of Muscarinic Binding in Relation to Other Indicators of Striatal Compartmentalization

AChE staining. The present results link the patchy distribution of heaviest striatal [^{3}H]-PrBCM binding to macroscopic patterns of AChE staining both in development and adulthood: zones of dense binding match AChE-rich patches in the immature striatum and at least some AChE-poor patches (striosomes) in the mature striatum. The fact that the AChE-rich patches appear to be the forerunners of the AChE-poor (striosomal) patches of the mature striatum (Graybiel, 1984a) suggests that the relationship between the patches of dense muscarinic binding and levels of AChE staining would be reversed during maturation. This was shown to be the case here, though the meaning of such results depends upon the cellular localization and the physiological action of the AChE involved.

Much of the striatal AChE in adult rats is thought to be intrinsic to the caudoputamen (McGeer et al., 1971b; Lehmann et al., 1979), but there is evidence that a small percentage of the esterase exists within dopaminergic nigrostriatal fibers (Lehmann and Fibiger, 1978; Butcher and Woolf, 1982). Greenfield et al. (1980, 1982) have shown that stimulation of the rat's substantia nigra elicits changes in AChE release there and in the caudoputamen. In terms of the classic cholinergic catabolic actions of AChE, the relationship between [^{3}H]-PrBCM

binding and AChE staining patterns found here may have significant functional consequences because the local concentration of AChE could affect the efficiency of muscarinic receptor activation. In the adult, the heterogeneity of striatal AChE staining would then mean that even if muscarinic ligand binding seems close to uniform, the activation of muscarinic receptors may be differential and compartmentalized across the striatum. As a consequence, topographic variations in the distribution of striosomes (see Graybiel and Ragsdale, 1978, 1983) as well as in the levels of background AChE staining could be functionally important when considering the distribution of muscarinic binding sites. By similar reasoning, the early alignment of AChE-rich zones with sites of dense muscarinic binding suggests that cholinergic activation could be readily depressed at these sites. It is conceivable, for example, that this might account for the findings of Nomura et al., (1981) who did not see cholinergic effects on dopamine release in striatal slice preparations from newborn rats, but did see such effects, which were atropine-sensitive, in older rat pups (where presumably the AChE levels within dopamine islands had fallen with age). However, because AChE may have non-classical effects (for example, there is evidence for its action as a slow peptidase; Chubb et al., 1980, 1982), other interpretations of the relationship between muscarinic binding and the esterase distributions could hold.

Other neurotransmitter-related compounds. Acetylcholinesterase staining is only one of a number of neurotransmitter-related marker techniques that can serve to delineate the striosomal system. In fact, the striatal distribution of each neuropeptide so far localized by immunohistochemistry has been found to follow striosomal ordering by being concentrated either in or out of striosomes, or at least to be patchy where correlations with striosomes have not yet been made (Graybiel et al., 1981a; Gerfen, 1983; Gerfen et al., 1985; Goedert et al., 1983;

Graybiel, 1984a). This is also true for GAD-positive neuropil, which is dense within at least some striosomes (Graybiel et al., 1983), and as discussed above, for CAT (Graybiel et al., 1987a) and tyrosine hydroxylase (Graybiel et al., 1987b). For some of the neuropeptides, the corresponding receptor localizations have also been found to be distributed in or out of the striosomal units (Herkenham and Pert, 1981; Goedert et al., 1984). A major implication of these findings is that cholinergic interactions in the striatum occur within a neurochemical context that is strongly influenced by the compartmental architecture of this tissue.

Trans-striatal channeling. Though not studied in the present experiments, both the cell bodies giving rise to striatal efferent connections (Graybiel et al., 1979; Gerfen, 1983; Parent and DeBellefeuille, 1983) and a number of fiber systems projecting to the striatum (Herkenham and Pert, 1981; Ragsdale and Graybiel, 1979; Ragsdale and Graybiel, 1981; Ragsdale and Graybiel, 1984; Donoghue and Herkenham, 1983; Gerfen, 1984; Jiminez-Castellanos and Graybiel, 1985; Jiminez-Castellanos and Graybiel, 1986; Jiminez-Castellanos and Graybiel, 1987a) follow a striosomal organization. Depending on the activities of the afferent pathways innervating striosomes and nonstriosomal regions, and their interactions with cholinergic interneurons, certain subsets of striatal efferent systems may thus be differentially active or inactive.

The present results extend this conclusion by suggesting that at least during development, and probably in adulthood as well, cholinergic-dopaminergic interactions in the striatum are themselves compartmentalized according to a similar plan. Major questions remain outstanding in regard to this modular form of interaction, including the degree of compartmentalization that can be expected to exist in the adult, the differential nature of patch and non-patch binding, the role of muscarinic receptor subtypes, the relation of the patterns to the distribution

of striatal nicotinic receptors and the cellular localization of the molecules involved. These unknowns limit the specific functional implications that can be drawn from the present results, but the general implication of the findings is clear: the functions subserved by striatal muscarinic receptors may vary across the striatum in a manner concordant with its compartmental organization during development, and may reflect a residual compartmentalization in accord with the heterogeneity expressed by mature striatal tissue.

Chapter 3

Autoradiographic Localization and Biochemical Characteristics of M1 and M2 Muscarinic Binding Sites in the Striatum of the Cat, Monkey and Human

ABSTRACT

The autoradiographic distribution of M1 and M2 muscarinic cholinergic binding sites was studied in the striatum of the cat, monkey and human, and concurrent binding assays were carried out on striatal tissue sections from the cat. M1 sites were directly labeled with [^{3}H]-pirenzepine; M2 sites were labeled as a consequence of binding competition between pirenzepine and [^{3}H]-N-methylscopolamine. Serial section analysis with autoradiograms and stained tissue sections allowed for comparisons among M1 and M2 binding distributions and acetylcholinesterase (AChE) staining patterns.

The two subtypes of binding sites demonstrated distinct striatal distributions. M2 sites were virtually homogeneous except in the ventral striatum where zones of sparse and especially dense binding were observed. Striatal M1 sites were generally more abundant than M2 sites and showed similar heterogeneity in the ventral striatum. Dorsally, however, patches of dense M1 binding were found, and proved to correspond with AChE-poor striosomes, hallmarks of striatal compartmentalization. The finding of differing distributions for the two subtypes of muscarinic cholinergic binding site suggests a mechanism for the intrinsic spatial segregation of striatal cholinergic function. Further, the striosomal patterning of M1 binding indicates that certain aspects of cholinergic function in the striatum

may be constrained and thus regulated by the compartmental ordering characteristic of this region of the basal ganglia.

INTRODUCTION

Subtypes of muscarinic cholinergic binding sites have been defined based upon analysis of binding assays for agonists (Birdsall et al., 1978) and for the nonclassical antagonist pirenzepine (Hammer et al., 1980). Such assays yield binding curves that most closely approximate curves modeling heterogeneous populations of binding sites. Classes of binding site subtypes showing low, high or super high affinity for agonists have been termed L, H or SH; alternatively, binding sites demonstrating high affinity for pirenzepine have been termed M1 while those having low affinity for pirenzepine are called M2. Further distinctions among muscarinic subtypes have been characterized by their differential binding affinities in the presence of the sulfhydryl reagent N-ethylmaleimide (Ehlert et al., 1980; Korn et al., 1983; Flynn and Potter, 1985) or in varying concentrations of divalent cations (Potter et al., 1984) or sodium (Watson et al., 1983). Such effects may reflect variations in the coupling of receptor molecules to associated regulatory proteins, or G proteins. However, a full understanding of the molecular mechanisms specifying particular subclasses of muscarinic binding sites is not yet in hand. Possibilities include the ability of receptor molecules to interconvert among different affinity states, differences in local membrane environments, and the existence of more than one species of receptor molecule. The latter hypothesis is supported by the recent cloning of a muscarinic receptor thought to be the M1 subtype (Kubo et al., 1986), and by further evidence that muscarinic receptors are encoded by more than one gene (Bonner et al., 1987; Braun et al., 1987; Fukuda et

al., 1987). Nonetheless, all of these possibilities probably contribute in some capacity to an explanation of the pharmacological observations indicating the presence of multiple muscarinic binding site subtypes. They are also likely to be involved in specifying among a variety of cellular responses mediated by muscarinic receptors, including breakdown of phosphoinositides (Fisher and Agranoff, 1987), inhibition of adenylate cyclase (Olianas et al., 1983a) and the regulation of certain potassium, sodium and calcium channels (North, 1986).

The first efforts to localize muscarinic binding sites to specific regions of the mammalian brain involved autoradiography with ligands that did not recognize subtypes, such as [^{3}H]-quinuclidinyl benzilate ([^{3}H]-QNB) and [^{3}H]-propylbenzilylcholine mustard ([^{3}H]-PrB). These early studies pointed to the striatum as a brain region with a notably dense, uniform level of [^{3}H]-QNB and [^{3}H]-PrB binding (Kuhar and Yamamura, 1976; Rotter et al., 1979b; Brand, 1980). It was later possible to show with autoradiograms of varying exposure times that in the cat there were hints of patterning in striatal [^{3}H]-PrB binding, and serial section analysis revealed that patches of particularly dense binding coincided with AChE-poor zones known as striosomes (Nastuk and Graybiel, 1985). Further, vivid patches of [^{3}H]-PrB binding were seen in the developing striosomal system of the fetal striatum of several species including human (Rotter et al., 1979a; Nastuk and Graybiel, 1985). These findings raised the possibility that striatal muscarinic cholinergic function might be spatially parcelled. The fact that the patterning was obscure at maturity, though, suggested that either the heterogeneity was only subtle at adulthood or (as is true for striatal opiate receptors (Moskowitz and Goodman, 1984)) a more overt compartmentalization was present but masked due to the simultaneous demonstration of muscarinic binding site subtypes having different distributions.

Autoradiographic and biochemical methods have been developed for studying subclasses of muscarinic binding sites directly with subtype-selective ligands such as [^{3}H]-pirenzepine and others, and indirectly through competition among more than one ligand (Potter et al., 1984; Wamsley et al., 1984; Yamamura et al., 1985; Giraldo et al., 1987). With methods such as these we have analyzed the distributions of M1 and M2 muscarinic binding sites (see also Nastuk and Graybiel, 1986) in the striatum of the cat, monkey and human after first confirming that the binding to be studied in this way had a valid biochemical basis. The principal autoradiographic finding is that in all three species, striatal M1 sites in the dorsal striatum are especially concentrated in dense patches aligned with striosomes whereas M2 sites do not demonstrate this type of patchiness. In mid-ventral and ventral regions of the dorsal striatum, zones of sparse binding are evident for both types of muscarinic binding site. In the ventral striatum, small patches of especially dense M2 binding are evident. These results suggest that some but not all aspects of striatal cholinergic function may be compartmentalized, with such spatial organization reflecting the molecular and functional characteristics of muscarinic receptor subtypes.

METHODS

Observations were made on striatal tissue from seven adult cats, three adult monkeys (cynomolgus) and five adult humans (three male and two female, ages 74-84). Human tissue was obtained at autopsy (postmortem delay 4-24 hours) from individuals with no known history of neurologic disease. At autopsy, blocks from the striatum were quickly dissected out and frozen on crushed dry ice. The blocks were kept at -70°C prior to sectioning as described below for the animal tissue.

Tissue from the cats and monkeys was obtained without perfusion under conditions of deep barbiturate anesthesia. Brains were quickly removed, frozen on crushed dry ice and mounted on cryostat chucks. For biochemical experiments, brains were cut into left and right halves before freezing; once mounted and in the cryostat, blocks were trimmed as close to the edges of the striatum as possible. Coronal sections through the striatum were cut in the cryostat at -12°C to -14°C. Section thickness was either 15 μm (for autoradiography and histochemistry) or 10 μm (for binding assays). Sections for binding assays were taken from mid-rostral levels of the striatum, where rostro-caudal variability in cross-sectional area was minimal. Sections were thaw-mounted onto gelatin-coated slides, to be processed for M1 or M2 ligand binding autoradiography, AChE staining by a modified Geneser-Jensen and Blackstad protocol (Geneser-Jensen and Blackstad, 1971), or for binding assays. For all procedures involving ligand binding, sections were placed temporarily after thaw-mounting into racks at about 4°C, and then kept under vacuum at 0°C for two to four hours in a vacuum desiccator buried in crushed ice and containing Drierite capsules. Slides were then stored at -20°C in sealed boxes containing Drierite for at least two weeks before further processing (Lewis et al., 1982).

For ligand binding autoradiography, sections were preincubated in 50mM sodium phosphate ($NaHPO_4$) buffer at pH 7.4 containing 10mM ethylenediaminetetraacetic acid (EDTA) and 0.1mM N-ethylmaleimide (NEM) for 15 minutes at 4°C to uncouple binding of endogenous agonist without affecting antagonist binding (Potter et al., 1984). Incubations were then carried out for one hour at room temperature in 50mM $NaHPO_4$ buffer containing 1mM EDTA and either 10nM [^{3}H]-pirenzepine ([^{3}H]-PZ; 76.0 Ci/mmol, New England Nuclear) for M1 binding or 0.3nM [^{3}H]-N-methylscopolamine ([^{3}H]-NMS; 85.0 Ci/mmol, New

England Nuclear) and 100 or 200 nM unlabeled PZ (gift of R. Hammer) for M2 binding. These concentrations of PZ were chosen to occlude as many M1 sites (K_d ca. 10 nM) as possible while leaving most M2 sites (K_d ca. 600 nM) free for labeling. For blanks, 1μm atropine was added to the incubation solution. To terminate binding, the sections were immersed for five minutes in chilled (4° C) 50mM $NaHPO_4$ buffer containing 1mM EDTA. Two very brief rinses in distilled water at 4°C followed, and the sections were then dried under a stream of cool air. Slides were apposed to LKB tritium-sensitive film for 12 to 29 days at room temperature. Films were developed in Kodak D19 for four minutes at 20° C then fixed in Kodak rapid fixer. Serial section comparisons were made among striatal M1 binding distributions, M2 binding distributions and AChE staining patterns. Densitometry was performed on M1 autoradiograms of feline and human tissue to estimate the degree of variability in binding density within a given tissue section. For each of five sections per case, five to 14 pairs of measurements of grain density were made from visible patch and neighboring non-patch regions in the dorsal striatum of one cat and one human. The percent difference in grain density in and out of patches was averaged for each section, then an overall mean percent difference was determined for each case.

For direct binding assays, sections from blocks trimmed down to the striatum as described were preincubated under the same conditions as were sections destined for autoradiography. Groups of three or four sections were then incubated in various concentrations of [^{3}H]-PZ or [^{3}H]-NMS (under the same conditions as for autoradiography) with and without 1μm atropine. Concentrations of[^{3}H]-PZ ranged from 0.3nM to 50nM, and [^{3}H]-NMS concentrations ranged from 0.03nM to 30nM. Following binding termination and rinsing, sections were wiped off slides with Whatman GF/B glass fiber filters or were dried and scraped off, and were

placed individually into scintillation vials. One ml of Protosol (New England Nuclear) was added to each vial, and the vials were capped and left overnight at 4°C. A few hours prior to counting in a liquid scintillation counter, 0.1 ml of 30% hydrogen peroxide (to prevent coloration) was added to each vial, followed by 10 ml of Betafluor (National Diagnostics). Specific and nonspecific binding were calculated from counts, and the Lowry method (1951) was applied to estimate the amount of protein per section. Binding curves were plotted and Scatchard analysis was performed for each of the two ligands. Linear regression analysis with the RS1 statistics program was applied both for nonspecific binding curves and Scatchard plots.

For competition experiments, the same procedures were followed as for direct binding assays except that the incubation solutions contained 0.3nM [^{3}H]-NMS and concentrations of unlabeled PZ ranging from 0.1nM to 10μM. Nonspecific binding of [^{3}H]-NMS was determined in the presence of 1μm atropine. Counts were expressed as percent occupancy, with 100% being the specific counts in the absence of any displacer. Points for a competition curve were plotted from the resulting counts, and nonlinear curve fitting was performed with the LIGAND program (Munson and Rodbard, 1980) to determine whether there was a better fit to a one-site or a two-site model. A Hill plot was also constructed from the occupancy concentration data, and a Hill coefficient was calculated.

RESULTS

Biochemical studies. Figure 1 (top) shows a direct binding curve for low concentrations of [^{3}H]-PZ (incubations in very high ligand concentrations were not included here, as the present experiments serve to characterize high affinity [^{3}H]-PZ

binding, *i.e.*, binding to the M1 site). For this concentration range, [^{3}H]-PZ binding had a saturable specific component and a nonspecific component that increased linearly (correlation coefficient r=0.99) as ligand concentration was increased. At 10nM [^{3}H]-PZ, the concentration chosen for subsequent autoradiographic experiments, nonspecific binding comprised less than 0.5% of total binding. Scatchard analysis (Fig. 1, bottom) yielded a linear plot (r=0.97) and revealed that, for our experimental conditions, [^{3}H]-PZ bound to a population of striatal sites with a K_d of 8.9.

Specific direct binding of [^{3}H]-NMS to striatal tissue was saturable (Fig. 2, top), and nonspecific binding rose linearly with increasing ligand concentration (r=0.97). Less than 4% of total binding was nonspecific at an incubation concentration of 0.3nM [^{3}H]-NMS, the concentration used for autoradiography. The plot obtained with Scatchard analysis (Fig. 2, bottom) demonstrated a linear fit (r=0.79) and indicated that [^{3}H]-NMS binding in the striatum of the cat had a K_d of 0.47. However, it was found that [^{3}H]-NMS adhered relatively readily to the glass walls of the incubation vessel and to the glass slides on which the sections were mounted.

The occupancy concentration curve for the competitive binding of PZ and [^{3}H]-NMS (Fig. 3) shows that under the present experimental conditions, PZ competes with [^{3}H]-NMS for binding to striatal sites. The data points fit well ($p<.05$) to a curve describing two populations of PZ binding sites. High affinity (M1) sites predominated in number over low affinity (M2) sites with a ratio of approximately 14:1, as determined from curve-fitting to a two-site model with LIGAND analysis. The Hill coefficient, n_H, for the competition data was 0.44, indicating also the presence of more than one PZ binding site.

Autoradiographic studies. In all species studied, high affinity [^{3}H]-PZ

Figure 3-1: Saturation analysis (top) of [^{3}H]-PZ binding to striatal tissue sections from the cat. Specific binding (●) is the difference between total binding and nonspecific binding. Nonspecific binding (○) was determined in the presence of 1 μm atropine. Each point represents the mean counts from three experiments, each carried out in quadruplicate (three animals, four sections per animal per point). Scatchard analysis of the specific binding of [^{3}H]-PZ is shown at bottom. Linear regression analysis was performed to determine K_d and B_{max}.

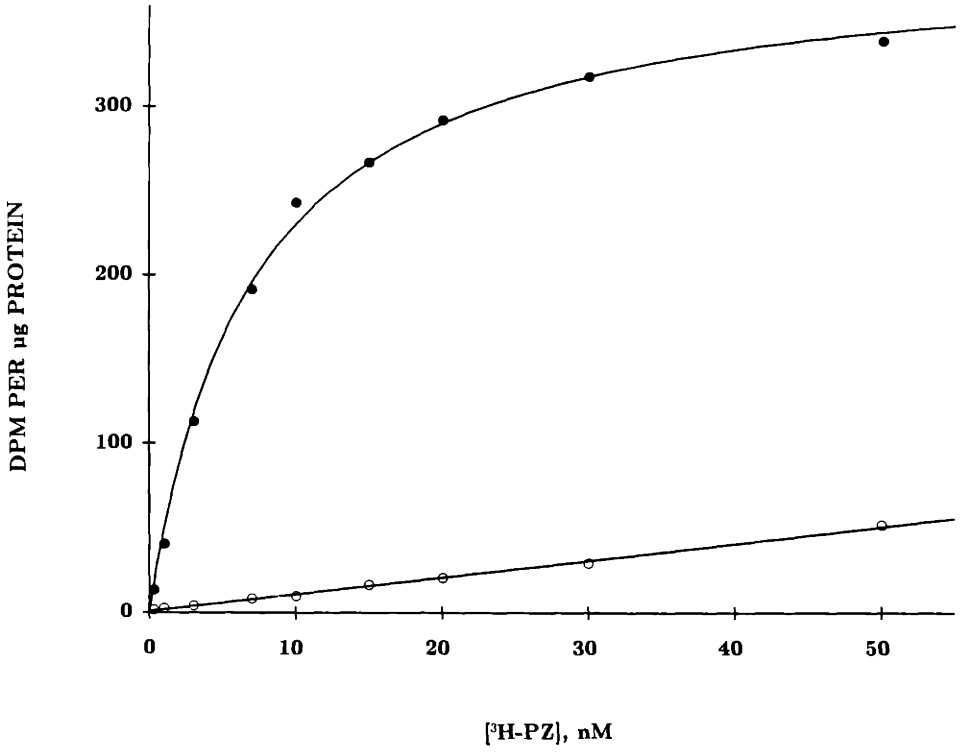
DPM PER µg PROTEIN
300
200
100
0
0
10
20
30
40
50
[3H-PZ], nM

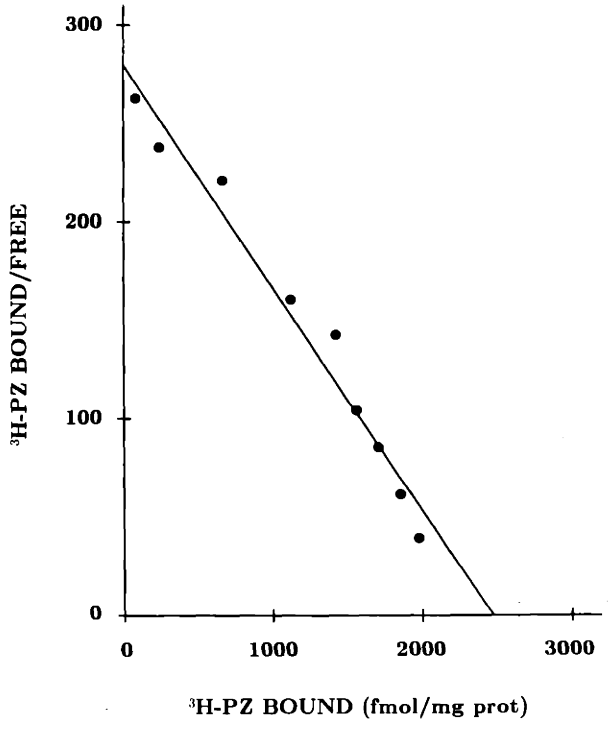
3H-PZ BOUND/FREE
300
200
100
0
0
1000
2000
3000
3H-PZ BOUND (fmol/mg prot)

Figure 3-2: Saturation analysis (top) of [^{3}H]-NMS binding to sections from the striatum of the cat. Specific (●) and nonspecific (o) binding were determined in the same way as was done for [^{3}H]-PZ. Each point represents mean values for three experiments performed in quadruplicate. Scatchard analysis (bottom) of the specific binding of [^{3}H]-NMS. Linear regression analysis was performed to determine K_d and B_{max}.

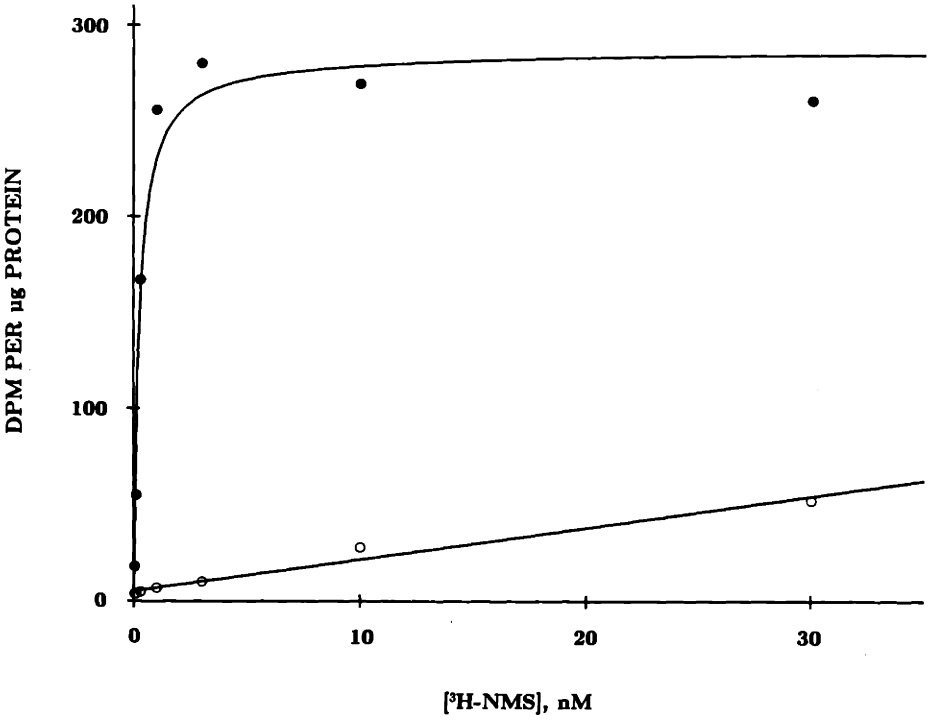
300
200
100
0
DPM PER ug PROTEIN
0
10
20
30
[3H-NMS], nM

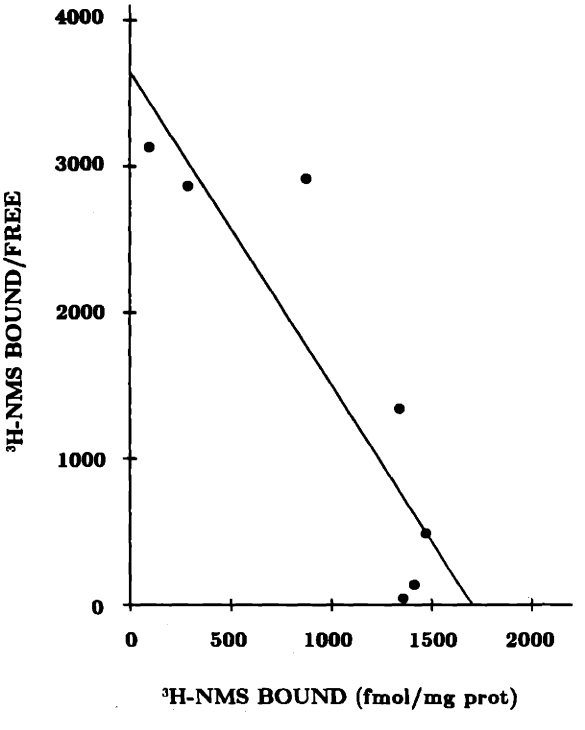
4000
3000
2000
1000
0
3H-NMS BOUND/FREE
0
500
1000
1500
2000
3H-NMS BOUND (fmol/mg prot)

Figure 3-3: Ability of PZ to compete with [^{3}H]-NMS (0.3 nM) for binding to striatal tissue sections from the cat. Concentrations of PZ ranged from 0.1 nM to 10 μM. Each point represents the mean percent occupancy in three experiments, each conducted in quadruplicate. Specific binding of [^{3}H]-NMS in the absence of displacer was taken as 100% occupancy. Curve fitting was performed with nonlinear regression analysis.

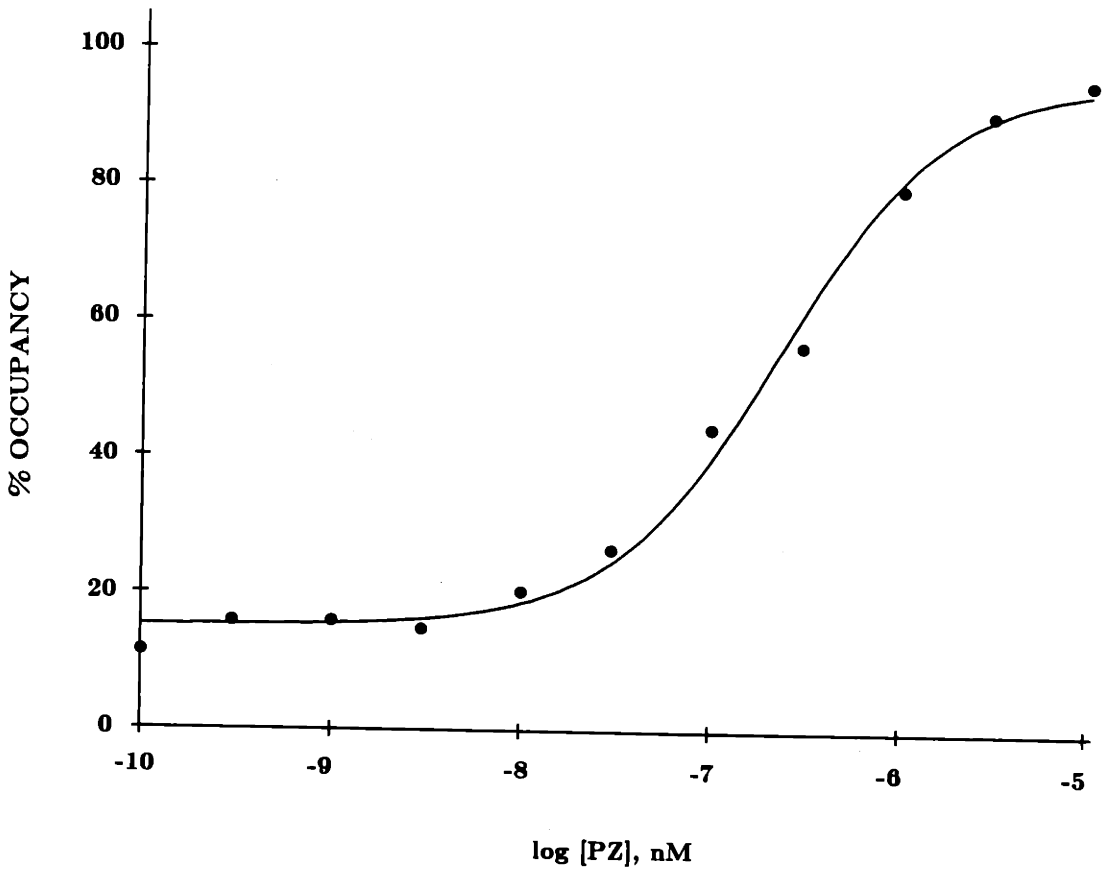
100
80
60
40
20
0
% OCCUPANCY
-10
-9
-8
-7
-6
-5
log [PZ], nM

binding (M1 binding) to striatal tissue sections was dense but not uniform. Figure 4A shows M1 binding in the cat's striatum, where zones of elevated binding density can be seen. These patches were irregularly shaped with widths of about 0.5-0.8mm. The patches were most often found mid-dorsally in the striatum (see asterisk in Fig. 4A); they rarely appeared in the extreme dorsolateral quadrant (the region to the right of the label "CN" shown in Fig. 4B), and when found mid-ventrally (in the region at the level of the X in Fig. 4A-C) they were not well delineated. Irregularly shaped patches of dense M1 binding also were found in the dorsal striatum of the monkey (Fig. 5A) and human (Fig. 6A), where their widths ranged from about 0.5-1.0mm.

Autoradiograms of tissue sections processed for the binding of [^{3}H]-NMS in the presence of PZ (M2 binding) exhibited few or no densities in the dorsal striatum (Fig. 4C, 5C and 6B). Most sections showed virtually uniform binding that was less dense than the M1 binding (optimal exposure times were nearly twice as long for M2 binding as for M1 binding). For the dorsal striatum, exceptions to this uniformity were found caudally in all three species, where occasional patches of very slightly elevated M2 binding were in register with particularly marked M1 patches (results not shown).

Serial-section comparisons between striatal M1 binding distributions and AChE staining demonstrated that patches of dense binding corresponded to zones of pale AChE staining, or striosomes (Graybiel and Ragsdale, 1978), in the dorsal striatum of the cat (Fig. 4), monkey (Fig. 5) and human (Fig. 7). It was observed in the cat that at certain rostro-caudal levels the M1 patches were more distinct medially whereas striosomes stood out best laterally (though both macroscopic labeling patterns showed patch-for-patch alignment). Another topographical difference between the two marker patterns was that the M1 patches were more

Figure 3-4: Photographs of consecutive serial coronal sections through the striatum of a cat showing the M1 binding distribution (A, darkfield), AChE staining (B, lightfield) and M2 binding distribution (C, darkfield). For darkfield photographs, areas rich in binding sites appear lighter than areas of sparse binding. Zones of particularly dense M1 binding in the dorsal striatum correspond to AChE-poor striosomes (asterisks). Farther ventrally, some sparse zones are present in all three marker patterns (X's). The insula major of Calleja (arrows), intensely stained with AChE, is weakly labeled with M1 binding and partially labeled with dense M2 binding. CN: caudate nucleus, P: putamen, NA: nucleus accumbens, IC: internal capsule. Scale bar = 1mm (A, B and C at same magnification).

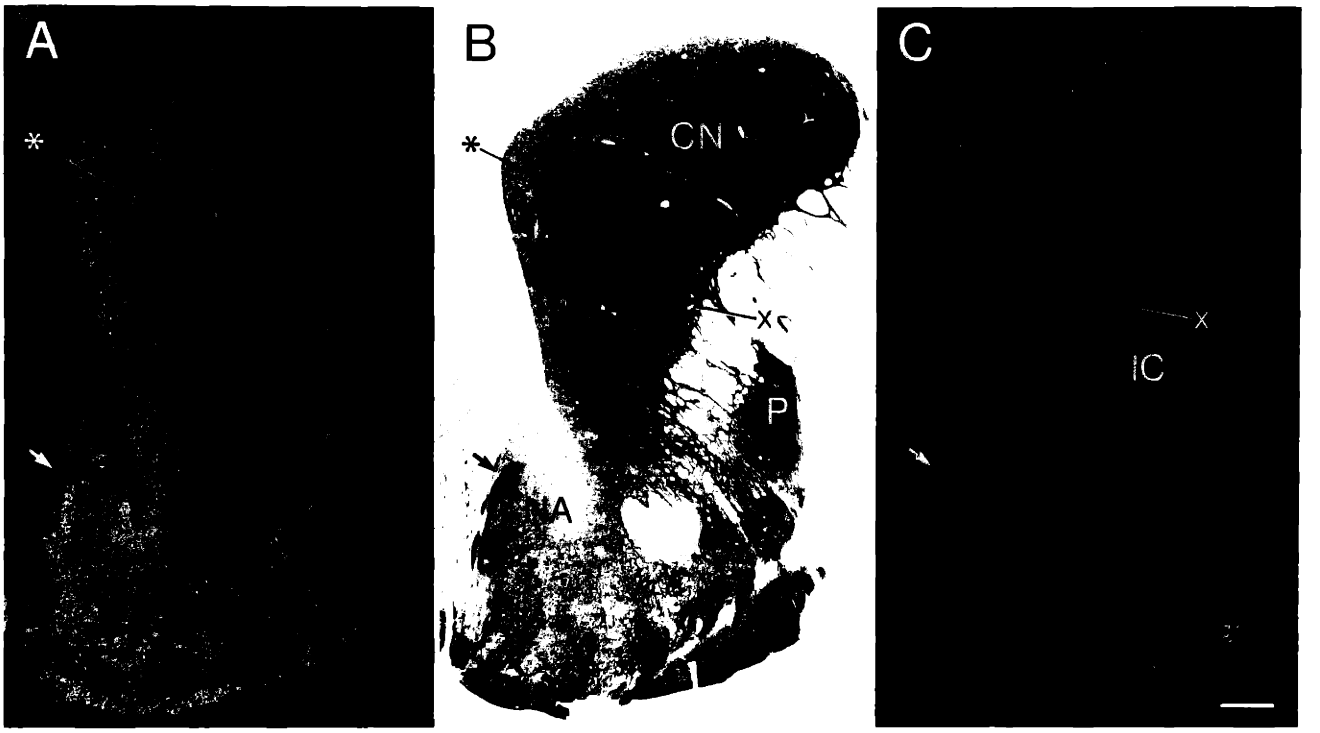
A
B
C
CN
X
P
A
X
IC

crisply delineated caudally than rostrally but the striosomes seemed equally well demarcated at all levels. This rostro-caudal difference in clarity of M1 patches was noted in all three species studied, and can be seen in the human tissue if Fig. 6A and Fig. 7A are compared. Figure 7 also reveals that in the dorsal putamen of the human, the M1 binding distribution is more decidedly patterned than is the AChE staining.

To substantiate the visual impression of greater M1 binding in the patches relative to that in the surrounding non-patch regions, densitometry was performed on autoradiograms of feline and human tissue. For sections from the cat, M1 patches were found to be an average of 20% denser than their surround, and for the human this average percent difference was 16%. In general there was variability of difference in grain density for patches and matrix measured within each section; this perhaps was due to mediolateral and dorsoventral differences in patch and matrix grain density, but a quantitative topographic analysis was not done.

Patterns of autoradiographic labeling in the ventral striatum and nucleus accumbens differed from those found dorsally, both for M1 and M2 binding. This ventral region in the cat (Fig. 8A,A'), monkey (Fig. 8B,B') and human (Fig. 9A,C) contained not only zones of dense M1 and M2 binding, but also areas of sparse binding for each receptor subtype. The labeling patterns appeared very complicated, especially in the human tissue with its instances of interdigitation among zones dense and sparse in binding sites. Comparison of the M1 and M2 binding distributions in all species yielded examples of correlations between areas sparse in both types of binding. Such patches were often found ventrally within the putamen (see Fig. 9A and C for the human and Fig. 8A and A' for the cat), and corresponded to AChE-rich zones. But as Fig. 8A and A' also shows, patches

Figure 3-5: M1 binding (A, darkfield), AChE staining (B, lightfield) and M2 binding (C, darkfield) in serially adjacent sections from the striatum of a cynomolgus monkey. Patches densely labeled with M1 binding are in register with striosomes (see asterisks). Such patches are absent in the M2 binding autoradiograph. P: putamen, IC: internal capsule. Scale bar = 1mm (A, B and C at same magnification).

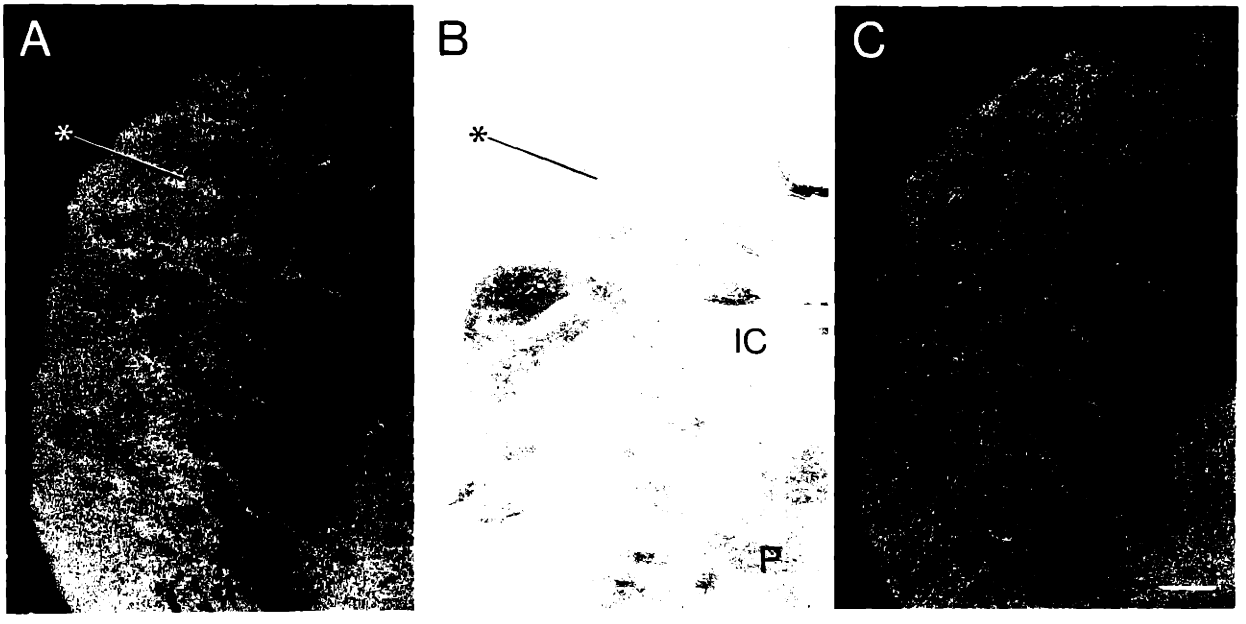
A
*
B
*
IC
P
C

Figure 3-6: Darkfield photographs of M1 (A) and M2 (B) binding in serial sections through the human caudate nucleus and putamen. M1 binding is patchy and generally denser than M2 binding, which lacks discrete patterning. Both types of binding are densest in the region of the ventral striatum (arrows indicate its rostral pole). CN: caudate nucleus, P: putamen. Scale bar = 3mm (A and B at same magnification).

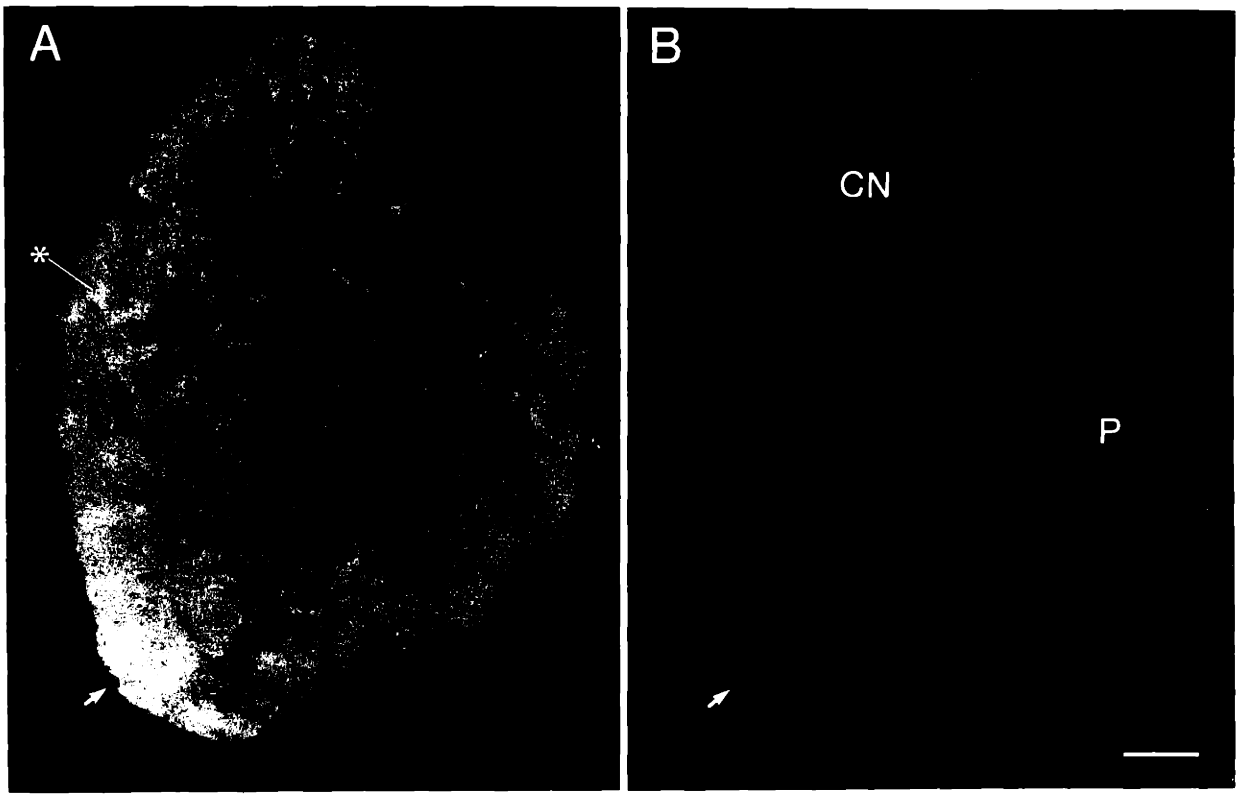
A
*
B
CN
P

of sparse binding also occurred ventral to the caudate nucleus. In addition, in the olfactory tubercle there were patches dense in both M1 and M2 binding sites (see Figs. 7, 8 and 9) that were rich in AChE as well. It is unclear whether all of these small patches corresponded to islands of Calleja. Nissl staining of adjacent sections (results not shown) indicated that there was some degree of overlap among patches and islands. The insula major of Calleja was distinct in Nissl staining (not shown) and in autoradiograms (see arrows in Fig. 4 and asterisks in Fig. 8) for the cat and monkey and was noteworthy because it contained sparse M1 binding, though a part of it was dense with M2 binding.

DISCUSSION

The primary findings of this study are that tissue sections processed for ligand binding autoradiography show differing macroscopic distributions of striatal M1 and M2 binding sites in the cat, monkey and human, and that striatal tissue sections from the cat demonstrate valid biochemical characteristics when processed for M1 and M2 muscarinic binding under experimental conditions that were the same as those employed to generate sections for autoradiographic study.

Ligand binding to striatal tissue. Both [^{3}H]-NMS binding and high affinity [^{3}H]-PZ binding exhibited saturable specific and linear nonspecific components. Levels of nonspecific binding for each radioligand were extremely low, a phenomenon substantiated by the near invisibility of autoradiographic film images for sections incubated in the presence of atropine. The K_d values obtained here for [^{3}H]-NMS binding and high affinity [^{3}H]-PZ binding in the cat's striatum agreed with values reported by several groups for the binding of these ligands to brain tissue from other mammalian species (Birdsall et al., 1976; Hulme et al.,

Figure 3-7: M1 binding (A, darkfield) and AChE staining (B, lightfield) in a serial pair of sections through the human striatum at a level caudal to that shown in Fig. 6. Patches of dense M1 binding in the caudate nucleus correspond to striosomes (see asterisks), although in the putamen the pattern of binding does not have a ready counterpart in the enzyme staining. There are virtually no silver grains over the GPe. Note ventrally the punctate zones of dense binding, some of which are matched by AChE-rich patches. IC: internal capsule, AC: anterior commissure, GPe: external segment of globus pallidus. Scale bar = 3mm (A and B at same magnification).

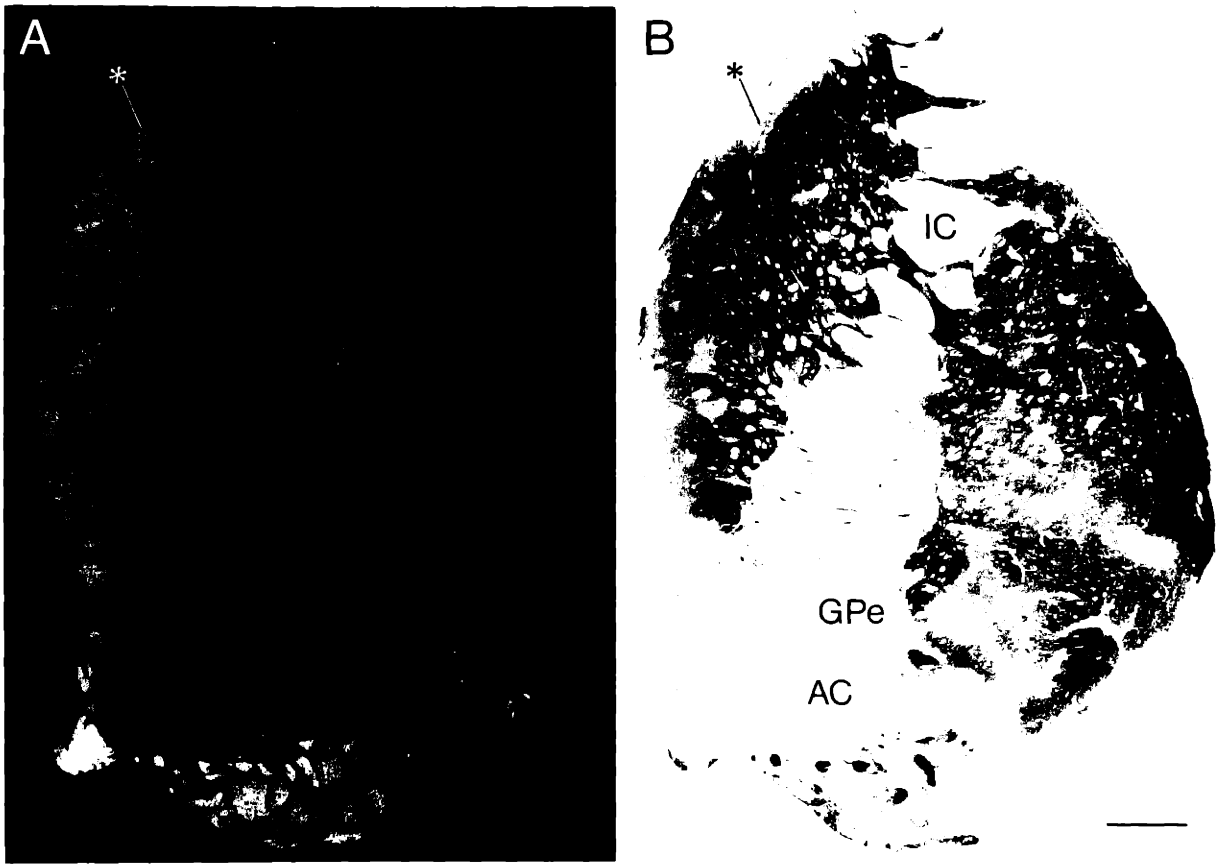
A
*
B
*
IC
GPe
AC

Figure 3-8: Darkfield photographs showing muscarinic ligand binding in the ventral striatum of the cat (A, A') and cynomolgus monkey (B, B'). Serial pairs of sections are shown for each species; M1 binding is depicted in A and B, and M2 binding is shown in A' and B'. Inhomogeneities are present for both M1 and M2 binding. Islands of Calleja are prominently labeled in the monkey for both M1 and M2 binding. The insula major of Calleja (see asterisks) in both species is notable because it is particularly sparse in M1 binding, though a zone within it contains very dense M2 binding. Scale bar = 1mm (A,A') and 1mm (B,B').

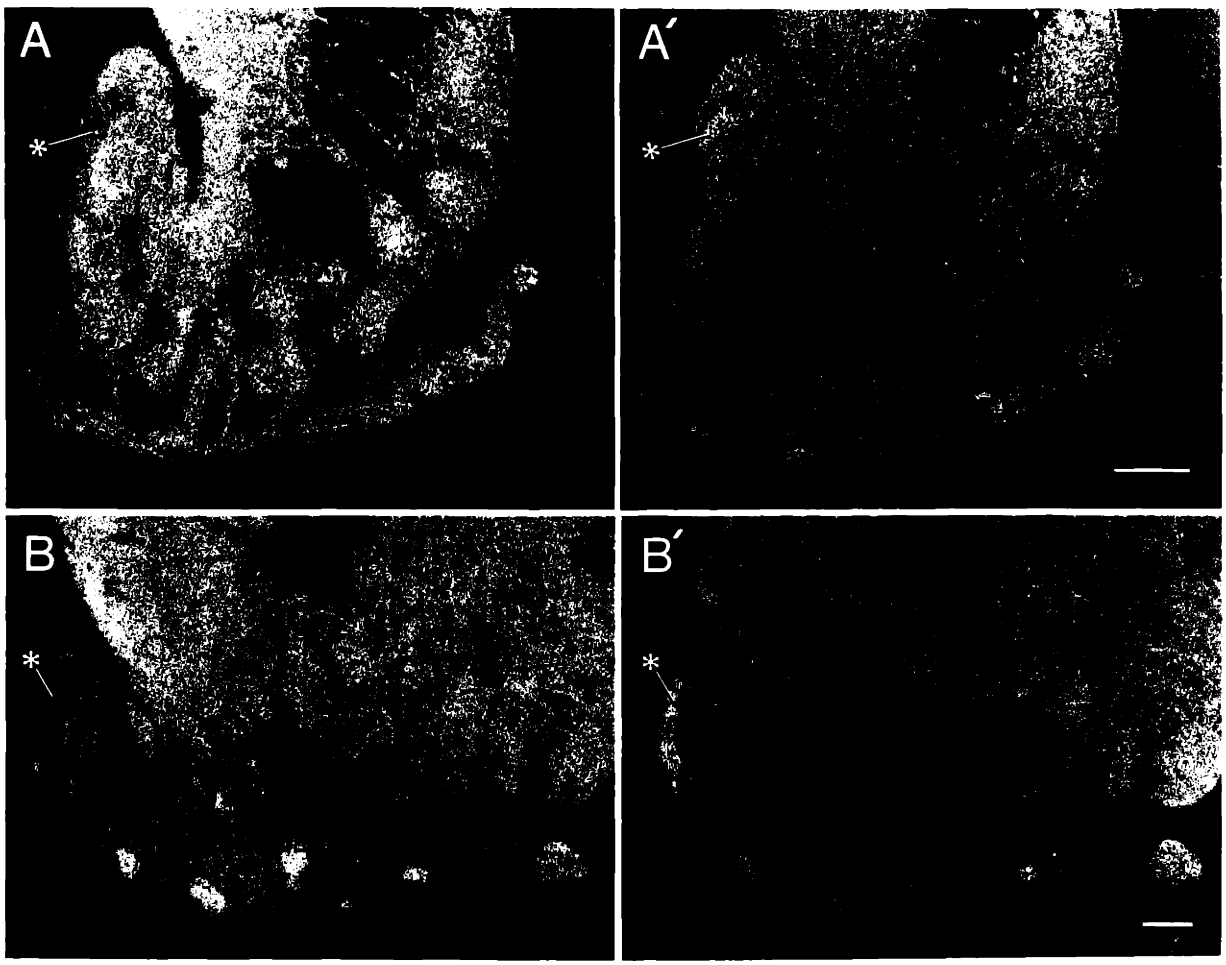
A
A′
B
B′

Figure 3-9: A comparison of M1 binding (A, darkfield), AChE staining (B, lightfield) and M2 binding (C, darkfield) in serial sections through the ventral striatum of the human. All three labeling patterns are intricate, showing instances of heavily and lightly labeled patches that are not always on complete register. Patches of dense M2 binding stand out particularly well against a surround of sparser binding. Scale bar = 3mm (A, B and C at same magnification).

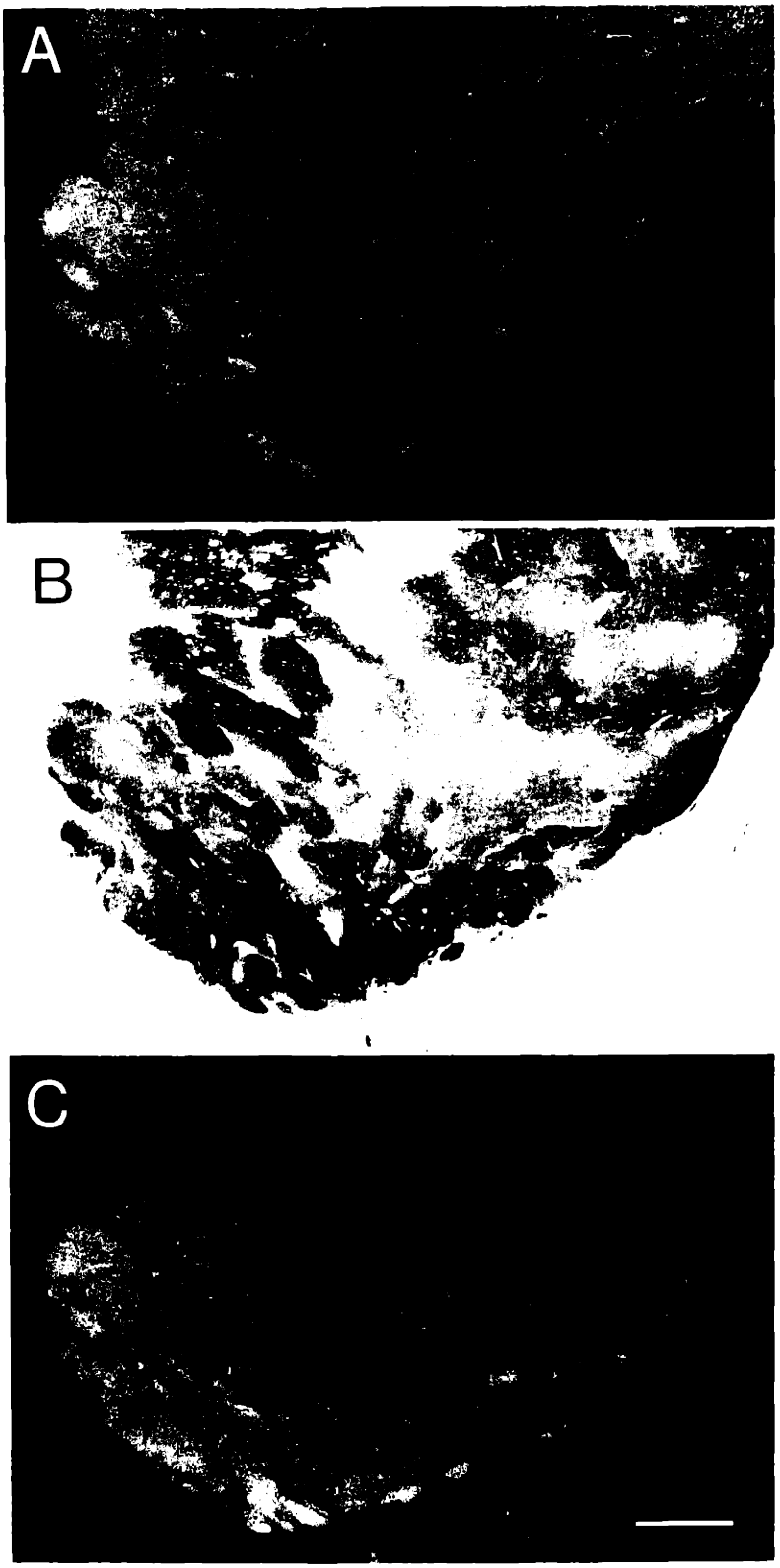
A
B
C

1978; Hammer et al., 1980; Hammer and Giachetti, 1982; Watson et al., 1983; Yamamura et al., 1983; Luthin and Wolfe, 1985). The B_{max} for nonselective [^{3}H]-NMS binding to striatal tissue was not greater than that for high affinity [^{3}H]-PZ binding. Cortes et al. (1986), who reported a similar discrepancy for B_{max} values, suggested that the problem may arise from an underestimation of the K_d for high affinity [^{3}H]-PZ binding. However, another possible explanation may reside in our finding that [^{3}H]-NMS sticks to glass fairly readily. Thus, values for total bound [^{3}H]-NMS could be erroneously low when tissue samples, which contain relatively small amounts of the ligand, are placed in glass scintillation vials for counting.

The competition between PZ and [^{3}H]-NMS for binding to striatal muscarinic sites in the cat yielded a curve that was best fit to a two-site model in which M1 sites were much more abundant than M2 sites. The autoradiography supported this in that longer exposure times were necessary to obtain appreciable striatal M2 labeling than were required for M1 labeling. However, the autoradiographic findings also demonstrate especially concentrated M2 sites in certain regions of the ventral striatum. This indicates that, although M1 binding sites are generally viewed as predominating in the striatum (and certainly they do in the dorsal striatum in our material), striatal M2 sites are also likely to be of importance, and in particular may be of unique importance in the ventral striatum. This may be of relevance in the case of clinical syndromes such as Alzheimer's disease that include degenerative changes in the basal forebrain.

Our autoradiographic analysis shows that for a range of mammalian species, subtypes of striatal muscarinic cholinergic binding sites have different anatomical distributions. Local concentrations of M1 binding correspond to the striosomal compartments inherent to the dorsal striatum, whereas the distribution of M2

binding sites is nearly uniform except in the olfactory tubercle and nucleus accumbens. Even in the ventral striatum where both subtypes have heterogeneous distributions, their density profiles are not fully matched, and in some sections appear inverse.

Functional meaning of different striatal M1 and M2 binding distributions. The present findings may prove critical for understanding the spectrum of cholinergic function in the striatum. First, the spatial distributions of muscarinic binding sites, where heterogeneous, are aligned with the compartmental arrangement characterizing almost all known connections and neurotransmitter-related markers in the striatum, including other cholinergic markers. Second, because the receptors thought to be represented by the M1 and M2 binding are likely to have distinct cellular functions and to be located on different cellular elements, the nature of cholinergic receptor function in the striosomal and matrix compartments may differ. This means that, depending upon their location in striosomes or matrix, certain striatal pathways and neurotransmitter systems could be affected in unique ways by M1 and M2 muscarinic stimulation or inhibition.

It is reasonable to ask whether all the binding sites that are made visible in an autoradiographic study would be functional under physiological conditions. To obtain direct evidence linking the observed macroscopic heterogeneity of striatal muscarinic binding sites with true functional heterogeneity is not yet possible given the presently available experimental approaches. However, a wide variety of cellular effects has been ascribed to muscarinic receptor activation in the striatum, including changes in the spontaneous and evoked release of acetylcholine and dopamine (see Chesselet 1984), inhibition of adenylate cyclase (Olianas et al., 1983a), and enhancement of phosphatidylinositol turnover (see Fisher and Agranoff 1987). Subtype-selective muscarinic stimulation results in discrete

electrophysiological effects that have not yet been characterized in striatal tissue but that include both inhibition (M2) and slow excitation (M1) of cortical pyramidal cells (McCormick and Prince, 1985) as well as hyperpolarization of cells in the parabrachial nucleus (Egan and North, 1986) and the reticular nucleus of the thalamus (McCormick and Prince, 1986) with a resultant increase in membrane potassium conductance. Further analysis of muscarinic receptor function in the striatum should take into account the distinctions in anatomical distribution of M1 and M2 binding sites.

Muscarinic binding sites in relation to cholinergic neurons and neuropil. Markers for the striatal cholinergic system other than muscarinic binding sites also exhibit macroscopic heterogeneity. Acetylcholinesterase staining, choline acetyltransferase (ChAT)-positive cells (Graybiel et al., 1983) and neuropil (Graybiel et al., 1987a), and choline uptake sites (Lowenstein et al., 1986) are all distributed more densely in the extrastriosomal matrix than in striosomes. These distributions are in direct contrast to that of M1 binding sites (which show the reverse compartmentalization), and differ also from the largely uniform M2 binding site distribution.

These discrepancies suggest that although cholinergic cell bodies and processes are concentrated outside striosomes, either cholinoceptive cell bodies and processes are more concentrated in striosomes than in matrix, or the striosomal cholinoceptive elements maintain greater densities of muscarinic receptors than do cholinoceptive elements found in the matrix. For the subset of muscarinic receptors termed autoreceptors, the second explanation is more likely to hold since such receptors would be found on cholinergic neurons themselves, and ChAT-like immunoreactivity is sparse in striosomes (although it cannot be discounted that cholinergic processes within striosomes merely may express lower levels of ChAT

than do those in the matrix). Pharmacological evidence obtained from acetylcholine release studies (James and Cubeddu, 1987) indicates that striatal muscarinic autoreceptors in the rabbit may be of the M2 subtype, though M2 receptors may well subserve other functions in this tissue, and there may also be more than one kind of M2 receptor in the brain (Hammer et al., 1986). It will be necessary to accumulate more evidence of the type that has been found in the cortex (Raiteri et al., 1984; Mash et al., 1985; Meyer and Otero, 1985) to show whether some or all striatal M2 receptors are presynaptic. The present autoradiographic results cannot distinguish autoreceptors from among the entire pool of striatal muscarinic receptors (which may include spare receptors lacking function); but it is an interesting possibility nonetheless that differing distributions of autoreceptors in striosomes and matrix could provide for differential and perhaps compartmentalized self-regulation of acetylcholine release across the striatum. More generally it may be the case that greater numbers of muscarinic receptors are required within striosomes, where, judging from ChAT immunoreactivity, less acetylcholine seems to be available. Higher densities of receptors there could serve as a form of local amplification of cholinergic transmission.

Muscarinic binding and the nigrostriatal dopamine-containing innervation. Several studies have shown that muscarinic agonists can facilitate the release of dopamine from nigrostriatal terminals, presumably through presynaptic action (see Chesselet 1984). It has been suggested also that cholinergic augmentation of striatal dopamine release may be mediated by the M1 muscarinic receptor (Raiteri et al., 1984; deBelleroche and Gardiner, 1985). If so, then striosomes may represent sites where such an effect preferentially occurs. Quite another level of interaction between the two systems has been proposed with the

suggestion that dopamine itself can regulate the affinity of striatal muscarinic receptors (Ehlert et al., 1981). Interactions such as this between the two neurotransmitter systems may be governed at least in part by the compartmentalization of striatal muscarinic receptors. In addition, many lines of evidence indicate that the nigrostriatal dopaminergic system also obeys striosomal ordering. Tyrosine hydroxylase-like immunoreactivity is more concentrated in the extrastriosomal matrix than in striosomes in both human (Graybiel et al., 1987b) and cat (Newman-Gage and Graybiel, 1988). In the rat, fibers labeled by [^{3}H]-dopamine uptake are concentrated in patches (Doucet et al., 1986), and islandic dopamine-containing fibers may have lower rates of dopamine turnover than do fibers in the matrix (Olson et al., 1972). Such compartmentalization may be related to differences in the sites of origin of mesostriatal fibers innervating striosomes and matrix (Jiminez-Castellanos and Graybiel, 1985, 1986, 1987a). There is now also evidence that striatal dopaminergic binding sites are ordered striosomally. Dopaminergic binding sites of the D2 type are distributed more densely in the extrastriosomal matrix (Joyce et al., 1986; Loopuijt et al., 1987) whereas D1 binding sites are more concentrated in striosomes (Besson et al., 1987). The above findings, taken together with the present observations, suggest that a functional parallel exists at a macroscopic level between the striatal dopamine and acetylcholine systems: for both, neurotransmitter availability as well as action may differ with location in striosomes or matrix.

At a molecular level, striatal dopamine and acetylcholine receptors may be linked through mutual coupling of certain receptor subtypes to adenylate cyclase. There is evidence that in the striatum of the rat, enhancement of adenylate cyclase activity by dopamine can be inhibited by muscarinic receptor stimulation, and coupling of both neurotransmitter receptors to the same domain of adenylate

cyclase has been proposed as a mechanism for this interaction (Olianas et al., 1983b). It is thought that the D1 subtype of dopamine receptor is involved in this phenomenon (Kelly and Nahorski, 1986). A possible subtype for the muscarinic receptor in question has not yet been identified. Based on studies of the pharmacology of pirenzepine in the rat brain, however, it has been suggested that low-affinity pirenzepine binding sites may mediate muscarinic inhibition of adenylate cyclase activity. By contrast, high-affinity pirenzepine binding sites may be responsible for muscarinic enhancement of the breakdown of phosphatidylinositol, another important second messenger system (Gil and Wolfe, 1985). Though it is generally far from clear that for all tissue, the same muscarinic receptor subtype is necessarily always linked to the same second messenger system (Harden et al., 1986; Ashkenazi et al., 1987), differential effector coupling of M1 and M2 receptors in the striatum would provide for topographically distinct actions of acetylcholine there. If such a spatial distinction among striatal muscarinic receptors exists at the level of second messenger systems, then it might provide for the compartmentalization of at least some sequelae of cholinergic receptor activation, including changes in intracellular calcium levels and alterations in neurotransmitter release.

Compartmentalization of cholinergic function in the striatum. Modulation of neurotransmitter release and receptor affinity, as well as direct or indirect action on ion channels and second messenger systems, could be expected to lead to changes in the electrical activity of single neurons or collective groups of neurons. If striatal M1 and M2 receptors involved in such effects act and are acted upon in distinct ways, then their differing anatomical distributions might provide a substrate for trans-striatal sorting of information flow as it is represented by local perturbations in electrical activity. Such alterations, if present, would likely be

subtle because the striatum is well known to be electrically quiescent; but in the face of such quiescence, even small changes in electrical activity could be expected to assume greater relative importance as signalling mechanisms. The inhomogeneities in density of muscarinic binding site subtypes, as well as of other binding sites found in the striatum (Herkenham and Pert, 1981; Goedert et al., 1984; Moskowitz and Goodman, 1984; Faull and Villiger, 1986; Joyce et al., 1986; Besson et al., 1987), raise the possibility that variations in physiological activity are spatially as well as temporally ordered within the striatum, perhaps with respect to its striosomal compartmentalization.

The present findings indicate that compartmentalization may critically effect receptor-mediated function of the striatal cholinergic system at levels ranging from molecular to macroscopic. At the molecular level, muscarinic receptors serve as part of the linkage between the binding of acetylcholine and subsequent local membrane effects mediated by various ion channels. At the cellular level, muscarinic receptors mediate events such as changes in levels of cytosolic calcium and in the dynamics of neurotransmitter release. Macroscopically, by virtue of their distributions, at least some muscarinic receptors are in a position to exert different molecular and cellular effects on groups of neurons depending upon the locations of these cells relative to striosomes. Muscarinic receptor activation occurring in striosomes may have profoundly different effects on neuronal communication than that occurring extrastriosomally or at the borders separating striatal compartments.

Chapter 4

Ontogeny of M1 and M2 Muscarinic Binding Sites in the Striatum of the Cat: Relationships to One Another and to Striatal Compartmentalization

ABSTRACT

The ontogeny of striatal M1 and M2 muscarinic cholinergic binding sites was studied with autoradiographic localization in cats ranging in age from embryonic day 40 to postnatal day six. Direct labeling with [^{3}H]-pirenzepine revealed M1 sites, and M2 sites were labeled with [^{3}H]-N-methylscopolamine in the presence of pirenzepine. In serial tissue sections, distributions of striatal M1 and M2 sites were compared to one another and to patterns of acetylcholinesterase staining and tyrosine hydroxylase-like immunoreactivity.

In the younger fetal material both subtypes of muscarinic binding sites demonstrated heterogeneous distributions, with patches of dense binding corresponding to islands of dopaminergic nigrostriatal innervation. For both M1 and M2 binding, lateral to medial and caudal to rostral density gradients were observed in the patches and in the surrounding matrix. During fetal development and into the perinatal period, overall binding increased, but more so in the matrix than in the patches. Thus, by postnatal day six striatal M2 binding appeared nearly homogeneous. M1 binding, however, was still slightly more concentrated in patches than in matrix. At maturity, the patches of elevated M1 binding proved to correspond to striosomes. These findings suggest that the ontogenetic regulation of muscarinic binding sites is influenced by location relative to striatal compartments, and that expression of M1 and M2 binding site subtypes is differentially regulated.

INTRODUCTION

The compartmental organization of the mammalian striatum is a relatively early developmental landmark that undergoes ontogenetic modification but persists to adulthood. Nigrostriatal dopaminergic fibers initially have uniform terminal fields but during early fetal development these afferents come to be arranged in an islandic pattern (Olson et al., 1972; Tennyson et al., 1972; Specht et al., 1981a; Moon Edley and Herkenham, 1984; Newman-Gage and Graybiel, 1988). Afferents from the cortex have been observed to change from a homogeneous to a patterned striatal distribution during gestation (Goldman-Rakic, 1981). Striatal neurogenesis is also spatially constrained for some neuronal types, with early-born medium sized neurons forming patches and later-born medium sized neurons filling in the matrix around the patches (Angevine and McConnell, 1974; Brand and Rakic, 1979; Donkelaar and Derderen, 1979; Graybiel and Hickey, 1982; Marchand and Lajoie, 1986; van der Kooy and Fishell, 1987).

An important issue in striatal development concerns the relative contributions of extrinsic and intrinsic elements in pattern formation, and several investigators have worked to clarify this issue (Fishell and van der Kooy, 1987; Foster et al., 1987; Johnston et al., 1987; Newman-Gage and Graybiel, 1988). Equally important, however, are questions concerning the ways in which particular groups of striatal neurons are regulated with respect to the production of neurotransmitter-related molecules. Such questions apply not only to the stage of early island formation but also to the perinatal period when further changes occur. For example, during the first postnatal weeks the distribution of μ opiate receptors is transformed from uniform to patchy (Kent et al., 1982; Moon Edley and

Herkenham, 1984; Murrin and Ferrer, 1984). At this time patterns of striatal acetylcholinesterase (AChE) staining and tyrosine hydroxylase-like immunoreactivity (TH-like immunoreactivity) go through a complicated conversion: islands of heavy marker in a light surround become the palely labeled zones known as striosomes arranged upon a dark matrix (Graybiel, 1984b).

In an attempt to better understand the developmental regulation of an important molecule in the striatal cholinergic system, the muscarinic cholinergic receptor, this study charts the changing distributions of M1 and M2 muscarinic binding sites as compared to patterns of AChE staining and TH-like immunoreactivity in fetal cats and kittens. It has been previously shown that striatal muscarinic binding sites labeled with the antagonist [^{3}H]-propylbenzilylcholine mustard have patchy distributions in fetal tissue and are close to uniform in array at maturity (Rotter et al., 1979a; Nastuk and Graybiel, 1985); however, these studies did not include separate consideration of muscarinic receptor subtypes. Biochemical studies have suggested independent ontogenetic schedules for the expression of muscarinic receptor subtypes in the brain of the rat (Kuhar et al., 1980), although anatomical localization was not performed. A recent report has provided indirect autoradiographic evidence that M1 and M2 muscarinic binding sites have differing distributions during postnatal development of the rat's brain, but the only change noted for the caudoputamen was an age-related increase in total and M1 binding (Miyoshi et al., 1987). It is clear that no single study has yet considered the developmental rates of M1 and M2 binding site populations while also following possible changes in their macroscopic arrangement in the striatum.

For this investigation, the distributions of striatal M1 and M2 sites were observed in cats ranging in age from mid-fetal to early postnatal. The

distributions of the two subtypes were initially similar: both were concentrated in patches corresponding to dopamine islands. Perinatally, differences arose such that M2 binding sites became close to uniform in distribution and M1 binding sites retained especial denseness within the striosomal compartment. These findings suggest that striatal M1 and M2 binding sites follow related but distinct schedules of ontogenetic regulation.

METHODS

For these experiments, muscarinic ligand binding assays and autoradiographic distributions were studied in striatal tissue sections from six fetal cats, three kittens and six adult cats. The fetal cats ranged in age from embryonic day 40 (E40) to E58 of a 65-day gestation period. Fetuses were obtained by sterile laparotomy from timed-pregnant cats that had been bred in an in-house colony. Immediately following delivery of the fetuses, their brains were removed and quickly frozen in crushed dry ice. Kittens and cats were deeply anesthetized with Nembutal prior to removal and freezing of brains. For biochemical experiments, selected adult brains were hemisected before freezing, and once mounted on cryostat chucks the tissue was trimmed to make a rectangular block face with its edges as close as possible to the borders of the striatum. Coronal cryostat sections were cut at a temperature of -12°C to -14°C; section thickness was 15 μm for autoradiography and histochemistry or 10 μm for binding assays. Sections for binding assays were taken from mid-rostral striatal levels, where rostro-caudal variability in cross-sectional area was minimal. Sections were thaw-mounted onto gelatin-coated slides and were processed for muscarinic ligand binding autoradiography, AChE histochemistry by a modified Geneser-Jensen and Blackstad protocol (Geneser-Jensen and Blackstad,

1971), Nissl staining, immunohistochemistry for TH, or for binding assays. All sections to be processed for ligand binding were thaw-mounted then placed temporarily into racks kept at 4°C; filled racks were kept under vacuum at 0°C for 2-4 hours in a vacuum desiccator buried in crushed ice and containing Drierite capsules. Slides were stored at -20°C in sealed boxes containing Drierite for at least two weeks before further processing (Lewis et al., 1982).

For ligand binding autoradiography, it was necessary that fetal and kitten material be lightly postfixed for 15 minutes in 0.05% glutaraldehyde in 50mM sodium phosphate buffer at 4°C prior to incubation. This served to minimize tissue loss from slides (binding assays, described below, were performed in parallel with fixed and unfixed adult tissue sections). Sections were then preincubated in 50mM sodium phosphate ($NaHPO_4$) buffer at pH 7.4 containing 10mM ethylenediaminetetraacetic acid (EDTA) and 0.1mM N-ethylmaleimide (NEM) for 15 minutes at 4°C to uncouple binding of endogenous agonist without affecting antagonist binding (Potter et al., 1984). Incubations were carried out for one hour at room temperature in 50mM $NaHPO_4$ buffer containing 1mM EDTA and either 10nM [^{3}H]-pirenzepine ([^{3}H]-PZ; 76.0 Ci/mmol, New England Nuclear) for M1 binding or 0.3nM [^{3}H]-N-methylscopolamine ([^{3}H]-NMS; 85.0 Ci/mmol, New England Nuclear) and 100 nM unlabeled PZ (gift of R. Hammer) for M2 binding. This concentration of PZ was chosen to occlude as many M1 sites (K_d ca. 10nM) as possible while leaving most M2 sites (K_d ca. 600nM) free for labeling. For blanks, 1μM atropine was added to the incubation solution. To terminate binding, the sections were immersed for five minutes in chilled (4°C) 50mM $NaHPO_4$ buffer containing 1mM EDTA. Two very brief rinses in distilled water at 4°C followed, and the sections were then dried under a stream of cool air. Slides were apposed to LKB or Amersham tritium-sensitive film for 12 to 29 days at room temperature.

Films were developed in Kodak D19 for four minutes at 20°C then fixed in Kodak rapid fixer. Serial section comparisons were made among M1 and M2 binding distributions, AChE staining, TH-like immunoreactivity and Nissl staining.

For direct binding assays, fixed or unfixed sections from trimmed striatal blocks were preincubated under the same conditions as were sections for autoradiography. In triplicate or quadruplicate, sections were then incubated in various concentrations of [^{3}H]-PZ or [^{3}H]-NMS (under the same conditions as for autoradiography) with or without 1μM atropine. Concentrations of [^{3}H]-PZ ranged from 0.3nM to 50nM, and [^{3}H]-NMS concentrations ranged from 0.03nM to 30nM. Following binding termination and rinsing, sections were dried and scraped off slides, and were placed individually into scintillation vials. One ml of Protosol (New England Nuclear) was added to each vial, and the vials were capped and left overnight at 4°C. A few hours prior to counting in a liquid scintillation counter, 0.1ml of 30% hydrogen peroxide (to prevent coloration) was added to each vial, followed by 10 ml of Betafluor (National Diagnostics). Specific and nonspecific binding were calculated from counts, and the Lowry method (1951) was applied to estimate the amount of protein per section. Binding curves were plotted and Scatchard analysis was performed for the binding of each of the two ligands to the fixed or unfixed tissue. Linear regression analysis with the RS1 statistics program was applied for both nonspecific binding curves and Scatchard plots.

For competition experiments, the same procedures were followed as for direct binding assays except that the incubation solutions contained 0.3nM [^{3}H]-NMS and concentrations of PZ ranging from 0.1nM to 10μM. Nonspecific binding of [^{3}H]-NMS was determined in the presence of 1μM atropine. Counts were expressed as percent occupancy, with 100% being the specific counts in the absence of any displacer. Points for competition curves generated with fixed and unfixed tissue

were plotted from the resulting counts. Hill plots were constructed from the occupancy concentration data, and Hill coefficients were calculated.

Sections to be stained for TH-like immunoreactivity yielded the crispest staining if they were dried under cool air immediately after thaw-mounting. Dried sections were returned to racks in the cryostat chamber, then were transferred to boxes stored at -20°C until further processing. Tissue was postfixed for one hour in a solution of 0.9% saline in 0.1M phosphate buffer containing 4% paraformaldehyde, then washed twice in a 0.9% saline solution in 0.1M Tris buffer. On-slide immunohistochemistry was carried out with antibody against TH (diluted 1:500) kindly provided by Dr. Tong Joh. Immunostaining was identified with the peroxidase-antiperoxidase method.

RESULTS

Striatal muscarinic binding of both the M1 and M2 subtypes was observed in the striatum of the cat at all the ages included in this study; in fact, relative to other brain regions the striatum was always notable for particularly dense binding. Light postfixation of adult striatal tissue sections in buffered 0.05% glutaraldehyde did not lead to significant elevations in nonspecific binding for either [^{3}H]-PZ or [^{3}H]-NMS, as Figs. 1 and 2 (top) show. Neither were the K_d values for either ligand (assessed by Scatchard analysis, Figs. 1 and 2, bottom) changed appreciably. [^{3}H]-PZ bound to M1 sites in unfixed tissue with a K_d of 8.9 nM, and to M1 sites in fixed tissue with a K_d of 12.2 nM. The K_d for [^{3}H]-NMS binding to muscarinic sites in unfixed tissue was 0.47 nM; for fixed tissue this value was 0.26 nM. The competition curves in Fig. 3 show that glutaraldehyde fixation did not change PZ's ability to compete with [^{3}H]-NMS binding to more than one population of striatal

muscarinic binding sites. The Hill coefficient for fixed tissue was 0.40 as compared to a value of 0.44 for unfixed tissue.

Autoradiograms of developing M1 and M2 muscarinic binding distributions revealed that with age there was an overall increase in the density of striatal M1 and M2 sites. The increase was not quantified, but was seen qualitatively when tissue sections from animals at ages E40 to adult were apposed against the same piece of tritium-sensitive film. In addition to this temporal gradient for muscarinic binding, spatial gradients that were most notable prenatally were seen along the mediolateral and rostrocaudal axes of the striatum. Thus, M1 and M2 binding in a given coronal section were both usually densest in the putamen and lateral caudate nucleus, and across a number of such sections muscarinic binding was densest caudally.

Striatal M1 and M2 binding both demonstrated local patterning that bore a relationship to striosomal organization and that changed during development. There were certain basic similarities in the distributions of the two subtypes of binding sites, especially for the younger fetal ages studied. However, some ontogenetic differences in striatal array were also evident for M1 and M2 sites, as will be described below.

E40. As shown in Fig. 4 A and C, virtually no binding above background levels to either muscarinic subtype was present in the ganglionic eminence, which was still relatively large at this age (the labeled line in Fig. 4C indicates the ventricular edge of the ganglionic eminence). In the striatum, muscarinic binding density was greatest caudally and laterally, being concentrated in the putamen and lateral caudate nucleus. Both M1 and M2 binding sites demonstrated heterogeneous striatal distributions, with patches of dense binding that were most prominent in the mid-rostral putamen and along the lateral border of the caudate

Figure 4-1: Saturation analysis (top) of [^{3}H]-PZ binding to striatal tissue sections from the cat, postfixed in 0.05% buffered glutaraldehyde (squares) and unfixed (circles). Specific binding (filled symbols) is the difference between total binding and nonspecific binding. Nonspecific binding (open symbols) was determined in the presence of 1 μM atropine. Each point represents the mean counts from either two or three experiments, each performed in quadruplicate (two or three animals, four sections per animal per point). Scatchard analysis of the specific binding of [^{3}H]-PZ to fixed (squares) and unfixed (circles) tissue is shown at bottom. Linear regression analysis was carried out to determine K_ds.

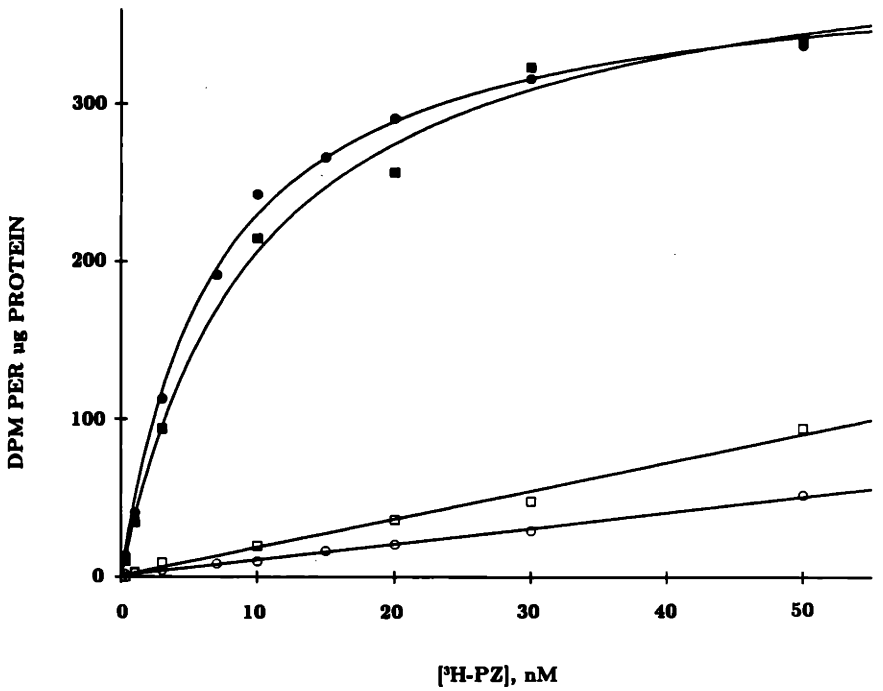
DPM PER ug PROTEIN
300
200
100
0
0
10
20
30
40
50
[3H-PZ], nM

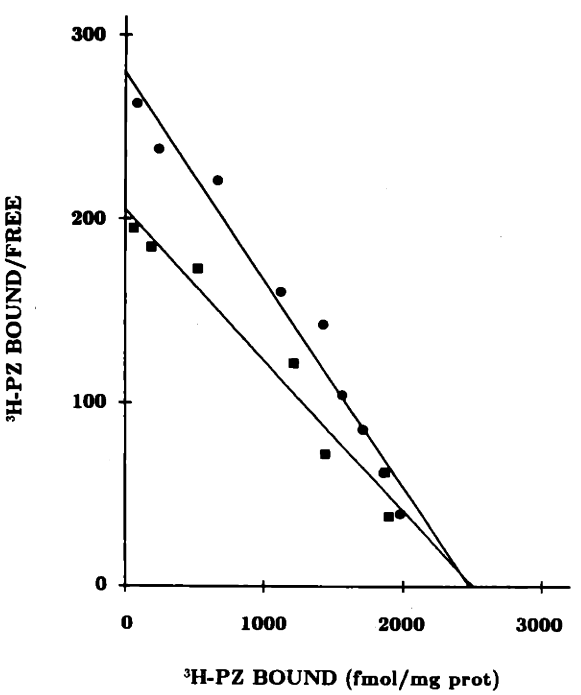
3H-PZ BOUND/FREE
300
200
100
0
0
1000
2000
3000
3H-PZ BOUND (fmol/mg prot)

Figure 4-2: Saturation analysis (top) of [^{3}H]-NMS binding to unfixed striatal sections (circles) as well as sections postfixed in 0.05% buffered glutaraldehyde (squares). Specific (filled symbols) and nonspecific (open symbols) binding was determined in the same way as for [^{3}H]-PZ. Each point represents mean values for two or three experiments, each performed in quadruplicate. Scatchard analysis (bottom) of the specific binding of [^{3}H]-NMS to fixed (squares) and unfixed (circles) tissue sections. Linear regression analysis was performed to determine K_ds.

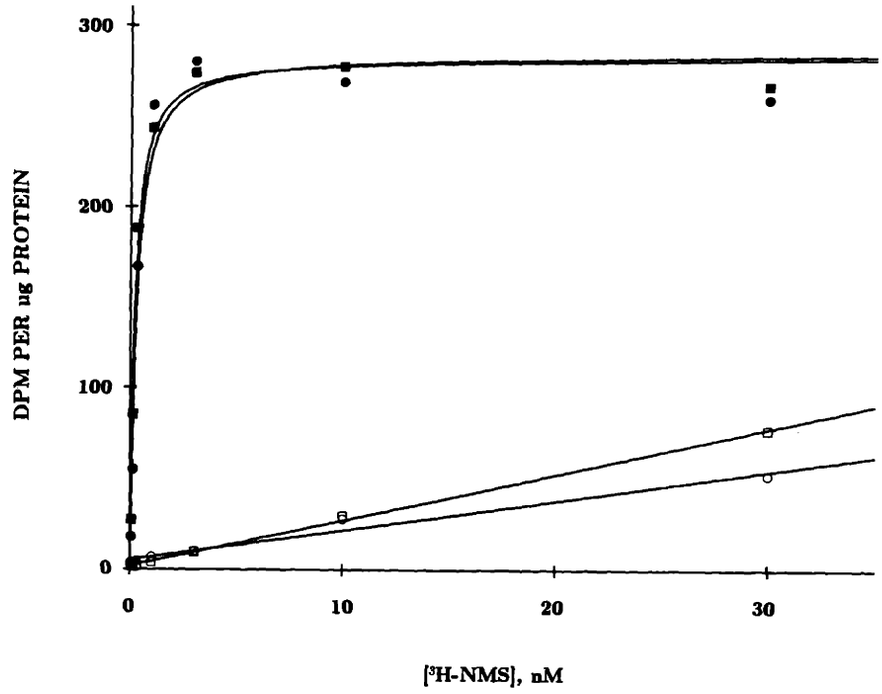
300
200
100
0
0
10
20
30
DPM PER ug PROTEIN
[3H-NMS], nM

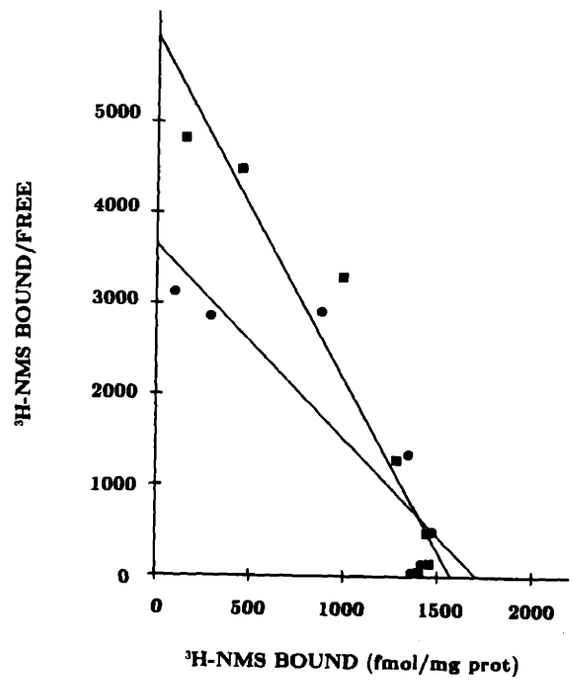
5000
4000
3000
2000
1000
0
0
500
1000
1500
2000
3H-NMS BOUND/FREE
3H-NMS BOUND (fmol/mg prot)

Figure 4-3: Competition curves for the binding of PZ to striatal tissue sections in the presence of [^{3}H]-NMS (0.3nM). Sections were postfixed in 0.05% buffered glutaraldehyde (squares) or left unfixed (circles). Concentrations of PZ ranged from 0.1nM to 10μM. Each point represents the mean percent occupancy in two or three experiments, each conducted in quadruplicate. Specific binding of [^{3}H]-NMS in the absence of displacer was taken as 100% occupancy. Curve fitting was performed with nonlinear regression analysis.

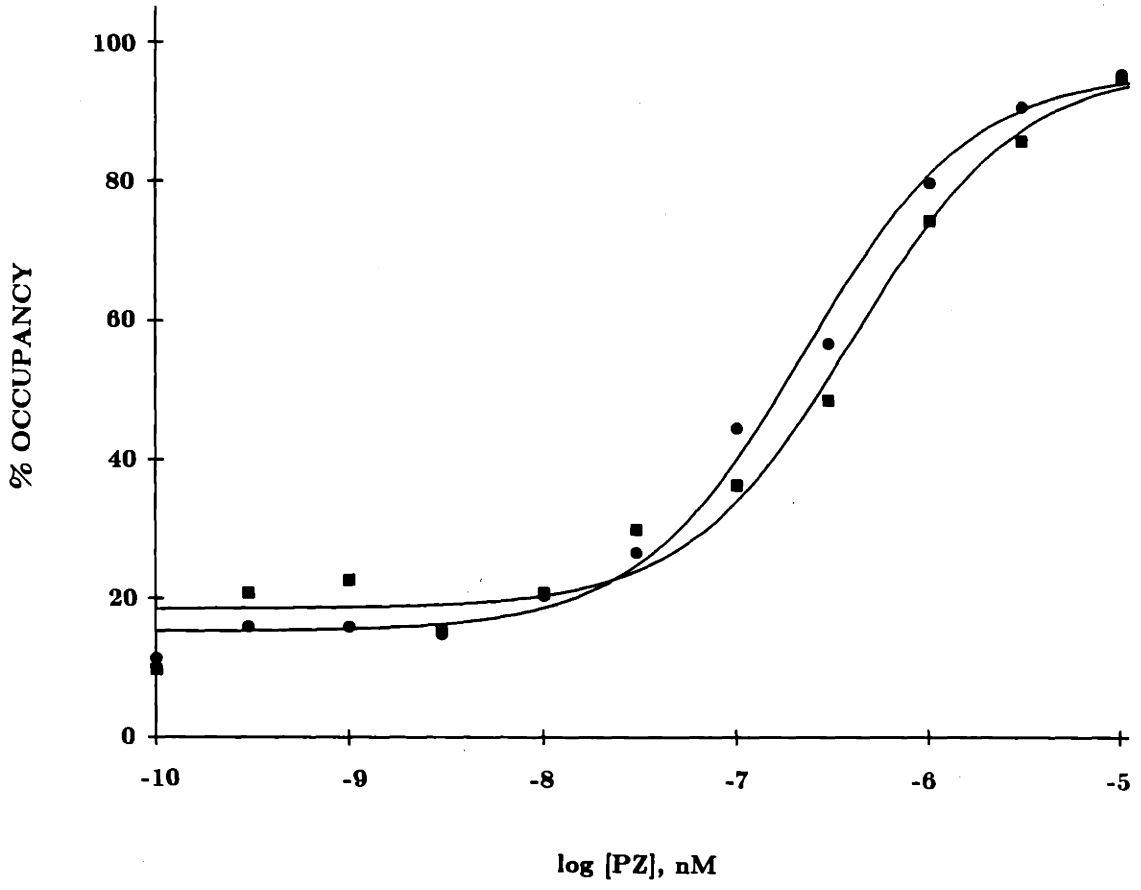
100
80
60
40
20
0
% OCCUPANCY
-10
-9
-8
-7
-6
-5
log [PZ], nM

Figure 4-4: Photographs of serial coronal sections through the striatum of a cat fetus at 40 days of gestation (E40). Acetylcholinesterase staining (A) is shown in lightfield while M1 (B) and M2 (C) muscarinic binding are shown in darkfield. For darkfield photographs, areas rich in binding sites appear lighter than areas of sparse binding. Asterisks indicate an area of dense M1 binding corresponding to an AChE-rich patch in the dorsolateral caudate nucleus. This patch is not obvious in the M2 binding autoradiogram, although zones of dense M2 binding are present in the putamen. CN: caudate nucleus, P: putamen, GE: ganglionic eminence (line indicates its ventricular edge). Scale bar = 0.5mm (A, B and C at same magnification).

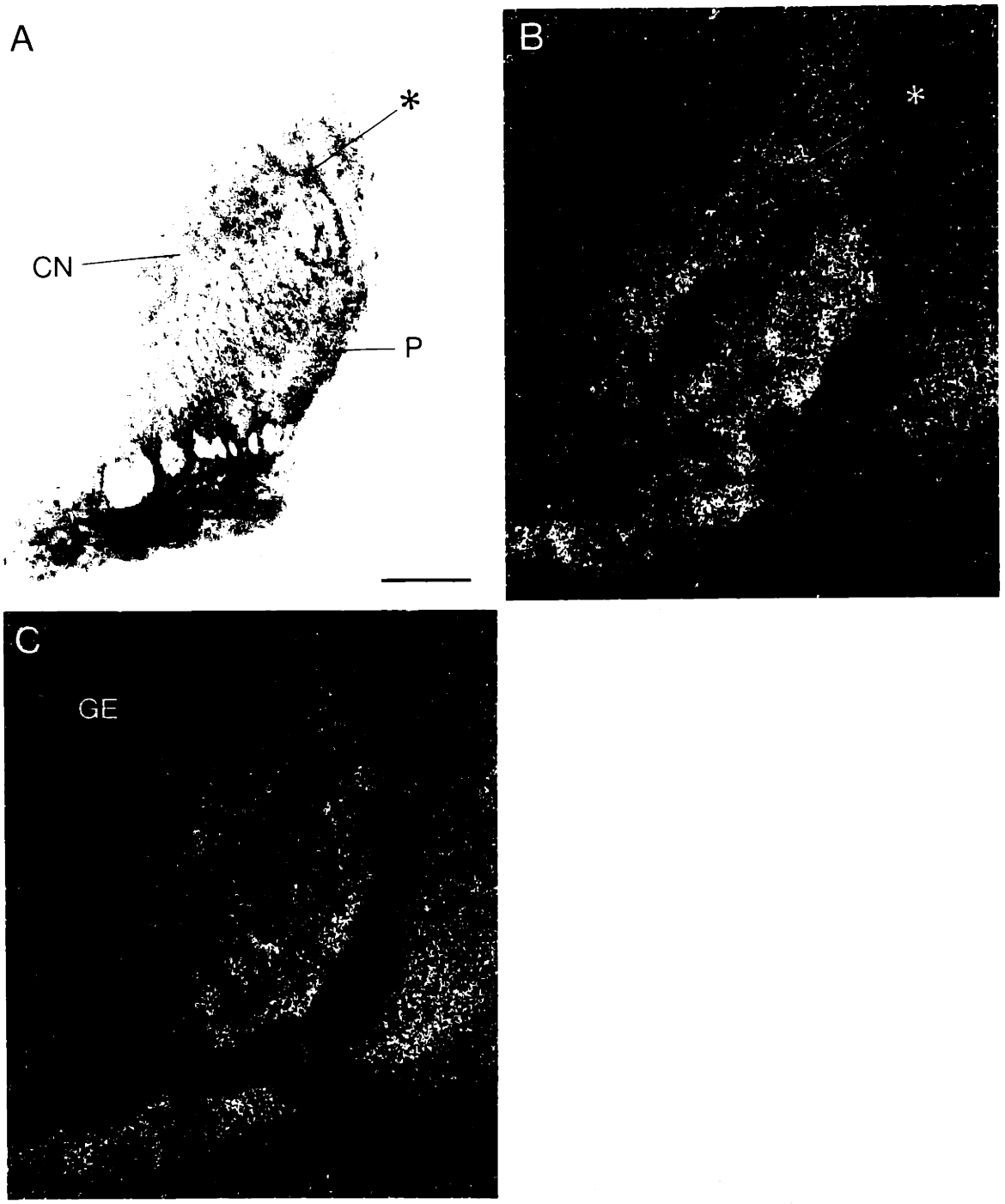
A
*
CN
P
B
*
C
GE

nucleus. Fewer and smaller patches were seen caudally where the cross-sectional area of the striatum was smaller. The olfactory tubercle and ventral region of the caudal nucleus accumbens contained ill-defined dense and sparse zones of M1 and M2 binding. For these ventral regions as well as in the dorsal striatum, M1 densities stood out better against the surrounding matrix than did zones of dense M2 binding. The asterisk in Fig. 4B shows such a patch in the dorsal caudate nucleus, clear in the M1 but not the M2 autoradiogram. Another distinction between the two binding site distributions was seen in the septum, which contained moderate M2 binding but little or no M1 binding.

At E40, AChE staining (Fig. 4A) and TH-like immunoreactivity (not shown) in the dorsal striatum both were concentrated in islands that were in register with the zones of elevated muscarinic binding density (see asterisks). Staining of these patches was also most intense in the lateral caudate nucleus and the putamen. However, AChE-rich patches often were less pronounced than receptor-dense zones in the putamen as Fig. 4 shows for both M1 and M2 binding.

E45. With its increasing size, the striatum also developed considerable clarity of patterning for M1 and M2 muscarinic binding (Fig. 5B and C), AChE staining (Fig. 5A) and TH-like immunoreactivity. In the dorsal caudate nucleus patches of intense labeling stood out more clearly against a matrix of paler labeling. For all markers, these patches again were in alignment with one another and were concentrated in the putamen and lateral caudate nucleus (see asterisks in Fig. 5A-C). Patches were seen at all rostrocaudal levels, although they were crispest mid-rostrally. In the ventral caudate nucleus zones of heavy and light label were present but were relatively poorly demarcated.

A mediolateral gradient of muscarinic binding density was seen within the striatal matrix surrounding the patches, and appeared more pronounced for M2

Figure 4-5: Serial sections through the striatum of a fetal cat at E45. Acetylcholinesterase staining (A, lightfield), M1 binding (B, darkfield) and M2 binding (C, darkfield) all demonstrate distinct, correlative patches of dense label (see asterisks) that are concentrated laterally in the striatum. Mediolateral gradients of labelling are present in the striatal matrix for all three markers but most markedly for M2 binding. CN: caudate nucleus, P: putamen, GE: ganglionic eminence. Scale bar = 0.5mm (A,B and C all at same magnification).

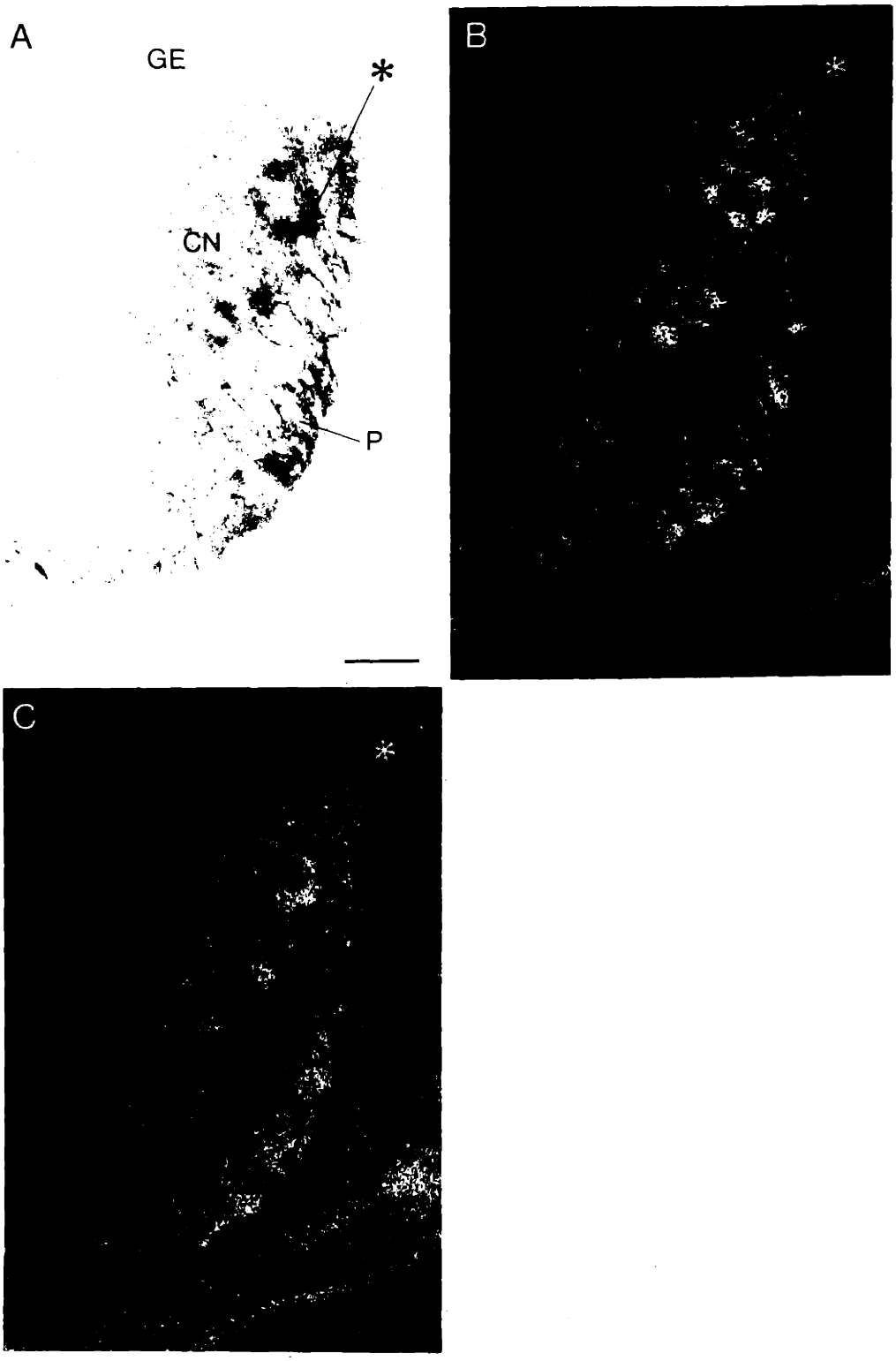
A
GE
*
CN
P
B
C
*

than for M1 binding. Both subtypes were visibly present in the lateral matrix of the caudate nucleus; medially, however, although some matrix binding was present up to the border of the ganglionic eminence for M1 sites, M2 binding there had faded to background levels (thus, the border of the ganglionic eminence could not be easily distinguished in M2 autoradiograms).

In the ventral part of the nucleus accumbens and particularly in the olfactory tubercle, M1 binding was present and patchy with zones of dense binding in the olfactory tubercle matching AChE-rich areas. M2 binding in these regions demonstrated similar heterogeneity but was less pronounced than M1 binding. Conversely, the septum contained moderate levels of M2 binding but almost no M1 binding except at its rostral tip where extremely sparse distributions of M1 sites were observed.

E53. In the dorsal caudate nucleus at this age, patches of dense M1 and M2 binding were present medially and still especially laterally. At all rostrocaudal levels, patches were more pronounced for M2 than for M1 binding (see Figs. 6A and B and 7A and B). This difference appeared to be due to a greater developmental increase in M1 matrix binding as compared to M2 matrix binding, and not due to increased M2 binding in the patches (in general striatal M2 binding was, as at all ages, less dense than M1 binding). Muscarinic binding at this age was less frankly patchy than either TH-like immunoreactivity (Fig. 6D, Fig. 7D) or AChE staining (Fig. 6C, Fig. 7C), both of which demonstrated crisp darkly staining patches against a pale matrix at all rostrocaudal levels.

Binding distributions in the ventral caudate nucleus were also heterogeneous. Patches of dense binding tended to be larger and less well defined than those found dorsally, and were often intercalated with zones of sparse binding. In the putamen, binding was densest peripherally and no longer demonstrated the degree of patchiness seen at earlier ages.

Figure 4-6: M1 binding (A, darkfield), M2 binding (B, darkfield), AChE staining (C, lightfield) and TH-like immunoreactivity (D, lightfield) in serially adjacent sections from the striatum of an E53 fetal cat. Patches of dense M2 binding are more pronounced than their M1 counterparts. For all markers, heavily labeled patches are crisper dorsally than they are ventrally in the caudate nucleus. CN: caudate nucleus, P: putamen, NA: nucleus accumbens. Scale bar = 1mm (A - D all at same magnification).

M1 and M2 binding were both now present in the dorsal as well as the ventral regions of the nucleus accumbens. Rostrally, the borders of this nucleus were easily distinguished in the M1 autoradiograms due to the sparseness of [^{3}H]-PZ binding in the adjacent septum. M2 binding also occurred in the rostral nucleus accumbens, although its density was not much greater than that in the septum. By contrast, AChE staining here was extremely faint. Farther caudal, binding of both subtypes in the nucleus accumbens was still present but was less dense than in the caudate nucleus and putamen. In some sections (not shown), heterogeneity was present in the form of a ventral curving streak of dense M1 and M2 binding. Acetylcholinesterase staining in the caudal nucleus accumbens, though still faint, was more intense than it was at rostral levels, and demonstrated complementarity to the binding distributions: rather than forming a ventral streak, the heaviest staining was concentrated in a mediodorsal rim that had no counterpart in the autoradiograms.

E58. Both M2 and particularly M1 binding were noticeably denser in the non-patch matrix of the caudate nucleus than was observed in the younger fetuses. Binding in the matrix was densest in the dorsolateral quadrant and sparsest ventrally (see Fig. 8B and C). Patches of light as well as heavy binding were visible in the dorsolateral caudate nucleus. The dense patches were often partially surrounded by rims nearly devoid of binding (and also of AChE staining), and they were still somewhat more pronounced in the M2 than the M1 autoradiograms. However, AChE (Fig. 8A) and TH (Fig. 8D) staining patterns were again the most overtly heterogeneous, demonstrating conspicuous dense patches that had less clear counterparts in the binding autoradiograms (see asterisks in Fig. 8). Nissl staining of a serially adjacent section (Fig. 8E) revealed that the marked neurochemical heterogeneity was not readily apparent in the striatum's cytoarchitecture. Some

Figure 4-7: Serial coronal sections through the striatum of the same animal shown in the previous figure, but at a caudal level. M1 (A) and M2 (B) binding, shown in darkfield, are still heterogeneous but are less frankly patchy than AChE staining (C) or TH-like immunoreactivity (D), shown in lightfield. CN: caudate nucleus, P: putamen. Scale bar = 1mm (A - D are all at same magnification).

large aggregations of cells were present (as was observed in Chapter 1), but these had no correspondents in any of the marker patterns.

In the caudal caudate nucleus, matrix staining was relatively more intense for AChE than for TH; thus, patches were best delineated in caudal sections processed for TH-like immunoreactivity. Caudal sections also demonstrated that the earlier observed mediolateral gradient of labeling across the caudate nucleus and putamen was now less obvious for M1 binding but was still noticeable for AChE staining and TH-like immunoreactivity.

The nucleus accumbens again exhibited differential patterning for muscarinic binding, AChE staining and TH-like immunoreactivity. Rostrally the nucleus accumbens contained very dense M1 binding, moderately dense M2 binding and TH-like immunoreactivity, and very pale AChE staining. With caudal progression as shown in Fig. 9C, a dorsal AChE-positive cap appeared (see arrow) that was sparse in muscarinic binding. At the same time, the previously observed ventromedial streak of dense M1 and M2 binding appeared (marked by asterisks in Fig. 9 A and B) and again had no ready counterpart in AChE staining.

P1. At this early postnatal age, patches of dense muscarinic binding (Fig. 10 B and C) were increasingly obscure and AChE staining patterns (Fig. 10A) were marbled and complex in appearance. Only TH-like immunoreactivity retained striatal patches that were clearly more heavily labeled than the surrounding matrix, itself nonetheless demonstrating staining of growing intensity. For both M1 and M2 autoradiograms it was still sometimes possible in the dorsal caudate nucleus to discern partial rims sparse in silver grains. Patches of binding with slightly elevated density relative to the surrounding matrix were often associated with such rims and were no longer necessarily more distinguishable for M2 than M1 binding (particularly in caudal sections). Comparisons between binding

Figure 4-8: Five serial sections through the striatum of a fetal cat at age E58. Both M1 (B, darkfield) and M2 (C, darkfield) binding are denser in non-patch regions than they were at earlier ages. Patches of particularly dense binding can still be discerned and matched to areas rich in AChE staining (A, lightfield) and TH-like immunoreactivity (D,lightfield). Zones of very light label are visible for all four marker patterns. Nissl staining (E, lightfield) fails to reveal heterogeneity corresponding to that seen in the other sections. CN: caudate nucleus, P: putamen, S: septum, Olf. T: olfactory tubercle. Scale bar = 1mm (A - E all at same magnification).

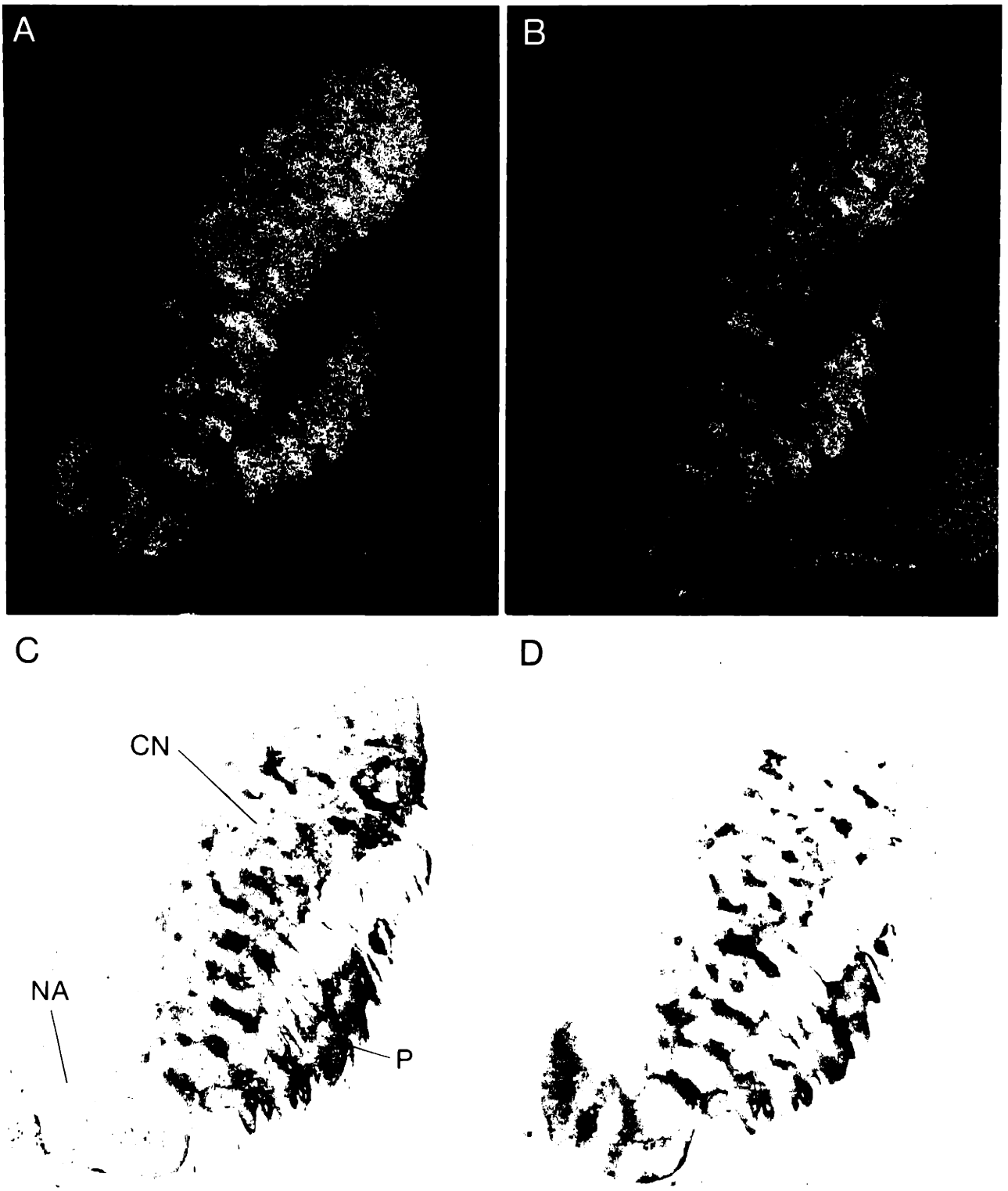
A
B
C
D
CN
NA
P

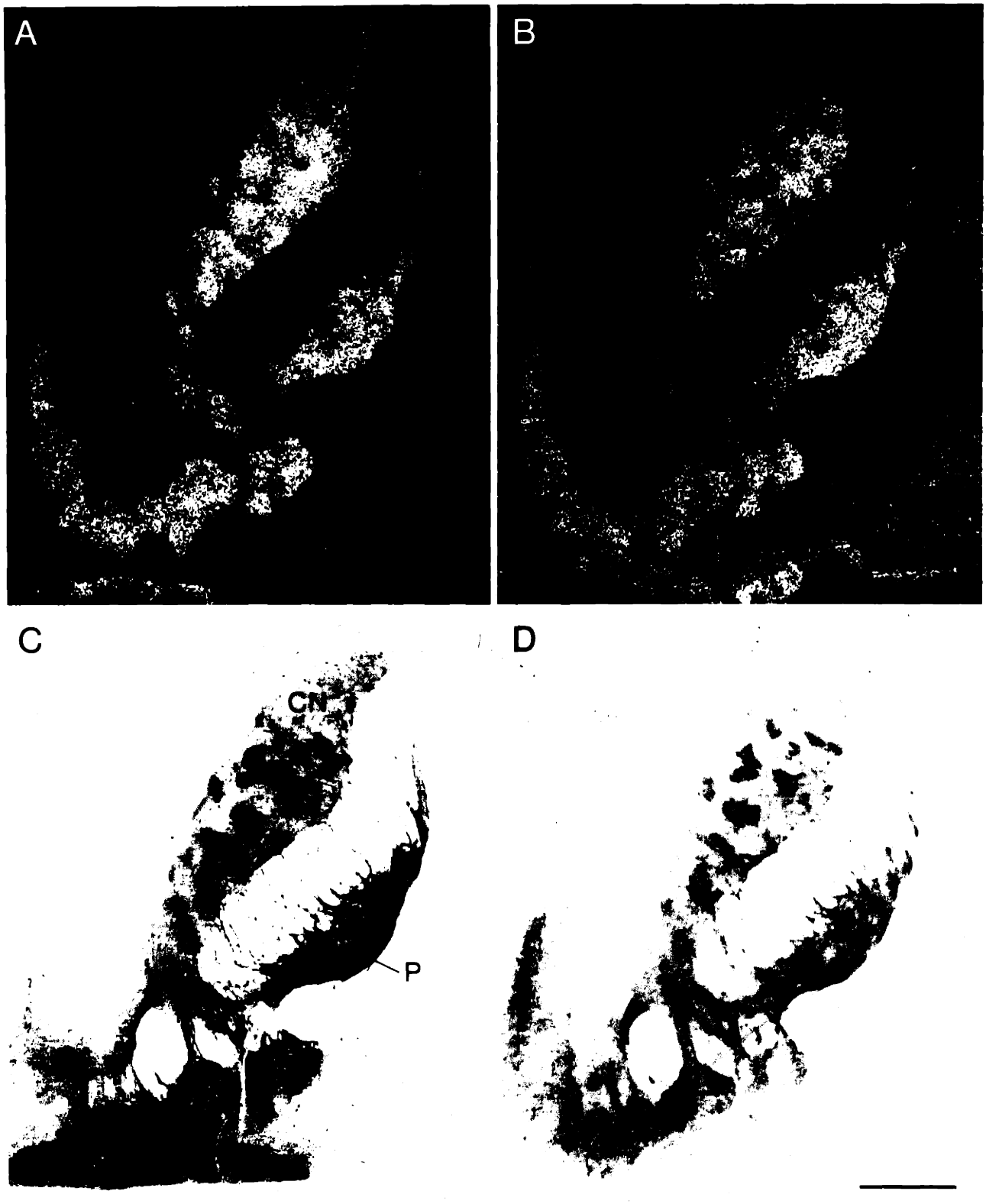
A
B
C
CN
P
D

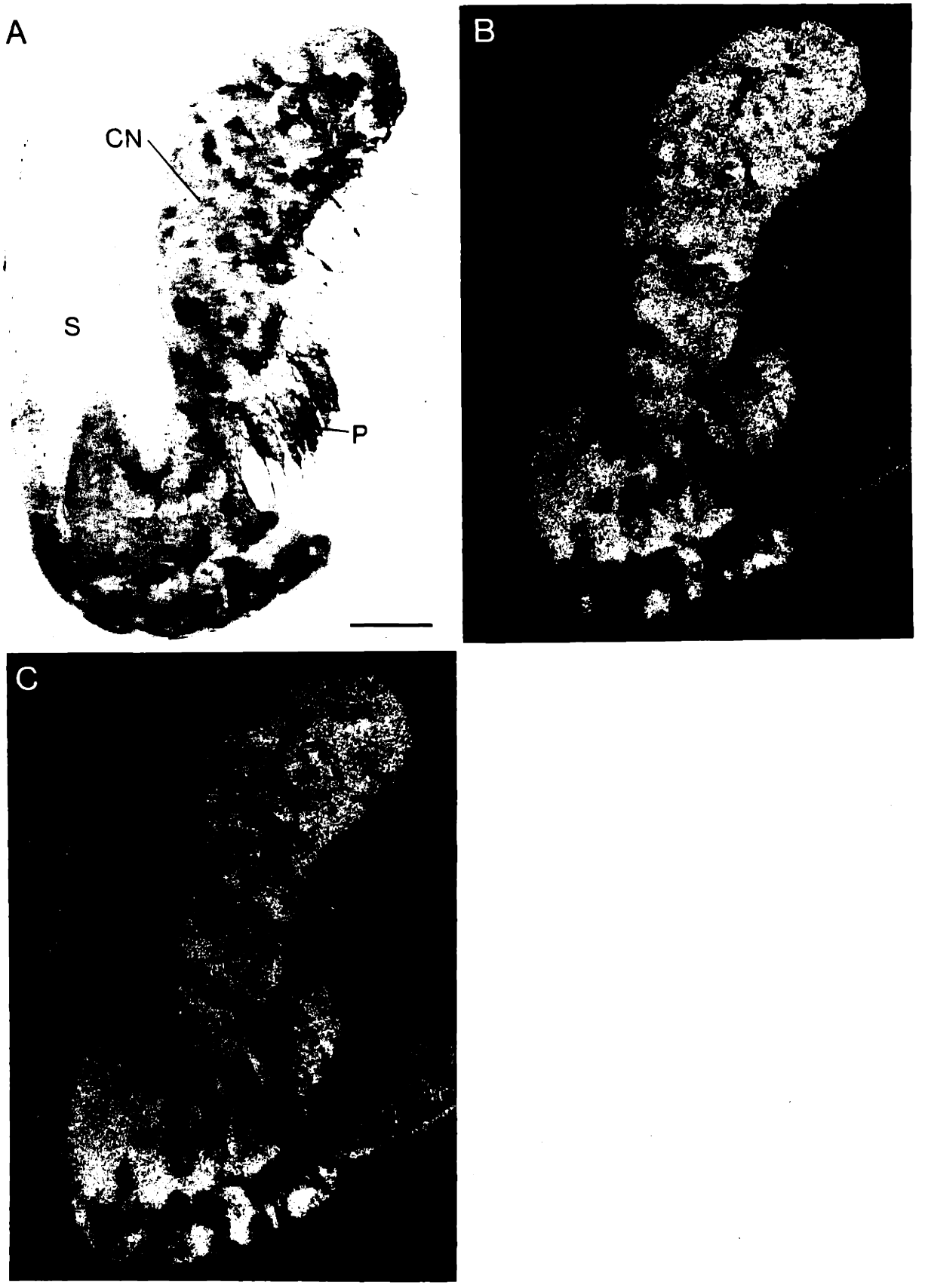
A
CN
S
P
B
C

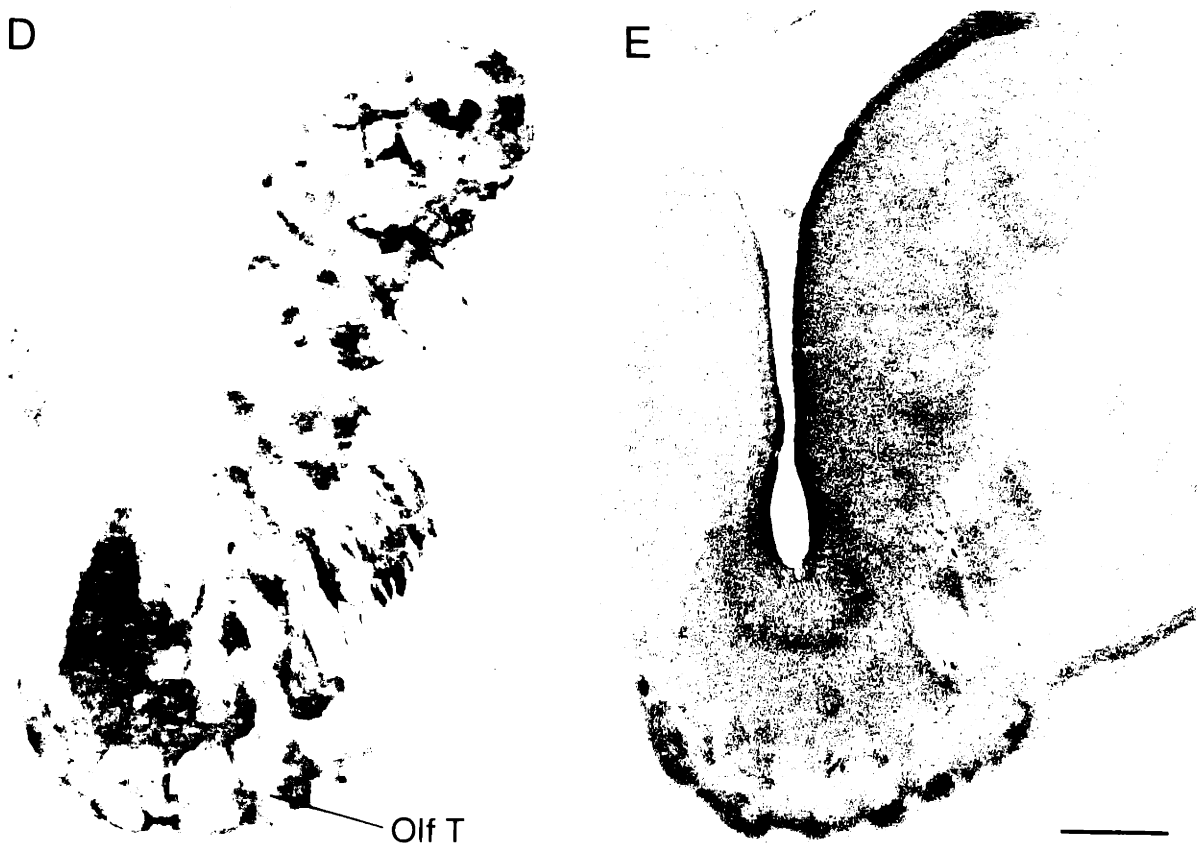
D
Olf T
E

Figure 4-9: Darkfield photographs of M1 (A) and M2 (B) binding compared to AChE staining(C, lightfield) and TH-like immunoreactivity (D, lightfield) in serially adjacent sections showing the nucleus accumbens at E58. Asterisks indicate a core of dense muscarinic binding that has no correspondent in AChE staining or TH-like immunoreactivity. Instead, AChE staining is concentrated in a dorsal-lying shell (see arrow) that is present but obscure in the section stained for TH-like immunoreactivity. NA: nucleus accumbens. Scale bar = 1mm (A - D all at same magnification).

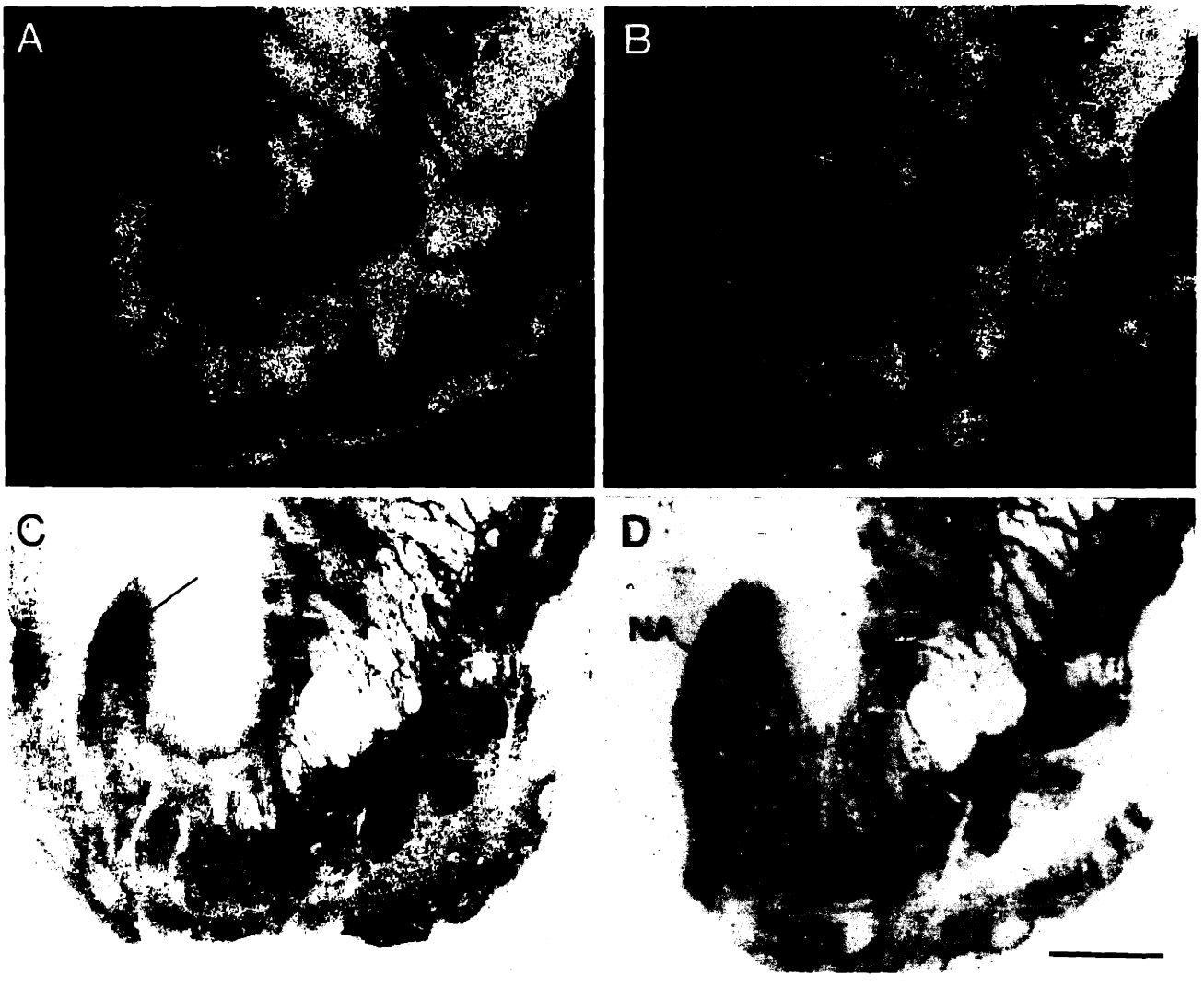
A
B
C
D

distributions and AChE staining profiles were difficult to make due to the complexity of the latter. However, it did appear in some sections that at least partial matches existed between receptor-dense and AChE-poor zones, as well as between receptor-dense and AChE-rich zones.

Ventrally in the caudate nucleus both types of muscarinic binding demonstrated large, poorly delineated areas of dense and sparse binding that matched respectively areas of heavy and light AChE staining (and also areas of heavy and light TH-like immunoreactivity). The asterisks in Fig. 10A-C indicate for binding and esterase staining such a densely labeled zone. The nucleus accumbens at birth again exhibited heterogeneity of M1 and M2 binding that varied with position along its rostrocaudal axis and that was similar in nature to earlier described examples.

P6. By the end of the first postnatal week, M1 and M2 binding site distributions, shown from rostral to caudal in Figs. 11-13A and B both were quite similar to their adult forms. Striatal M1 binding was heavy, with patches of particularly dense binding most often found mediodorsally in the caudate nucleus. The patches were less numerous than those seen in adult tissue, but in shape and contour they resembled mature M1-dense zones (particularly in caudal sections). Few areas of sparse M1 binding were observed, even in the ventral caudate nucleus. In the putamen, binding was virtually uniform.

Only rarely were any patches of dense M2 binding seen, and when present they were usually in the ventral or caudal caudate nucleus and were in alignment with zones rich in M1 binding, AChE staining and TH-like immunoreactivity (see asterisks in Fig. 13). For many sections, however, striatal M2 binding was close to homogeneous.

Figure 4-10: Acetylcholinesterase staining (A, lightfield), M1 binding (B, darkfield) and M2 binding (C, darkfield) in a serial triplet of sections from the striatum of a one-day-old kitten. Dorsally, esterase staining and M1 binding patterns are both complex relative to those seen earlier, while M2 binding is approaching uniformity. In the ventral caudate nucleus, however, patches rich in all three markers can still be seen (asterisks) and are in register. Scale bar = 1mm (A, B and C all at same magnification).

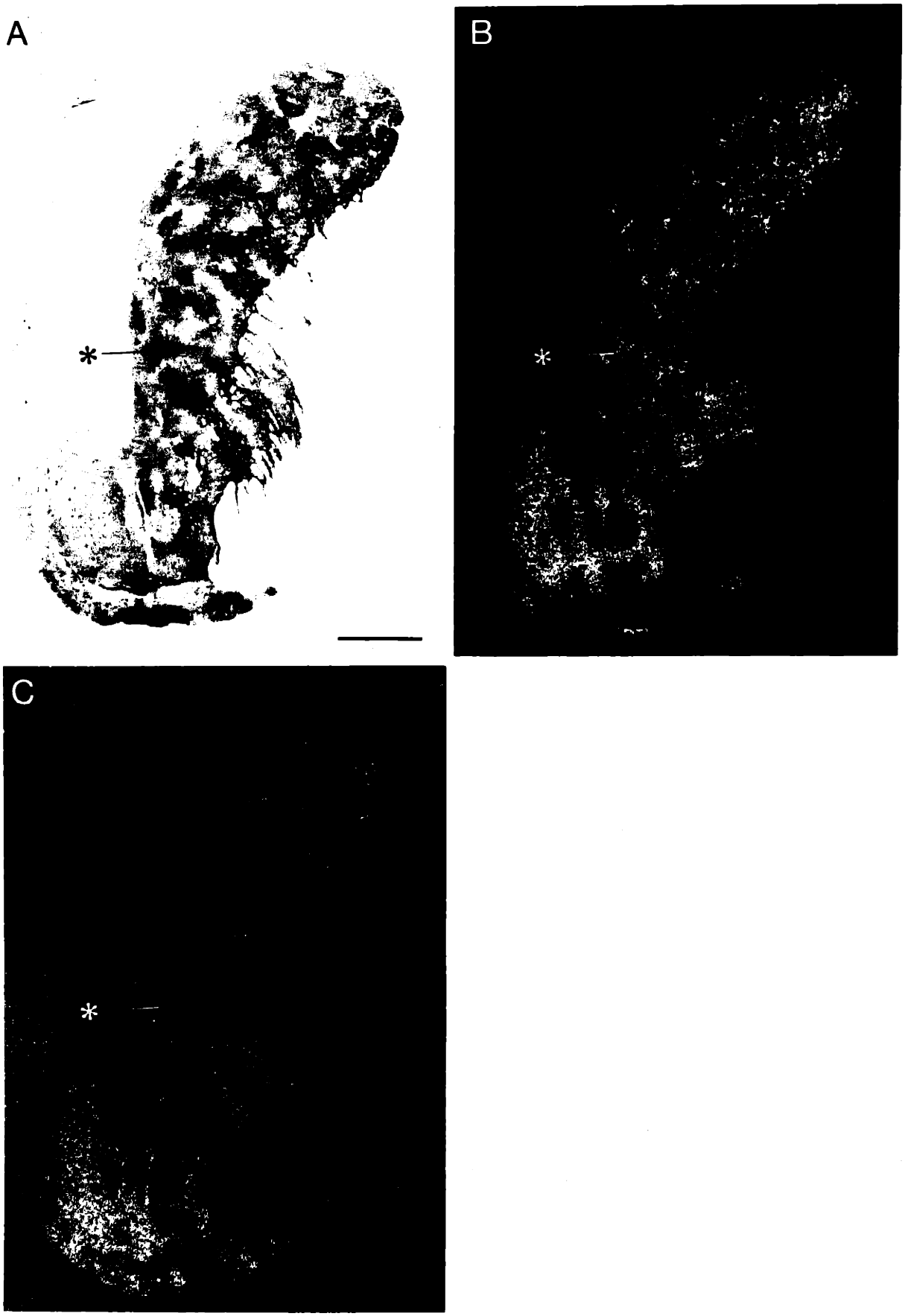
A
B
C

Sections stained for AChE still showed complex patterning. Staining in the matrix had come up in intensity but clearcut AChE-poor striosomes were not yet apparent. Rostrally, the marbled appearance characteristic of the mid-ventral caudate nucleus had no ready counterpart in muscarinic binding or TH-like immunoreactivity, as indicated in the four neighboring but not serially adjacent sections shown in Fig. 11. Nonetheless, isolated examples of M1-rich areas matching AChE-poor areas were noted in some serially adjacent rostral sections. Farther caudal, patches rich in AChE remained and matched areas of dense M1 (and sometimes M2) binding as well as heavy TH-like immunoreactivity (see asterisks in Fig. 12 and 13). However, in such sections there were also patches delineated by M1 muscarinic binding and TH staining that were not discernible in the AChE staining (see arrows in Fig. 12 A and D) as well as instances of patches rich in AChE and TH staining but lacking dense muscarinic binding (see arrows in Fig. 13C and D).

At this age, the most overt patchwork patterning was revealed in the sections processed for TH-like immunoreactivity. Although staining of the matrix was increasing in degree, pronounced islands of heavier immunolabeling were still readily apparent at all rostrocaudal levels. The islands became smaller and more punctate with caudal progression.

Adult. The findings concerning the distributions of M1 and M2 muscarinic binding in the mature cat's striatum were presented in detail in Chapter 2. Briefly, as during development, striatal M1 binding was heavier than M2 binding although the latter was considerably dense itself. Patches particularly rich in M1 binding were present, usually in the mid-dorsal caudate nucleus, and matched AChE-poor striosomes (known also to be TH-poor at maturity (Graybiel et al., 1987b)) seen in serially adjacent sections as shown in Fig. 14. These patches

Figure 4-11: A comparison of M1 and M2 binding (A and B, darkfield), AChE staining (C, lightfield) and TH-like immunoreactivity (D, lightfield) in serial sections through the rostral striatum of a kitten at six days of age. At this rostral level, M2 binding is virtually uniform in distribution (the gradient is artifactual) and M1 binding shows obscure patterning. Similarly, AChE staining is muddy in appearance. Only TH-like immunoreactivity demonstrates distinct dense patches against a pale matrix. Scale bar = 1mm (A - D all at same magnification).

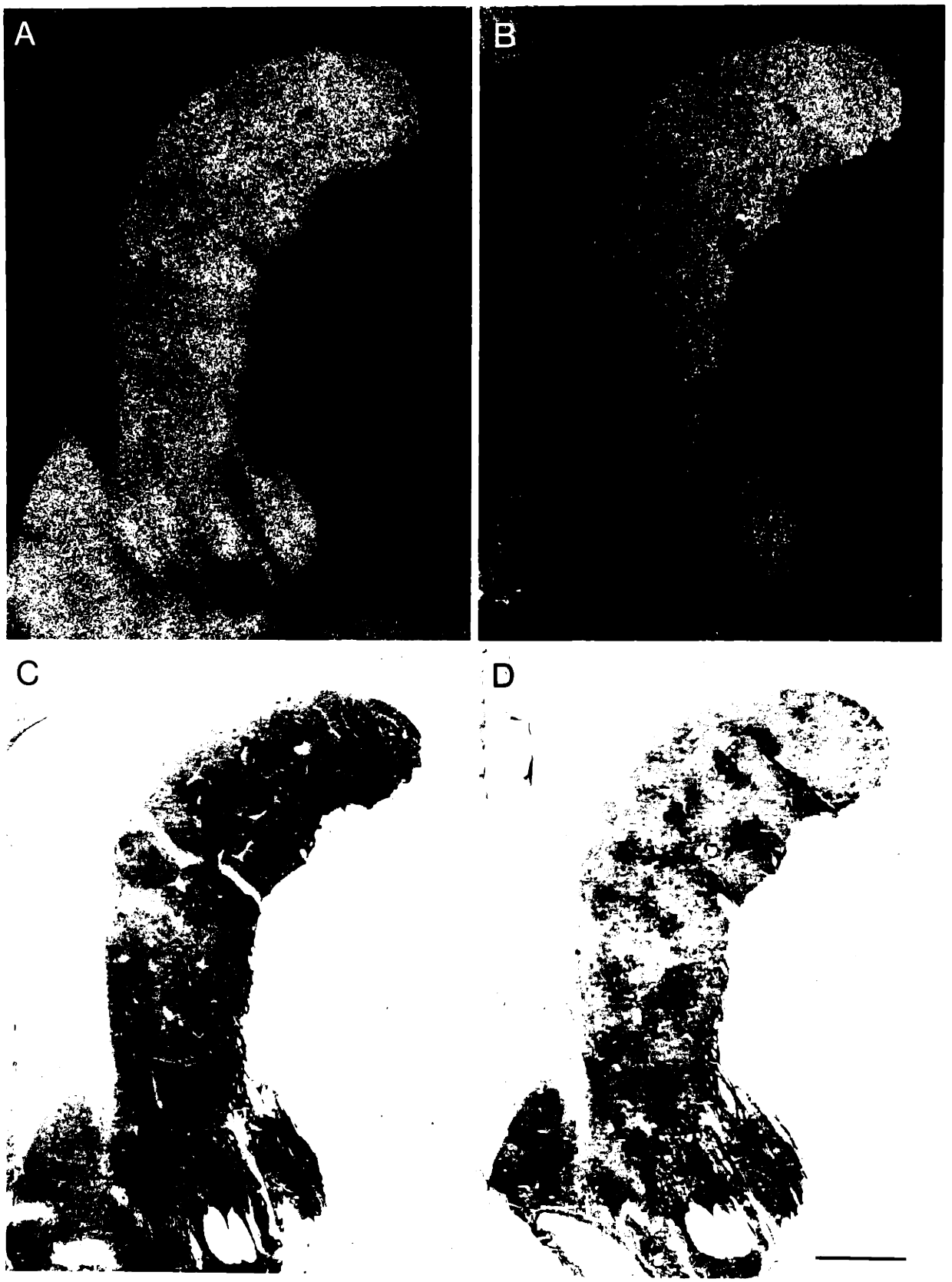
A
B
C
D

Figure 4-12: Striatal sections from the same kitten as in Fig. 3-11, showing the same four markers at a level farther caudal than in Fig. 3-11. At this level, TH-like immunoreactivity (D) again demonstrates the most discrete patch pattern in the caudate nucleus. The TH-rich patch marked with an asterisk also appears in AChE staining (C) and M1 binding (D). However, some heavily labeled patches are visible only in TH-like immunoreactivity and M1 binding (see arrows). Esterase staining in the corresponding region of the caudate nucleus is marbled in appearance. The autoradiograph of M2 binding (B) shows little heterogeneity in any striatal quadrant. Scale bar = 1mm (A - D all at same magnification).

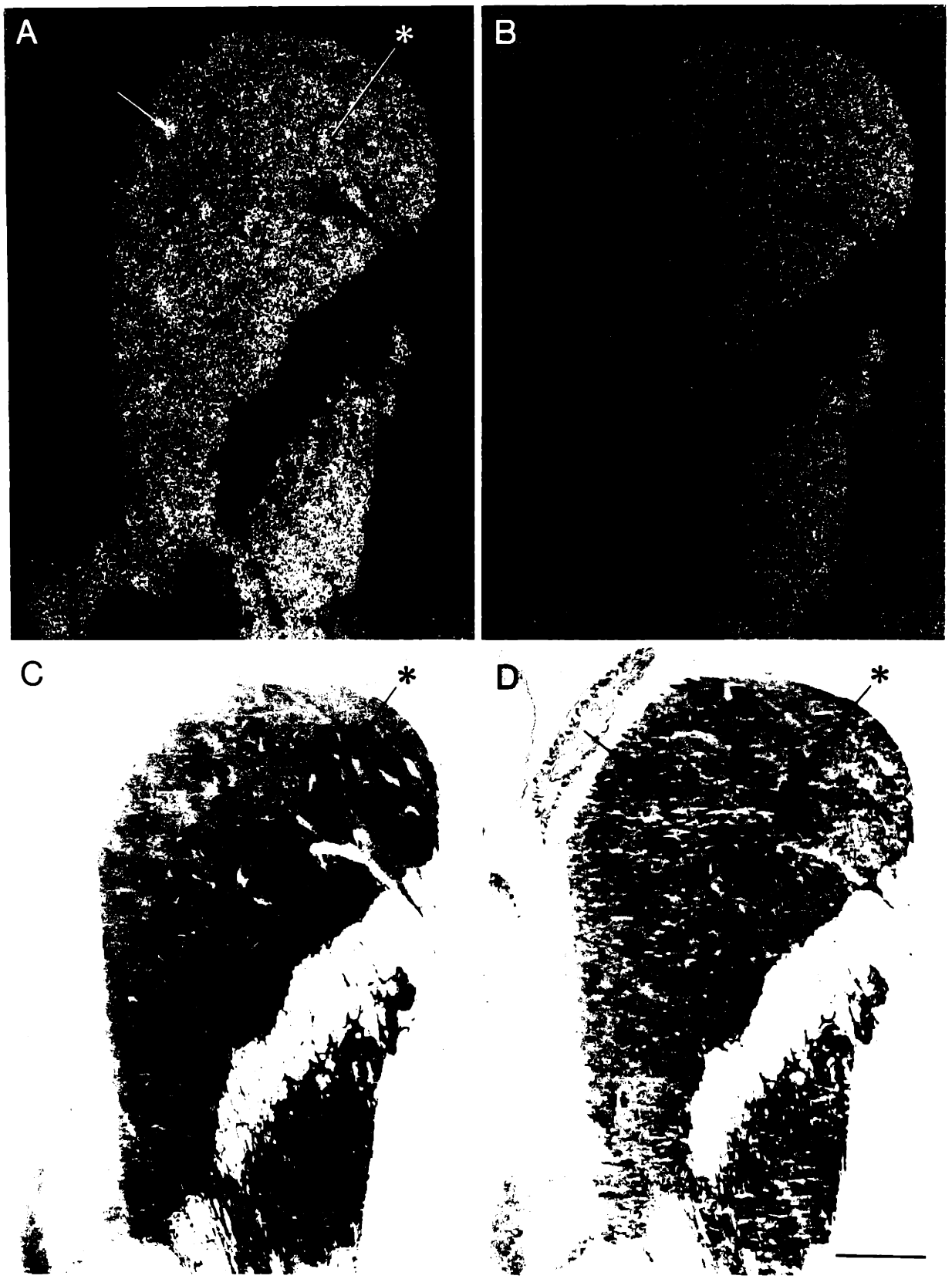
A
*
B
C
*
D
*

Figure 4-13: A third set of serial sections from the striatum of the same six-day-old kitten, at a posterior-most level. M2 binding this far caudal demonstrates some dense patches that are seen in all four sections (asterisks), although other patches visible in M1 binding (A), AChE staining (C) and TH-like immunoreactivty (D) are not represented in M2 binding. An example of a dorsolateral patch rich in AChE and TH-like immunoreactivity but not muscarinic binding is pointed out by arrows. The putamen at this and other rostro-caudal levels shows dim patterning of esterase staining and TH-like immunoreactivity but no landmarks in M1 or M2 binding. Scale bar = 1mm (A - D all at same magnification).

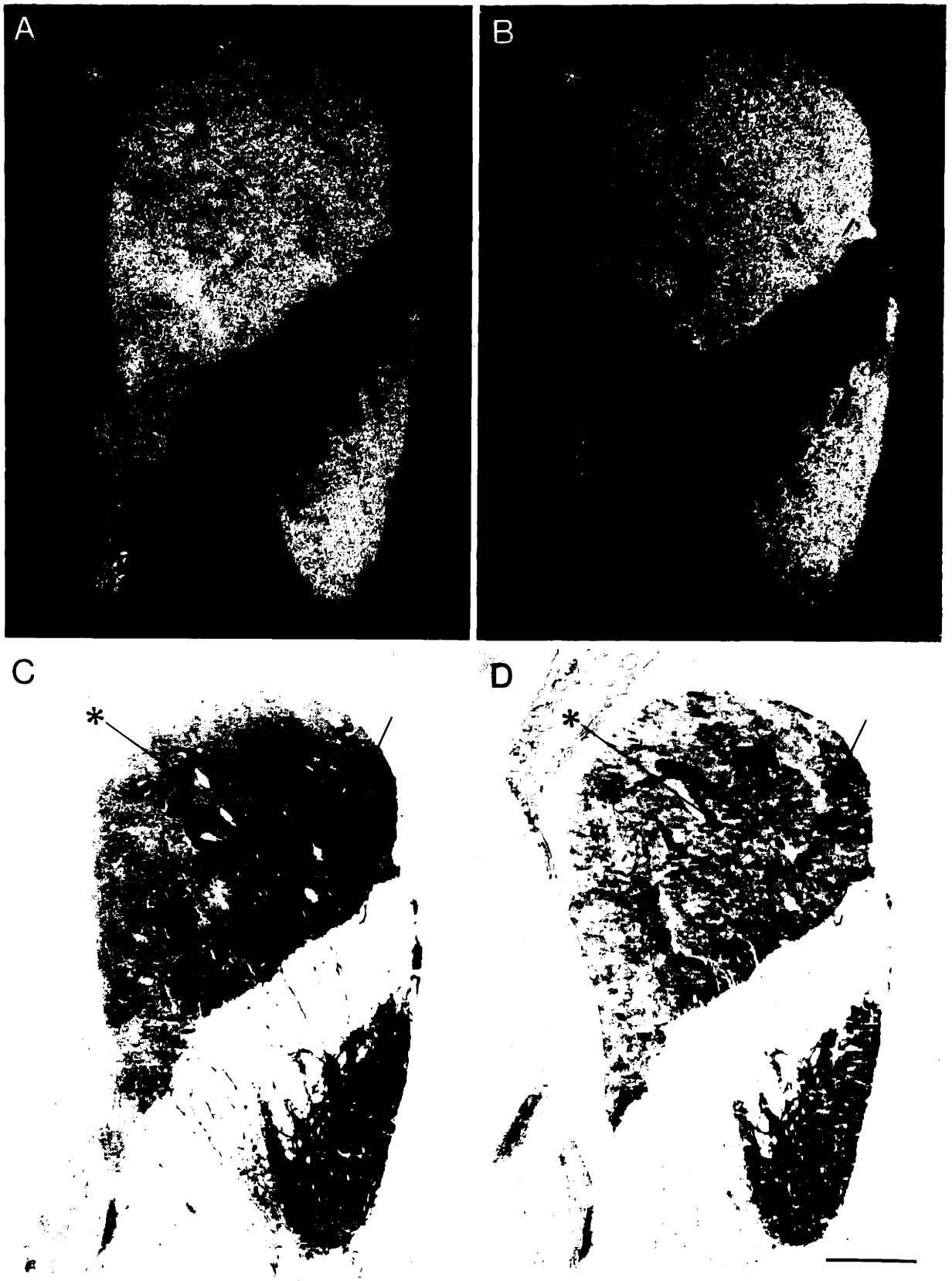
A
B
C
D
*
*

seldom had counterparts in the M2 autoradiograms, which were close to uniform except in some caudal sections. There, a few M1-dense patches also had slightly elevated M2 binding in some cases. In the ventral striatum and nucleus accumbens, both M1 and M2 binding distributions were heterogeneous and were similar to patterns of AChE staining.

DISCUSSION

This study demonstrates that muscarinic binding sites of both the M1 and M2 subtype are present prenatally in the striatum of the cat. These binding sites are distributed in patches coinciding with the early-developing nigrostriatal dopamine island system, the predecessor of the mature striatum's striosomal compartment. Perinatally, M1 and M2 binding distributions change and diverge as they approach their adult forms. M2 sites become close to uniform in distribution. M1 sites become less vividly patchy but are still heterogeneously distributed, reflecting to some degree the labile complexity of patterning observed for AChE staining at this stage of development. At maturity striatal M2 sites are nearly uniform in distribution whereas M1 sites, though dense in the extrastriosomal matrix, are especially concentrated in patches aligned with striosomes.

Muscarinic Binding Characteristics in Fixed and Unfixed Striatal Tissue

Light glutaraldehyde fixation was essential in preventing loss of fetal tissue from the slides as they were processed for muscarinic binding autoradiography. The effects of this fixation step were assessed in adult striatal tissue, where it was possible to carry out parallel binding assays with fixed and unfixed sections. The assays demonstrate that light fixation does not result in appreciable changes in K_d

Figure 4-14: Consecutive serial sections through the striatum of an adult cat showing M1 binding (A, darkfield), AChE staining (B, lightfield) and M2 binding (C, darkfield). Acetylcholinesterase-poor striosomes are matched by dense zones of M1 but not M2 binding. The latter is nearly uniform in distribution. Scale bar = 1mm (A, B and C all at same magnification).

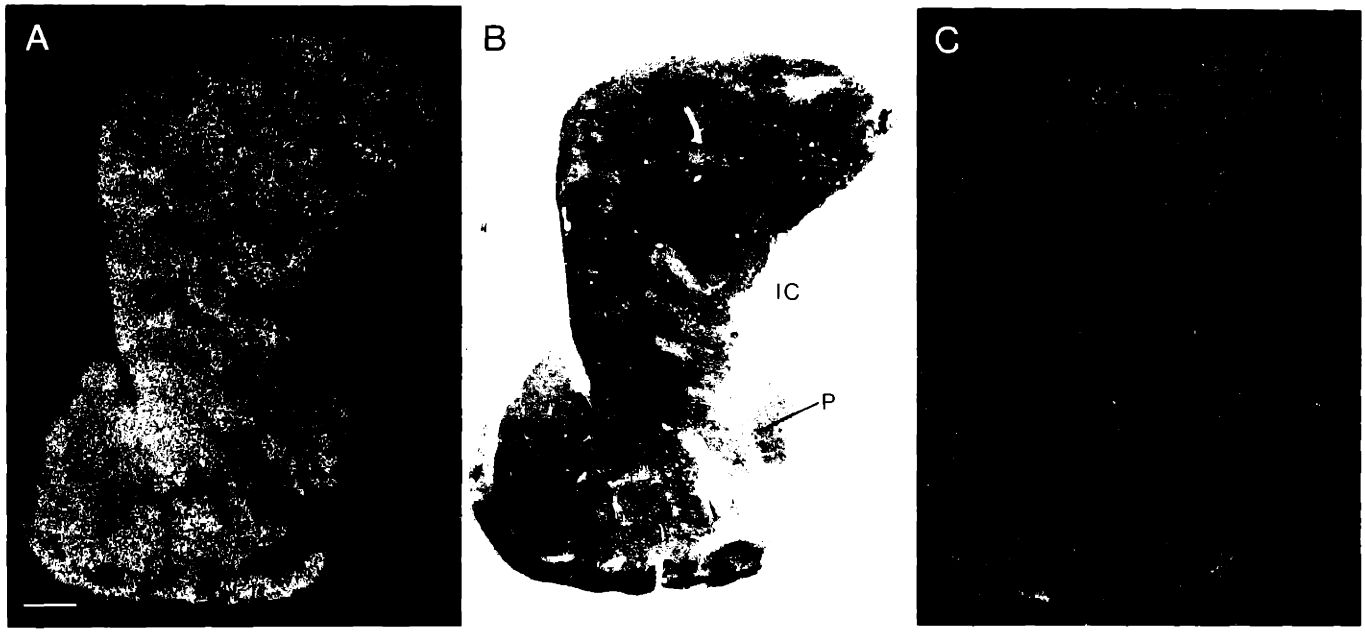
A
B
IC
P
C

or increases in nonspecific for either ligand involved. It was not possible to perform such parallel assays with fetal tissue sections, as the unfixed sections fell off the slides during incubations and rinsing. Although we have no direct proof that light fixation does not alter the binding affinities of M1 and M2 sites in fetal tissue, autoradiographic blanks prepared by incubating fetal tissue sections in the presence of excess atropine generated nearly invisible film images. Thus, nonspecific binding does not appear to increase greatly with fixation. Furthermore, other investigators have provided evidence with a variety of ligands that the K_ds of muscarinic binding sites do not change significantly during development in the central nervous system (Kuhar et al., 1980; Ravikumar and Sastry, 1985a; Large et al., 1986). This fact, taken together with the present finding that a discrete striatal subsystem (the striosomal system) can be marked with muscarinic ligands throughout development regardless of tissue fixation, strongly suggest that the present autoradiograms are valid.

Prenatal Ontogeny of Muscarinic Binding Site Distributions

Origins of striatal muscarinic binding sites. At embryonic day 40, the youngest fetal age included in this study, striatal M1 and M2 binding sites were both present and were heterogeneously distributed in accord with inhomogeneities observed for AChE staining. It was not possible to work with the extremely friable tissue from animals younger than E40, so the first appearance of striatal muscarinic binding sites was not documented. It is probable, however, that such binding sites are present early in development; by way of comparison, it has been shown that [^{3}H]-quinuclidinyl benzilate binding sites area present at least as early as 16 weeks in the human fetal striatum (Ravikumar and Sastry, 1985b). Furthermore, ^{3}H-thymidine studies of striatal neurogenesis indicate that large neurons are born

within an early developmental time window (Brand and Rakic, 1979; Bayer, 1984; Marchand and Lajoie, 1986). At least some of these neurons are likely to make up the class of large striatal neurons shown at maturity to be choline acetyltransferase-positive and therefore cholinergic (Bolam et al., 1984; Mesulam et al., 1984; Wainer et al., 1984b; Phelps et al., 1985; Vincent and Reiner, 1987; Izzo and Bolam, 1988). Early development of striatal cholinergic neurons would not be without precedent in the central nervous system: it has been shown that cholinergic cells in the nucleus of Meynert appear within the first three months of gestation in the human (Candy et al., 1985). As for the striatal cholinoceptive elements bearing the muscarinic binding sites, these may in fact form receptors prior to receiving cholinergic afferentation. Evidence presented by Coyle and Yamamura (1976) and discussed by Rotter et al. (1979c) suggests that muscarinic receptor formation parallels but precedes the development of choline acetyltransferase activity in the rat brain, in a manner perhaps analogous to the precocious appearance of nicotinic receptors at the neuromuscular junction. In the brain, other receptor systems also have been shown to antedate their presynaptic counterparts; these include substance P receptors (Quirion and Dam, 1986) and opiate receptors (Kent et al., 1982).

Muscarinic binding sites and synaptogenesis. It remains unknown whether early striatal muscarinic binding sites have a patchy distribution from their outset or whether, as for TH-like immunoreactivity, they are initially homogeneous and become aggregated into islands shortly thereafter (Specht et al., 1981b; Specht et al., 1981a; Foster et al., 1987; Newman-Gage and Graybiel, 1988). Likewise, we cannot say whether striatal muscarinic binding sites might have some regulatory role in patch formation or whether the clustering of muscarinic binding sites is merely a passive consequence of the intercalation of newly arriving neurons

lacking such binding sites. The presence of dense islandic muscarinic binding sites is certainly consistent with the suggestion of Newman-Gage and Graybiel (1988) that these islands, which are also high in synaptic vesicle immunoreactivity, are areas of elevated synaptogenesis. The present findings further indicate that the islands are selective sites of synaptogenesis involving the processes of cholinergic interneurons in particular. According to such a scheme, cholinergic synaptogenesis in the extrastriosomal matrix would postdate its islandic counterpart, as is reflected by the later appearance of binding sites in the matrix.

Muscarinic receptor formation and cholinergic synaptogenesis may have mutually supportive roles during development. Evidence suggests that much muscarinic receptor synthesis in the mammalian central nervous system occurs prior to synaptogenesis (Rotter et al., 1979a). Muscarinic receptors may even exert trophic effects as has been suggested for opiate receptors (Kent et al., 1982; Spain et al., 1985); such effects could then influence subsequent patterns of synaptogenesis among striatal cholinergic neurons. During synaptogenesis certain populations of striatal receptors may be stabilized through the phosphorylating action of calcium-calmodulin dependent protein kinase II (see Newman-Gage and Graybiel, 1988), thus influencing their final distribution. In addition, further biochemical differentiation of muscarinic receptors and their local microenvironments may occur during synaptogenesis as has been observed in the avian retina (Large et al., 1985).

Patterning and the cellular localizations of muscarinic binding sites during development. Studies of striatal neurogenesis and afferentation may shed light on the cellular localizations of muscarinic binding sites within patch and matrix compartments. Evidence in the rat suggests that striatonigral neurons in patches are born first and send out nigral projections before striatal neurons of the

matrix do (Fishell and van der Kooy, 1987). Early developing muscarinic binding sites of either the M1 or M2 subtype may reside on striatonigral neurons of the patch compartment, whereas later forming muscarinic binding sites may be located on striatonigral cells of the matrix. In fact, electron microscopic evidence in the adult rat shows that choline acetyltransferase-positive terminals do synapse on striatonigral neurons (Izzo and Bolam, 1988). Muscarinic binding sites associated with such cholinergic synapses, if functional during development, would be distinct depending upon their location in the patch or matrix compartment because striatonigral neurons of the patch and matrix have been shown to project respectively to the pars compacta and pars reticulata of the substantia nigra (Gerfen, 1985). Thus, muscarinic activation in striatal patches and matrix would influence different terminal fields in the substantia nigra.

Dopaminergic projections from the substantia nigra to the striatum also develop biphasically, with patch afferentation preceding matrix afferentation (Olson et al., 1972; Tennyson et al., 1972; Graybiel, 1984b; van der Kooy, 1984; Gerfen et al., 1987a). Evidence discussed in Chapter 1 suggests that a component of striatal muscarinic binding sites are located presynaptically on nigrostriatal terminals. Accordingly, some early appearing patch binding sites may be associated with early arriving patch afferentation while some binding sites in the matrix, appearing later in development, are associated with the second wave of ingrowing nigrostriatal fibers.

Topographic gradients of muscarinic binding site formation. Superimposed upon the local inhomogeneities in M1 and M2 binding site distributions are large scale density gradients along the rostrocaudal and mediolateral axes of the fetal and neonatal striatum. Muscarinic binding in both patches and matrix is densest caudally and laterally. In addition, patch patterns of

M1 and M2 binding differ grossly for the dorsal and ventral regions of the striatum, and the nucleus accumbens evinces its own heterogeneity of muscarinic binding.

The general caudal to rostral and lateral to medial gradients of striatal receptor expression have been previously noted in the rat (Coyle and Yamamura, 1976; Rotter et al., 1979a; Kuhar et al., 1980) and are in agreement with the findings in several species that striatal neurogenesis and synaptogenesis proceed along the same axes (Altman, 1969; Bayer, 1984; Marchand and Lajoie, 1986; Newman-Gage and Graybiel, 1988). In fact, other cholinergic markers including acetylcholine, acetylcholinesterase, choline acetyltransferase and hemicholineum binding sites also have been shown to develop from caudal to rostral and lateral to medial in the striatum (Butcher and Hodge, 1976; Coyle and Yamamura, 1976; Hohmann and Ebner, 1985; Fibiger et al., 1987; Lowenstein et al., 1987). Regulation of the developing striatal cholinergic system thus falls under spatial constraints acting at more than one level, with global programs controlling cholinergic expression overlying the regional program defined by striatal patches and matrix.

Perinatal Changes in Muscarinic Binding Distributions

Around the time of birth, the mammalian striatum is a site of continuing active cell differentiation and synaptogenesis among its several types of neurons and afferent fibers (see DiFiglia et al., 1980; Tanaka, 1980; Brand and Rakic, 1984; Levine et al., 1986). At any given time, neurons will be at different stages of maturation depending upon their type and their location with respect to striatal compartments and large scale developmental gradients. Just how cholinergic and cholinoceptive cells fit into this spatiotemporal spectrum of ontogeny is not yet

clear. Given such dynamism, however, it is not surprising that perinatal muscarinic binding site distributions and AChE staining patterns are as complex as they are before resolving into their adult forms, and that correlations among marker patterns are inconsistent.

Relationships among neurochemical staining patterns. Whereas the lack of material from very young fetuses precluded comparisons among early burgeoning striatal muscarinic binding patterns, AChE staining and TH-like immunoreactivity, it was possible to follow the progress of all three marker configurations as they underwent changes immediately following birth. The present findings show that the fundamental postnatal change in AChE (and also TH, not shown) staining in the caudate nucleus is a switch from a mosaic of dark patches upon a light matrix to one of pale patches, or striosomes, upon a dark matrix. By contrast, although [^{3}H]-PZ binding outside patches does increase greatly during development, M1 binding retains its initial characteristic of dense zones (that match striosomes) upon a less dense matrix. Striatal M2 binding is transformed from a similar patch pattern to a nearly homogeneous distribution. It is noteworthy that a like situation occurs in layer IV of the somatosensory cortex in the infant rat: there, AChE staining is transiently heavy while dense muscarinic binding remains through maturity (Kristt and Kasper, 1983).

By the end of the first postnatal week, arrays of both subtypes of muscarinic binding approximate their adult forms. Acetylcholinesterase staining still demonstrates transitory marbling and dense patches, and TH-like immunoreactivity is still concentrated in darkly staining islands (although this is subject to position along the rostro-caudal axis and within the coronal plane as Figs. 11-13 show). The situation is one of heterogeneous expression of three different molecules - a neurotransmitter receptor, a neurotransmitter catabolizer

and a neurotransmitter metabolizer - marking the same system of neuronal compartmentalization. It is likely that each molecule directly or indirectly participates in the regulation of the others' expression through mechanisms that are still far from clear.

Divergence of striatal M1 and M2 binding distributions. The differing expression of M1 and M2 muscarinic binding sites has its roots in prenatal development: then, each subtype is distributed in an islandic pattern, but it is patches of dense M2 binding that stand out best against the relatively sparse labeling of the matrix. Thus, there is a greater disparity between receptor density in patches and matrix for the M2 than for the M1 subtype. This situation is reversed perinatally so that there evolves a greater disparity of density between patches and matrix for M1 than for M2 binding; in fact, M2 binding at postnatal day 6 is nearly the same for patches and matrix, and M2 autoradiograms of mature tissue do not divulge striosomes.

Because quantitative autoradiography was not performed, it cannot be determined whether the disappearance of heterogenous M2 binding (as well as the obscuring of patchy M1 binding) occurs because of selective receptor elimination in patches or selective synthesis (or reduced degradation) in non-patch tissue. As a third possibility, all three phenomena could be occurring throughout the developing striatum, but to differing degrees in patches and matrix. Muscarinic receptor endocytosis as a means of down regulation, or reducing receptor number, has been extensively investigated in the developing central nervous system and myocardium (for a review see Nathanson, 1987). The idea of an ontogentic role for receptor elimination in the striatum is not without precedent; it has been proposed as a mechanism whereby the final distributions of μ opiate receptors are molded in the rat's caudoputamen (Kent et al., 1982). Interestingly, striatal μ receptors have also

been demonstrated to undergo up and down regulation that is largely selective to the patch compartment in adult rats (Tempel et al., 1984; Moon Edley, 1984).

The ontogenetic variance in distribution of striatal M1 and M2 binding sites suggests that expression of each muscarinic receptor subtype follows a distinct intrinsic genetic timetable (evidence does indicate that muscarinic receptors are encoded by multiple genes (Kubo et al., 1986; Bonner et al., 1987; Braun et al., 1987; Fukuda et al., 1987)). Alternatively or in addition, M1 and M2 receptor expression may be differentially sensitive to the regulatory effects of various extrinsic factors. Such factors include neurotransmitter availability, local electrical activity and feedback associated with linkages to second messenger systems. Further, the relative weights of these extrinsic influences could vary not only with receptor subtype but also with location in a particular striatal compartment.

Developmental Regulation of Striatal Muscarinic Binding Sites

Endogenous acetylcholine plays a critical part in controlling the density of its own receptors. *In vivo* administration of cholinergic agonists and antagonists has been shown to result respectively in down and up regulation of muscarinic binding sites in the striatum of the neonatal and adult rat (Ben-Barak et al., 1981). Exposure to anticholinesterase agents leads to decreases in striatal muscarinic binding site number, presumably because of elevated acetylcholine levels (Churchill et al., 1984). The mosaic nature of AChE staining makes it likely that the regulatory effects of acetylcholine are also heterogeneous across the striatum. Furthermore, by virtue of their differing affinities for acetylcholine, muscarinic receptor subtypes may be of unequal sensitivity to modulation by endogenous neurotransmitter. This distinction may contribute to the diversity of M1 and M2 binding patterns.

Ongoing electrical activity, though of a lowgrade nature in the striatum, may contribute to the maintenance of muscarinic receptors there. Electrical stimulation has been shown to regulate muscarinic receptor density in the intact central nervous system (Abdul-Ghani et al., 1981), and chronic membrane depolarization in neuroblastoma cells leads to an increase in receptor number, possibly through the inactivation of voltage-sensitive calcium channels (Liles and Nathanson, 1987). Local differences in muscarinic binding site density may be influenced by variations in electrical activity across populations of cholinoceptive striatal neurons.

In the striatum, cholinoceptive neurons are thought to be comprised at least in part of striatonigral medium spiny neurons (Izzo and Bolam, 1988). This cell type also receives dopaminergic input with a similar ultrastructural topography (Freund et al., 1984). If dopamine and acetylcholine actually share target neurons, then dopamine could be in a position to regulate muscarinic receptor number by influencing the electrical state of such neurons. Because dopamine availability varies with location in patches or matrix during development and at maturity (Olson et al., 1972; Graybiel et al., 1987b), such a regulatory mode would also be exerted unequally across striatal compartments. Furthermore, this would constitute divergent regulation of M1 and M2 muscarinic receptor subtypes if only one subtype is localized to striatonigral medium spiny neurons.

Another distinction between M1 and M2 muscarinic receptor regulation may exist at the level of the phosphatidylinositol second messenger system. Liles et al. (1986a) have provided evidence in neuroblastoma cells that activation of muscarinic receptors with its ensuing increase in phosphatidylinositol turnover, activation of protein kinase C, and elevation of cytosolic calcium leads to down regulation of muscarinic receptors. Thus, a negative feedback loop is completed. Because such regulation is agonist-induced, this mechanism, if active in the striatum, would be

closely tied to the modulatory role of acetylcholine availability and so would probably be spatially constrained by the striosomal system. Moreover, if striatal phosphatidylinositol turnover is linked to the M1 receptor as has been suggested (Gil and Wolfe, 1985), then this would constitute another instance of independent regulation of the two muscarinic subtypes.

In conclusion, a constellation of factors interact spatially, temporally, biochemically and perhaps genetically to produce the adult distributions of striatal muscarinic binding sites. Similar elements are likely to govern the other neurotransmitter binding sites in the striatum that have been shown to undergo ontogenetic changes in array (including putative receptors for substance P (Quirion and Dam, 1986), dopamine (Richfield et al., 1987) and GABA (Moon Edley, 1984), as well as μ opioid binding sites (Kent et al., 1982; Moon Edley and Herkenham, 1984; Murrin and Ferrer, 1984)). To garner information about why and how one receptor system changes during development is to gain insight into the nature of other receptor systems as they change with striatal maturation.

Chapter 5

M1 and M2 Muscarinic Cholinergic Binding Sites in the Cat's Substantia Nigra: Development and Maturity

ABSTRACT

Muscarinic cholinergic binding in the substantia nigra of the cat was investigated during development and at maturity by autoradiographically labeling the M1 and M2 subtypes of muscarinic binding sites. In cats from age embryonic day 40 to postnatal day six and at adulthood, M1 sites were labeled with [^{3}H]-pirenzepine and M2 sites were labeled with [^{3}H]-N-methylscopolamine in competition with pirenzepine. Comparisons were made among binding site distributions, acetylcholinesterase staining and tyrosine hydroxylase-like immunoreactivity in serial or neighboring nigral tissue sections.

M1 and M2 binding sites were present in the substantia nigra at all ages studied. Although quantitative comparisons were not performed, M1 binding delineated the substantia nigra more distinctly than did M2 binding. For M1 binding sites in particular, the embryonic pars reticulata of the substantia nigra was more prominently labeled than the pars compacta. At adulthood both nigral subdivisions clearly exhibited M1 and M2 binding, with the pars compacta demonstrating some internal heterogeneity of binding density. These findings provide further evidence that the substantia nigra is a site of cholinergic transmission and suggest that the functional balance between acetylcholine and dopamine in the basal ganglia may be active here as well as in the striatum.

INTRODUCTION

The substantia nigra is a major dopamine-containing cell group in the midbrain and supplies an extensive dopaminergic innervation to the striatum, to which it is reciprocally linked. This cell group plays a key but largely unelucidated role in the interplay between dopamine and acetylcholine in the basal ganglia. For example, it has been demonstrated that in the striatum, dopamine can regulate the release of acetylcholine (Guyenet et al., 1975; Bianchi et al., 1979; Sethy, 1979; Scatton, 1982; Stoof and Kebabian, 1982) and that conversely, striatal acetylcholine can modulate dopamine release (Westfall, 1974a; Westfall, 1974b; Giorguieff et al., 1976; Giorguieff et al., 1977; Giorguieff-Chesselet et al., 1979; deBelleroche and Bradford, 1978; deBelleroche and Gardiner, 1982; Lehmann and Langer, 1982; Raiteri et al., 1982; Sakurai et al., 1982).

At the level of the substantia nigra itself exogenously applied acetylcholine has an excitatory action on nigrostriatal cells (Dray and Straughan, 1976; Lichtensteiger et al., 1976; Walker et al., 1976; Greenfield et al., 1981). Furthermore, the dopamine-containing neurons of the substantia nigra's pars compacta and the neuropil of the pars reticulata contain acetylcholinesterase (AChE) and this enzyme can be released from nigral dendrites (Greenfield et al., 1980; Greenfield and Shaw, 1982; Weston and Greenfield, 1986). Although a primary function of AChE is to degrade acetylcholine (ACh), other metabolic roles have been ascribed to the enzyme (Chubb et al., 1980; Chubb et al., 1982), and AChE is not considered a definitive marker for cholinergic neurons or neuropil. Therefore, the presence of true direct cholinergic action in the substantia nigra has long been debated.

The development of sensitive immunohistochemical methods with monoclonal antibodies against choline acetyltransferase (ChAT), the synthetic enzyme for ACh, has recently yielded the first direct evidence for a cholinergic input to the substantia nigra. Choline acetyltransferase-positive fibers and terminals have been observed in moderate densities in the pars compacta, and more sparsely in the pars reticulata of the ferret (Henderson and Greenfield, 1987) and rat (Beninato and Spencer, 1987). The results of Beninato and Spencer's double labeling study suggest that the sources of this innervation are the pedunculopontine tegmental nucleus (cholinergic cell group Ch5 of Mesulam et al. (1983)) and to a lesser extent the lateral dorsal tegmental nucleus (cholinergic cell group Ch6 (Mesulam et al., 1983)).

Another anatomical marker for cholinergic pathways in the central nervous system is the autoradiographically localized muscarinic cholinergic receptor. Two muscarinic receptor subtypes have been defined based initially upon their binding affinities for agonists (Birdsall et al., 1978) and the antagonist pirenzepine (PZ) (Hammer et al., 1980), and these two receptors are likely to have distinct functions in a given tissue. High affinity PZ (M1) binding sites and low affinity PZ (M2) binding sites are differentially distributed across the brain. Although at the level of the midbrain it is M2 sites that predominate, the substantia nigra is notable because it has been observed to contain M1 sites as well (Cortes et al., 1986; Miyoshi et al., 1987). The present study demonstrates that M1 and M2 sites occur in the pars reticulata and pars compacta of the adult cat's substantia nigra and that, though both sites are present during embryonic development, their distribution across nigral subdivisions is different from that observed at maturity. At least some of these muscarinic binding sites could bear a functional relationship to the ChAT-positive terminals seen by others in the mature substantia nigra.

METHODS

Tissue sections from four fetal cats, one newborn kitten and two adult cats were studied. The ages of the fetal cats ranged from embryonic day 45 (E45) to E58 of a 65-day gestation period. Autoradiographic and binding assay procedures are described in detail elsewhere (see Chapter 3). Briefly, fetuses obtained by laparotomy from timed-pregnant cats (bred in an in-house colony), the newborn kitten, and the two adult cats were deeply anesthetized with Nembutal and their brains removed and frozen in crushed dry ice. Coronal cryostat sections of 15 μm thickness were cut at -12°C, thaw mounted and dried under vacuum at 0°C. For fetal and kitten material, light postfixation (15 min., 0.05% glutaraldehyde in 0.1M phosphate buffer at 4°C) prior to incubation with ligand was essential to minimize tissue loss from slides. Binding assays were performed in adult striatal tissue with and without this fixation step to determine that it did not lead to significant changes in nonspecific binding or binding affinity for the ligands involved (see Chapter 3). For autoradiography, sections were preincubated in 50 mM sodium phosphate buffer at pH 7.4 containing 10mM ethylenediaminetetraacetic acid (EDTA) and 0.1mM N-ethylmaleimide (NEM) for 15 minutes at 4°C to uncouple binding of endogenous agonists without affecting antagonist binding (Potter et al., 1984). Incubations were carried out for one hour at room temperature in 50mM sodium phosphate buffer with 1mM EDTA and either 10nM [^{3}H]-pirenzepine ([^{3}H]-PZ; 76.0 Ci/mmol, New England Nuclear) for M1 binding or 0.3nM [^{3}H]-N-methylscopolamine ([^{3}H]-NMS; 85.0 Ci/mmol, New England Nuclear) and 100 or 200 nM unlabeled PZ (gift of R. Hammer) for M2 binding. For blanks, 1μm atropine was added to the incubation solution. Following two brief post-incubation

washes in distilled water at 4°C, sections were dried under a stream of cool air and apposed to LKB-sensitive film for 12-43 days at room temperature. Films were developed in Kodak D19, fixed in Kodak rapid fixer and studied in comparison to serially adjacent or nearby sections stained for AChE by a modified Geneser-Jensen and Blackstad protocol (Geneser-Jensen and Blackstad, 1971), for tyrosine hydroxylase-like immunoreactivity (TH-like immunoreactivity; see Chapter 3 for procedure), or for Nissl substance.

RESULTS

Muscarinic binding sites of both the M1 and M2 subtype were seen in the fetal, neonatal and mature cat's substantia nigra. Characteristic binding patterns are described for each age below.

E45. At this age the substantia nigra was almost the only midbrain structure to show readily visible M1 binding above background levels (Fig. 1A); extremely sparse labeling was present over the mammillary bodies, but other regions showed little or no specific binding. Nigral M1 binding itself was quite light in comparison to binding observed in the striatum and hippocampus at the same age. The boundaries of the region of elevated nigral M1 binding were indistinct but appeared to include the pars reticulata and the ventral part of the pars compacta. M2 binding (Fig. 1C) was present over much of the midbrain, including the substantia nigra. However, it was not possible to delimit the borders of the substantia nigra in M2 autoradiographs because binding there was of approximately the same density as it was in the immediately surrounding tegmental regions (by contrast, the medial geniculate nuclei and superficial grey layer of the superior colliculus were easily identified due to their dense M2

Figure 5-1: A triplet of serial sections through the midbrain of a fetal cat at 45 days of gestation. The AChE staining (B) in this and subsequent figures was photographed in negative-image form so that areas rich in histochemical reaction product appear light. For M1 (A) and M2 (C) binding, darkfield photographs also show areas of dense label as light. At this fetal age, M1 binding to the substantia nigra is faint but stands out better against the surrounding tissue than does AChE staining or M2 binding. However, the boundaries of this zone of relatively dense M1 binding are difficult to define. M2 binding, though present in the substantia nigra, is denser by far in the medial geniculate bodies. The fasciculus retroflexus is visible in C by virtue of being notably poor in M2 binding. Note that M1 binding already predominates in the hippocampus. SN: substantia nigra, MB: mammillary body, SC: superior colliculus, MGB: medial geniculate body, FR: fasciculus retroflexus. Scale bar = 2mm (A, B and C at same magnification).

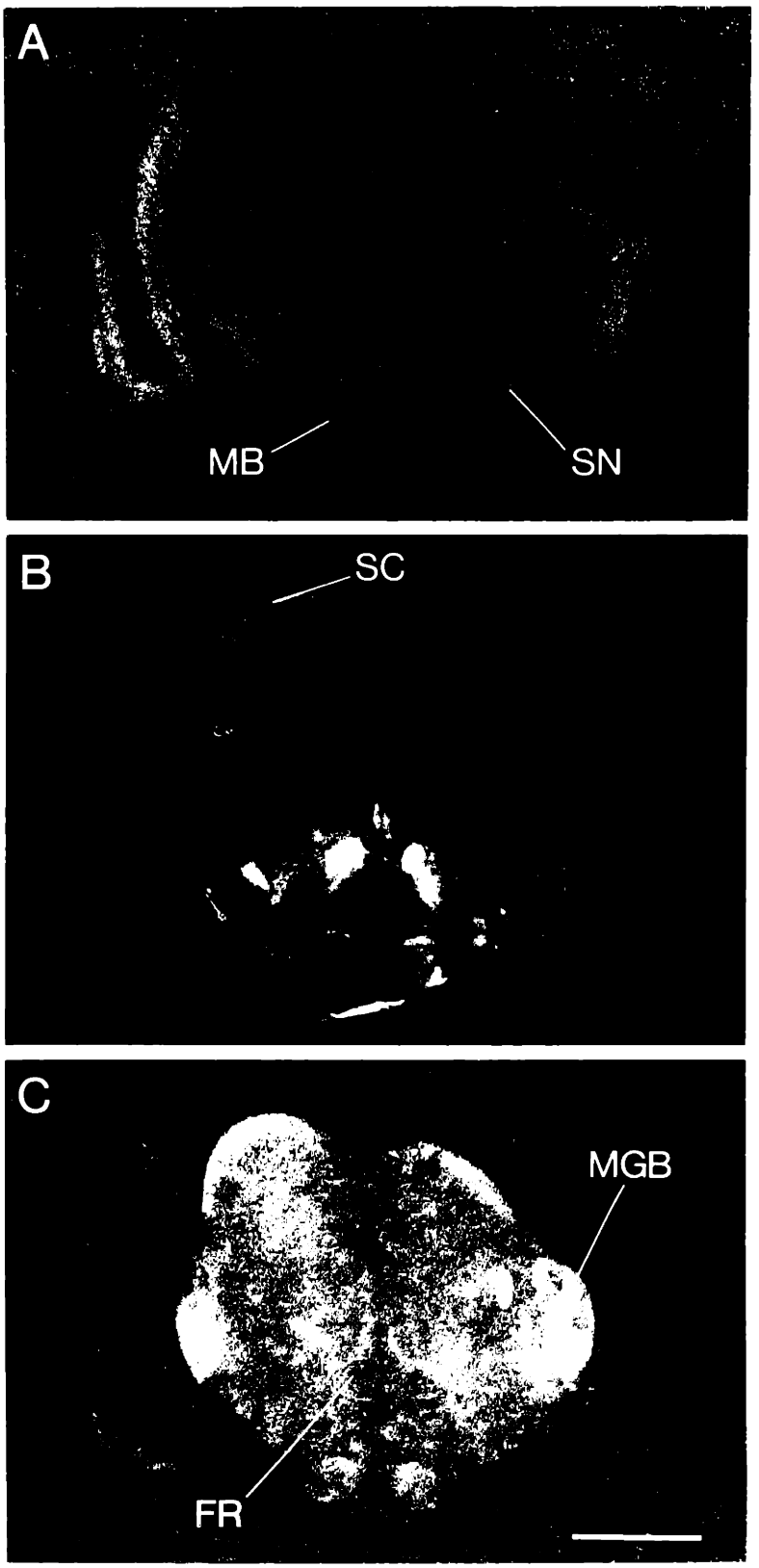
A
MB
SN
B
SC
C
MGB
FR

marking, and the fasciculus retroflexus stood out as two punctate zones having virtually no M2 binding). At E45, the substantia nigra's pars compacta demonstrated TH-like immunoreactivity (not shown) and, as shown in Fig. 1B, pale AChE staining. In the pars reticulata AChE staining was also present but was extremely light, made barely visible only after prolonged incubation times.

E58. M1 binding in the substantia nigra (Fig. 2A) was still relatively light but continued to increase in density relative to the rest of the midbrain. The labeling extended well laterally in the pars reticulata before fading, again with nondistinct borders. Medially, little or no M1 binding was present over the ventral tegmental area. By contrast, M2 binding approximately equal in density to that seen in the substantia nigra was observed in the ventral tegmental area (Fig. 2C). In the substantia nigra, M2 binding density was still low enough that it did not clearly demarcate the region. Staining for AChE was more apparent in the pars compacta than at earlier ages, but still notably pale in the pars reticulata (Fig. 2B).

P1. Figure 3A-D shows closely neighboring but not serial sections through the substantia nigra of a newborn kitten. The apparent faintness of M1 binding is due to variability in tritium-sensitive film exposure time and does not reflect an actual reduction of binding. M1 binding, as prenatally, was most notable in the substantia nigra's pars reticulata and decreased in density with dorsal progression into the pars compacta (Fig. 3A). There was again little or no M1 binding in the ventral tegmental area, shown by virtue of its TH-like immunoreactivity in Fig. 3C. M2 binding (Fig. 3D) also demonstrated little change in its appearance as compared to that seen in the late-fetal substantia nigra. For AChE staining (Fig. 3B), overall intensity was increased (to judge from the decreased incubation times needed to obtain observable staining) but the pars reticulata still lagged the pars compacta in the development of AChE content.

Figure 5-2: M1 binding (A), AChE staining (B) and M2 binding (C) in serial sections at the level of the substantia nigra in an embryonic day 58 cat. The substantia nigra pars compacta and, faintly, the pars reticulata are visible in AChE staining but do not contain levels of M2 binding high enough to distinguish them from the surrounding tegmentum. M1 binding is pronounced in the substantia nigra pars reticulata and decreases in density with dorsal progression into the pars compacta. SNpc: substantia nigra pars compacta, SNpr: substantia nigra pars reticulata. Scale bar = 2mm (A, B and C at same magnification).

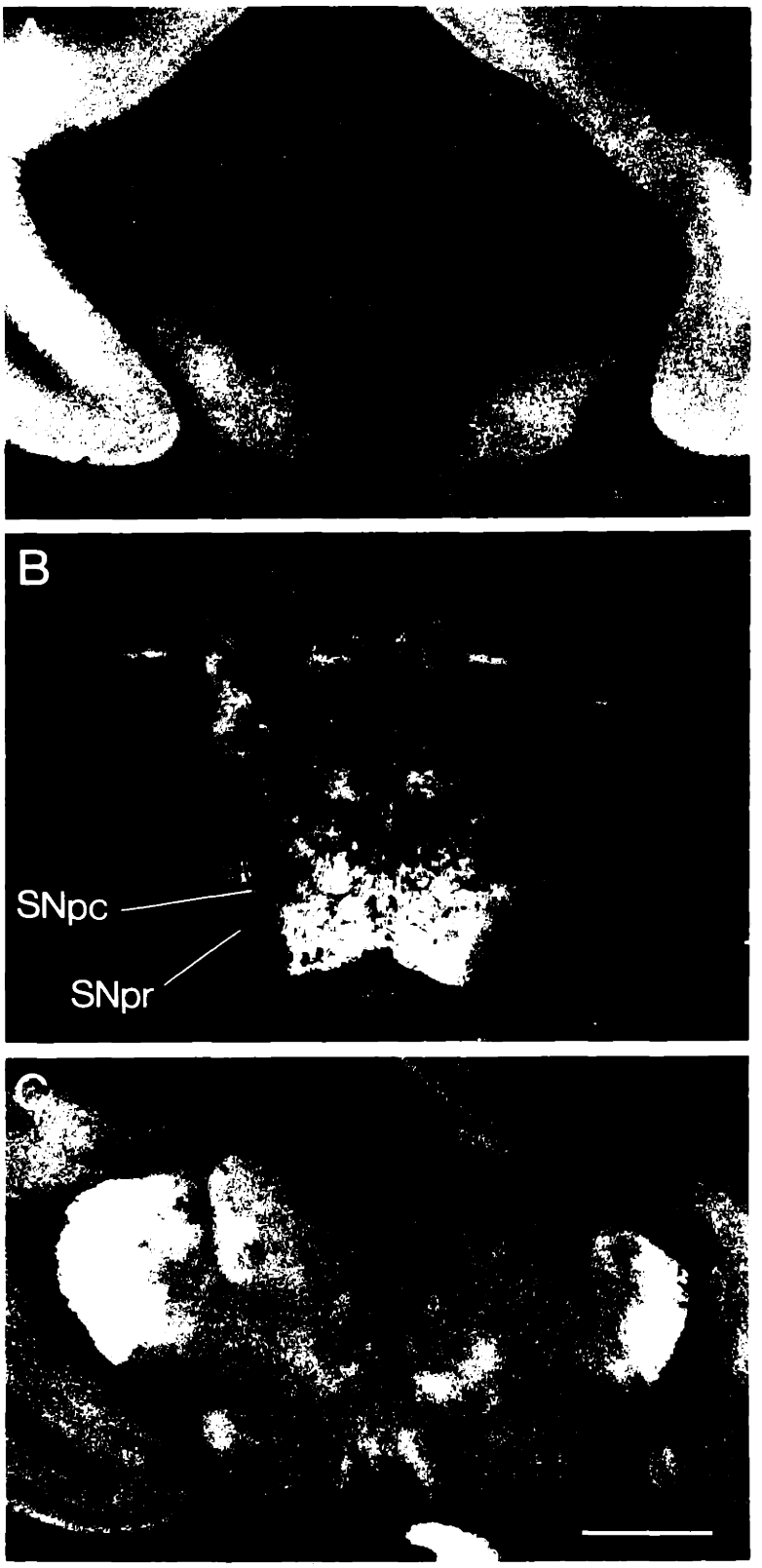
B
SNpc
SNpr

Figure 5-3: Four neighboring sections through the substantia nigra of a one-day-old kitten. Both subdivisions of the substantia nigra and the ventral tegmental area are intensely positive for TH-like immunoreactivity (C) but still demonstrate only faint AChE staining (B) and unremarkable M2 binding (D). M1 binding (A) is again best seen in the substantia nigra pars reticulata, wanes in density in the pars compacta and is almost nonexistent in the ventral tegmental area. Note that the superior colliculus shows bilaminar patterns of M2 binding and AChE staining. SNpc: substantia nigra pars compacta, SNpr: substantia nigra pars reticulata, VTA: ventral tegmental area, SCs: superior colliculus (superficial grey layer), SCi: superior colliculus (intermediate grey layer). Scale bar = 2mm (A, B and C at same magnification).

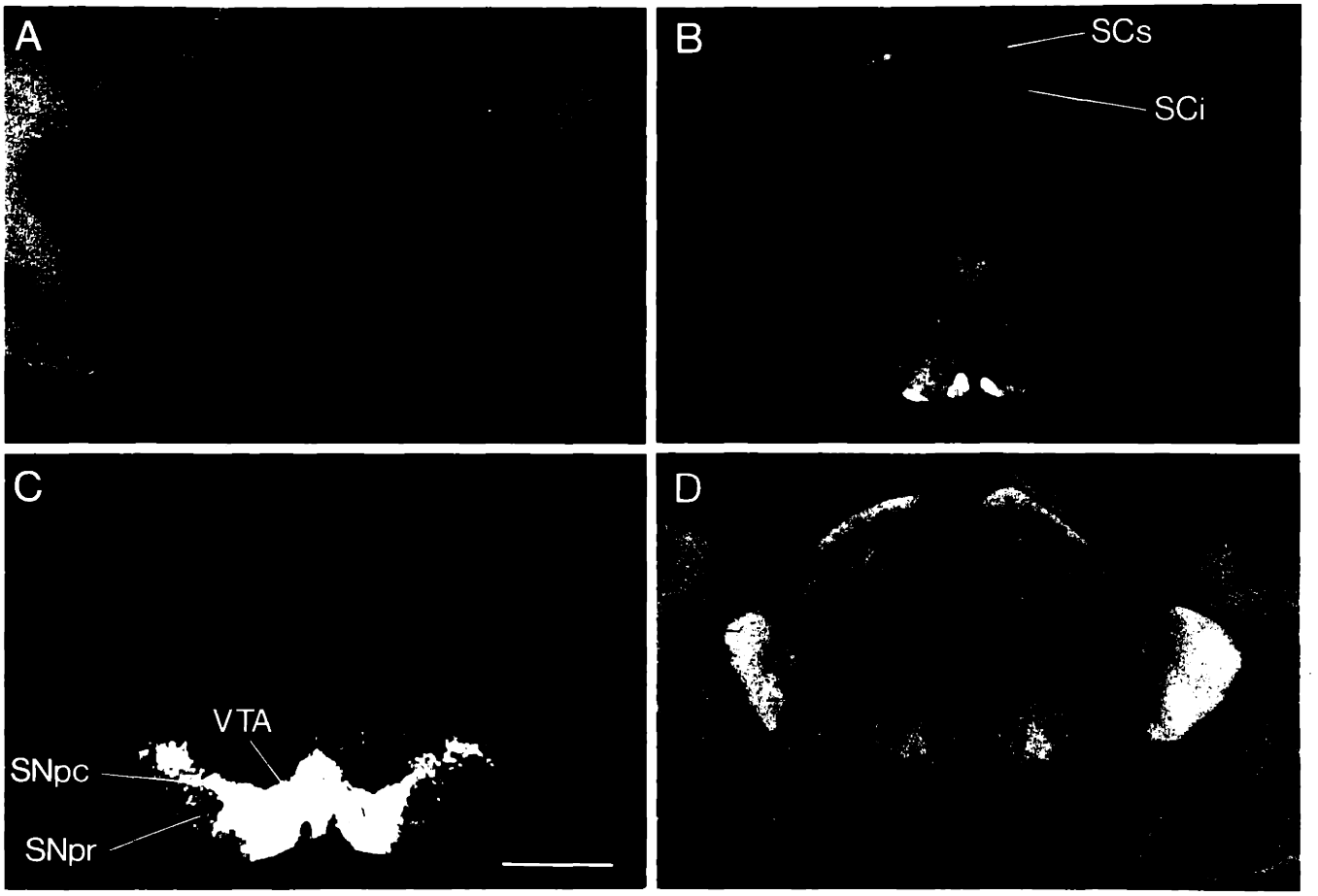
A
B
SCs
SCi
C
VTA
SNpc
SNpr
D

Adult. Both M1 and M2 binding were seen in the mature cat's substantia nigra (Fig. 4A and C). Nigral binding site density was much less than that seen in other brain regions particularly noted for the presence of one or the other subtype (for example, M1 binding in the striatum and M2 binding in the superior colliculus). Films exposed for the same number of days (not shown) demonstrated that in general, nigral M1 binding was somewhat denser than M2 binding, although no quantitation was performed to determine the ratios of the two subtypes.

Binding for both muscarinic subtypes was clearly present in the pars compacta as well as the pars reticulata of the substantia nigra. The subdivision of the pars compacta that has been referred to as the densocellular zone (Jiminez-Castellanos and Graybiel, 1987a) is shown at its rostral extremity in Fig. 4B. This zone was relatively sparse in both M1 and M2 binding (as well as in AChE staining as has been previously observed by Jiminez-Castellanos and Graybiel (1987b)). In the pars lateralis of the substantia nigra, AChE staining occurred but M1 and M2 muscarinic binding were both sparse.

DISCUSSION

This study establishes that M1 muscarinic cholinergic binding sites directly labeled with [^{3}H]-PZ, and M2 sites labeled with [^{3}H]-NMS in the presence of PZ both occur in the substantia nigra of the developing and adult cat. Ligand binding (more notably of the M1 subtype) predominantly in the pars reticulata is an early ontogenetic feature of the substantia nigra and precedes the development of marked nigral AChE staining. In the adult substantia nigra both the pars reticulata and the pars compacta demonstrate M1 and M2 binding that is of low density relative to binding in other brain regions particularly noted for the

Figure 5-4: Serial sections through the midbrain of an adult cat showing M1 binding (A), AChE staining (B) and M2 binding (C). Both subdivisions of the substantia nigra now demonstrate appreciable M1 and M2 binding (the pars reticulata is barely visible because most of it is out of the plane of section). AChE staining is intense in the substantia nigra pars compacta as well as the pars reticulata, excepting the less heavily stained dense zone of the pars compacta (labeled in A). The dense zone is also relatively sparse in both subtypes of muscarinic binding, as is the pars lateralis. SNpc: substantia nigra pars compacta, SNpr: substantia nigra pars reticulata, SNpl: substantia nigra pars lateralis, dz: dense zone. Scale bar = 2mm (A, B and C at same magnification)

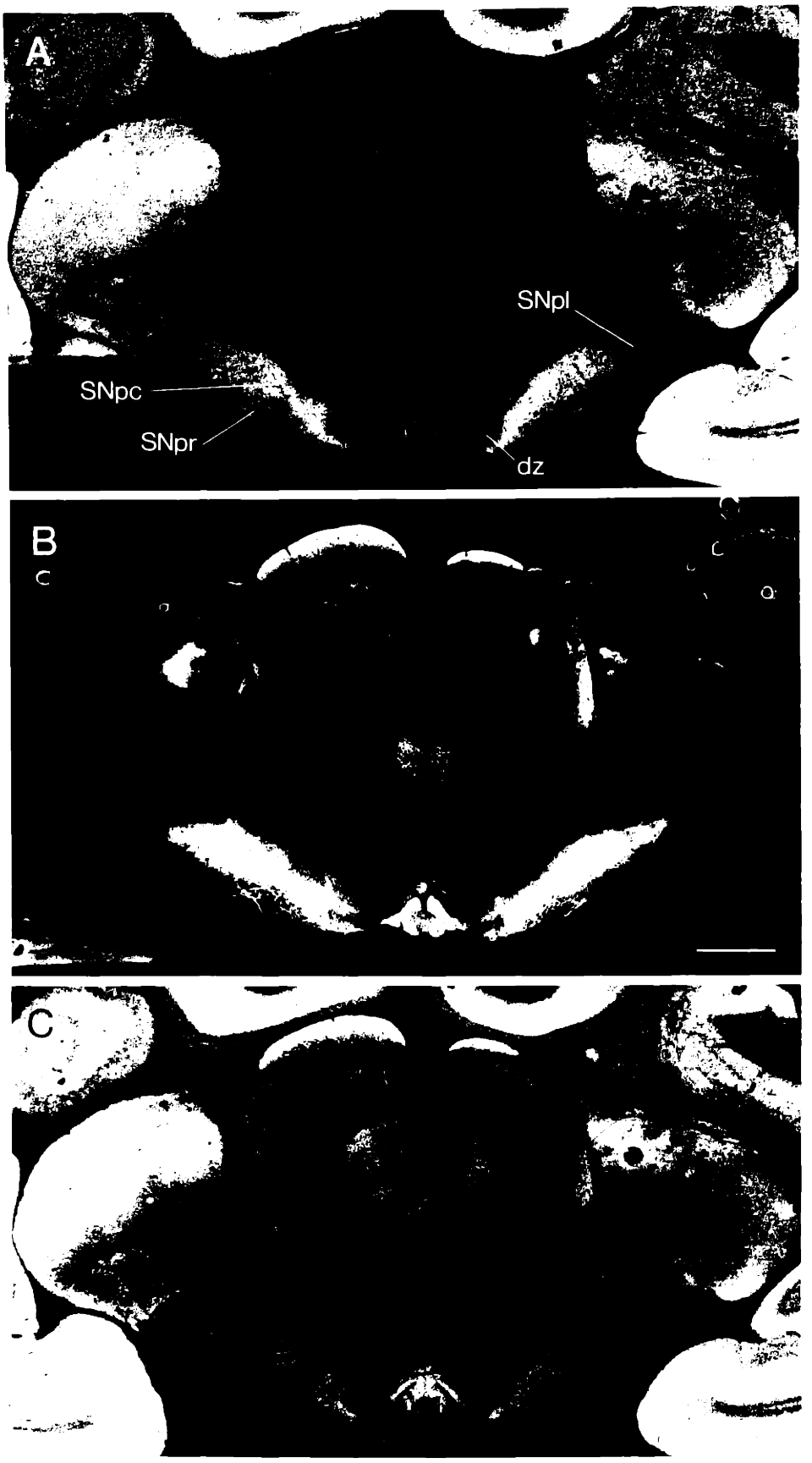
A
SNpl
SNpc
SNpr
dz
B
C

presence of either muscarinic subtype (*e.g.*, M1 binding in the striatum or hippocampus and M2 binding in the superior colliculus or medial geniculate nucleus).

Muscarinic Binding Sites in the Developing Substantia Nigra

Distinctions between subtypes. Very low levels of both M1 and M2 muscarinic binding sites were observed in the substantia nigra of the cat at the earliest fetal age studied, E40. At this and subsequent pre- and perinatal ages (as well as at maturity) nigral M1 binding appeared to be more pronounced than M2 binding. This impression may be due to the fact that elsewhere in the midbrain M1 binding appeared less prominent than M2 binding. However, Cortes et al. (1986) have noted that the substantia nigra of the human is exceptional as a midbrain structure for its predominance of M1 sites as determined with densitometric analysis. Furthermore, evidence from binding assays in various brain regions of the developing rat (Kuhar et al., 1980) indicates that low affinity agonist sites (which may be analogous to M1 sites) precede high affinity agonist sites (which may be analogous to M2 sites) in their expression. For the substantia nigra, temporal separation of the development of M1 and M2 binding may occur inasmuch as noticeably elevated nigral M1 binding appears earlier in development than does M2 binding. This could be due simply to the earlier establishment of a lifelong predominance of nigral M1 binding, or it could be a reflection of differing localizations of the two subtypes on cellular elements having distinct developmental time courses.

Distinctions among nigral subdivisions. Within the substantia nigra, the early appearance of M1 muscarinic binding mainly in the pars reticulata suggests that the pars compacta and pars reticulata are under different temporal

constraints during development. Neuronal birthdating studies in the rat (Altman and Bayer, 1981) indicate that cells of the embryonic pars compacta and pars reticulata are born contemporaneously. However, synaptogenesis and afferentation of the two nigral subdivisions could still occur differentially. If the establishment of incoming and outgoing connections as well as an increase in synaptic density (particularly for synapses requiring muscarinic receptors) occurs on an earlier schedule in the pars reticulata than in the pars compacta, such a distinction could well be reflected in the distribution of the receptors present in the substantia nigra.

The site of origin of afferents to the nigral subdivisions may play a role in determining the relative maturational time courses of such afferents. In the brain there is a general caudal to rostral gradient for many ontogenetic events, including the development of cholinergic systems as identified by markers such as ChAT activity and cholinergic receptors (Coyle and Yamamura, 1976; Rotter et al., 1979a; Kuhar et al., 1980; Hohmann and Ebner, 1985). If any of the muscarinic cholinergic binding sites that are in the pars reticulata (or that are related to dendrites of pars compacta neurons extending into the pars reticulata) are associated with the reported caudal-arriving cholinergic input from the pedunculopontine tegmental nucleus or the lateral dorsal tegmental nucleus, a sparse component of which does appear to terminate in the pars reticulata (Beninato and Spencer, 1987; Henderson and Greenfield, 1987), then such binding sites could be expected to develop relatively early in keeping with a caudal to rostral trend. In this light it is notable that muscarinic binding in the entopeduncular nucleus and the subthalamic nucleus also was observed (not shown) in the youngest brains studied. Both of these nuclei also have been proposed as possible targets of cholinergic input from the pedunculopontine tegmental nucleus and the lateral dorsal tegmental nucleus (Sugimoto and Hattori, 1984; Satoh and

Fibiger, 1986). The delayed appearance of definitive muscarinic binding in the substantia nigra's pars compacta might be expected if a significant component of these binding sites are destined for a presynaptic localization on nigrostriatal terminals, subserving cholinergic modulation of striatal dopamine release (see Chesselet, 1984). Such presynaptic binding sites would likely be under separate ontogenetic regulation from their postsynaptic counterparts found elsewhere in the substantia nigra.

Within the nigral pars compacta itself a pattern appears to characterize the emergence of muscarinic binding sites, most notably of the M1 type: autoradiographic silver grains are first present over the ventral reaches of the pars compacta and only later do they overlie its dorsal region. Such a pattern is reminiscent of Gerfen et al.'s description (1987a) of a dorsal and ventral tier in the pars compacta of the rat. Mesostriatal dopaminergic neurons in the ventral tier are thought to project to the striatal patches (and to develop earlier) while those in the dorsal tier project to the matrix compartment (and develop later). If an analogous dorsoventral division exists in the substantia nigra of the fetal cat, then it may be reflected in the early appearance of muscarinic binding sites in the ventral pars compacta. Perhaps some of these binding sites are specialized to be presynaptic and in particular to reside on nigrostriatal terminals within striosomes. In turn, later-appearing muscarinic binding sites in the dorsal pars compacta may be related to the striatal matrix, which is nigrally afferented mainly after the patch compartment (Olson et al., 1972; Tennyson et al., 1972; Graybiel, 1984b; van der Kooy, 1984; Gerfen et al., 1987a).

The present material demonstrates that muscarinic binding, particularly of the M1 subtype, is present in the substantia nigra's pars reticulata well in advance of appreciable AChE staining. A similar phenomenon was observed for M1 binding

in the entopeduncular nucleus, a structure that is closely allied to the pars reticulata (see Graybiel and Ragsdale, 1979) and that, like the pars reticulata, exhibits intense AChE staining at maturity and may be a target of cholinergic input from the pedunculopontine tegmental nucleus and the lateral dorsal tegmental nucleus (Sugimoto and Hattori, 1984; Satoh and Fibiger, 1986). In addition, M2 muscarinic binding was present in the intermediate grey layer of the superior colliculus at birth whereas it has been observed that patchy AChE staining does not develop there until postnatal day seven in the cat (McHaffie et al., 1986). The above findings are in agreement with the more general observation of Coyle and Yamamura (1976) that in the developing rat brain, cholinergic markers such as ChAT activity (termed presynaptic) lag ligand binding to muscarinic receptors (termed a postsynaptic marker) in their development. It is an interesting possibility that the early presence of muscarinic binding sites may underlie a guiding role for these sites in the development of central cholinergic pathways.

Nigral Muscarinic Binding Sites at Maturity.

Acetylcholine has been reported to have an excitatory effect on nigrostriatal neurons (Walker et al., 1976) and also to decrease endogenous AChE release from nigrostriatal neurons (Weston and Greenfield, 1986). The observation of ChAT-positive terminals and synaptic specializations in the substantia nigra's pars compacta and to a lesser extent in the pars reticulata suggests that effects such as these could be direct and could involve pars compacta neurons at the level of their somata and/or at the level of their dendrites extending into the pars reticulata. The presence of muscarinic cholinergic binding sites in both subdivisions of the mature cat's substantia nigra provides further important evidence that cholinergic transmission within the substantia nigra could be functional *in vivo*. However, although it has been demonstrated that nicotine has an excitatory effect on nigral

cells in the rat (Lichtensteiger et al., 1976) (and that nicotinic cholinergic binding sites are present in the substantia nigra of the rat (Clarke et al., 1984; Clarke and Pert, 1985)), a physiological role for nigral muscarinic binding sites of either subtype remains undefined.

The localization of muscarinic binding sites to the pars reticulata suggests that such binding sites could be in a position to modulate striatonigral input, perhaps in a manner analogous to that proposed for D1 dopamine receptors in the pars reticulata (Besson et al., 1988). Candidate neurotransmitters for such an interaction include GABA and substance P, both of which have been identified in striatonigral neurons (see Graybiel and Ragsdale, 1983). It has been demonstrated that nicotine diminishes potassium-evoked substance P release in nigral slices (Torrens et al., 1981), although possible muscarinic regulation of GABA or substance P release has not been extensively investigated in the substantia nigra.

Because at least some striatonigral afferents have been shown to terminate on ventrally-extending dendrites of dopamine-containing pars compacta neurons (Wassef et al., 1981), any cholinergic modulation of striatonigral input could indirectly influence the dopamine-containing nigrostriatal pathway. Alternatively or perhaps in addition, dopaminergic neurons of the pars compacta could be directly acted upon by the previously discussed cholinergic input arising from the pedunculopontine tegmental nucleus; in fact, there is evidence that neurons in the pedunculopontine tegmental nucleus project monosynaptically to nigrostriatal neurons in the pars compacta (Tokuno et al., 1988). Thus, the substantia nigra may represent a site of interaction between ACh and dopamine quite aside from that proposed to occur in the striatum, involving a cholinergic system distinct from the ChAT-positive striatal interneurons.

A full characterization of the muscarinic binding sites in the pars reticulata

and pars compacta must take into account the differential and well-ordered connectivity linking these nigral subdivisions with the histochemical compartments that are a hallmark of the striatum. Striosomes, macroscopic striatal zones that are relatively poor in AChE staining (Graybiel and Ragsdale, 1978) and TH-like immunoreactivity (Graybiel et al., 1987b), are the preferential targets of some nigrostriatal projections originating in the pars compacta (Jiminez-Castellanos and Graybiel, 1987a; Gerfen et al., 1987b) whereas the extrastriosomal matrix gives rise to the bulk of the striatonigral pathway to the pars reticulata (Gerfen, 1985). The pars compacta of the cat can be further subdivided: within it, a caudal densocellular zone that is AChE-poor (Jiminez-Castellanos and Graybiel, 1987b) sends projections to dorsolateral striosomes. The pars lateralis of the substantia nigra also projects to striosomes, but these are located caudally and ventrally in the caudate nucleus (Jiminez-Castellanos and Graybiel, 1987a). Because of this segregation within the nigro-striato-nigral loop, at least some muscarinic binding sites in various nigral subdivisions may be prefentially associated with the striosomal compartment or the extrastriosomal matrix. In this regard it is notable that the striosomally-projecting densocellular zone and pars lateralis both have reduced densities of M1 and M2 binding sites. Whether any of these sparsely present binding sites are destined for anterograde transport to a presynaptic location on striosomal dopamine-containing nigrostriatal fibers remains unknown, although there are findings to suggest that dopamine receptors are transported along the nigrostriatal pathway (van der Kooy et al., 1986). Nonetheless, it is evident that the phenomenon of compartmentalization extends well beyond the anatomical borders of the striatum proper, and underlies its interactions with principal linked nuclei such as the substantia nigra. Compartmental relationships, direct or indirect, borne by muscarinic binding sites in various nigral subdivisions are thus likely to be of functional importance.

Chapter 6

Epilogue

The foregoing investigations demonstrate that muscarinic cholinergic binding sites are a prominent component of the basal ganglia's chemoarchitecture. These studies show that there is both topographical and ontogenetic dissociation of M1 and M2 binding sites: the two subtypes have differing striatal distributions at maturity, and their developmental expression proceeds according to distinct schedules in both the striatum and the substantia nigra. Findings such as this point to interesting possibilities about the functional segregation of muscarinic binding sites in the basal ganglia. However, labeling of binding sites does not directly define their function. To shed light on the issue of receptor function in different striatal compartments or nigral subdivisions, one approach is to observe with anatomical means the sequelae of recetor activation. Given the wealth of information about the linkages between muscarinic receptors and intracellular second messenger systems, a natural course of action is to determine whether these linkages occur differentially in, for example, striosomes and matrix.

As was discussed in Chapters 2 and 3, one second messenger mechanism with which striatal muscarinic receptors are associated is the hydrolysis of phosphatidylinositol (PI). The autoradiographic localization of acetylcholine-stimulated PI turnover was first attempted by Hokin (1965) in the superior cervical ganglion of the cat. Since then with the advent of more sophisticated autoradiographic techniques, light-stimulated PI turnover has been mapped in retinal cells as a function of increased uptake of [^{3}H]-inositol (Anderson and Hollyfield, 1981; Anderson et al., 1983). In the brain itself these anatomical

techniques have not been applied although regional distributions of receptor coupling to PI turnover have been studied biochemically (Mantyh et al., 1984; Fisher and Bartus, 1985; Gonzales and Crews, 1985). Moreover, the relationship between striatal muscarinic receptors and PI turnover has been at least partially characterized (Fisher and Bartus, 1984; Gil and Wolfe, 1985). It would be of great value to draw on this body of knowledge in order to study striatal compartmentalization at the level of muscarinic cholinergic stimulation of PI turnover.

As an adjunct to the present thesis work, a series of experiments was undertaken in striatal slice preparations to localize autoradiographically the muscarinic stimulation of PI hydrolysis and to see whether the occurrence of this event is spacially constrained by striosomal organization. Coronal slices from adult cat striata were prepared and allowed to equilibrate in chambers perfused with oxygenated physiological buffer at 37°C. To each chamber was then added [^{3}H]-inositol alone or in conjunction with the muscarinic agonist carbamylcholine, with or without lithium. The reason for including lithium was to boost labeling of the slices, as lithium has been shown to inhibit the degradation of inositol phosphate (see Fisher and Agranoff, 1987). After an incubation period and rinse, some slices were frozen between a coverslip and a cryostat chuck and cut into thin (10 μm) sections that were thaw-mounted onto slides and apposed to tritium-senstitve film. Following exposure the same sections were stained for AChE. In parallel with the autoradiographic processing, the remaining slices were assessed biochemically for uptake of [^{3}H]-inositol; these slices were subjected to chloroform:methanol extraction and aliquots were taken from the resulting aqueous and organic phases for scintillation counting. Thin layer chromatography was also performed to show that the accumulated lipid-bound label was specific to PI and not found in any of the other phospholipid species.

Preliminary results of the biochemical experiments indicate that, in slices large enough to include the entire cross sectional area of the cat's caudate nucleus and putamen, it is possible to show increased incorporation of [^{3}H]-inositol in the presence of carbamylcholine. Labeling of the slices was further elevated by lithium. As for the autoradiography, sections cut from the incubated slices did produce images on the tritium-sensitive film. In these images, the caudate nucleus and putamen could be readily distinguished by virtue of their dense labeling. For most sections this labeling was close to uniform and bore little or no relationship to the striosomal pattern of AChE staining that was revealed when the sections were restained. However, a few film images of sections contained ill-defined zones of slightly reduced grain density that partially matched AChE-poor regions in the caudate nucleus. It is possible that the near uniformity of striatal PI turnover observed under these conditions may accurately reflect the *in vivo* state; alternatively, spatial heterogeneity of the cholinergic links to PI turnover may be present but clouded here by background labeling, lack of specificity of this approach for receptor subtypes, or transsynaptic effects. Nonetheless, these initial results are most promising and suggest that further work will yield a suitable method for anatomically localizing receptor-stimulated PI hydrolysis in striatal tissue, thus providing new insight into the functional significance of striatal compartmentalization.

References

Abdul-Ghani, A.S., M.M. Boyar, J. Coutinho-Netto, H.F. Bradford, C.P. Bernie, E.C. Hulme and N.J.M. Birdsall (1981) Effect of Tityus toxin and sensory stimulation on muscarinic cholinergic receptors in vivo. *Biochem. Pharmacol.* **30,** 2713-2714.

Altman, J. (1969) Autoradiographic and histologic studies of postnatal neurogenesis. *J. Comp. Neurol.* **136,** 269-294.

Altman, J. and S.A. Bayer (1981) Development of the brain stem in the rat. V. Thymidine-radiographic study of the time of origin of neurons in the midbrain tegmentum. *J. Comp. Neurol.* **198,** 677-716.

Amenta, F., G. Bernardi, V. Floris and M.G. Marciani (1979) Localization of α-bungarotoxin binding sites within the rat corpus striatum. *Neuropharmacol.* **18,** 319-322.

Anderson, R.E. and J.G. Hollyfield (1981) Light stimulates the incorporation of inositol into phosphatidylinositol in the retina. *Biochim. and Biophys. Acta* **665,** 619-622.

Anderson, R.E., M.B. Maude, P.A. Kelleher, M.E. Rayborn and J.G. Hollyfield (1983) Phosphoinositide metabolism in the retina: localization to horizontal cells and regulation by light and divalent cations. *J. Neurochem.* **41,** 764-771.

Angevine, J.B., Jr. and J.A. McConnell (1974) Time of origin of striatal neurons in the mouse: an autoradiographic study. *Anat. Rec.* **178,** 300.

Arikuni, T. and K. Kubota (1984) Substantia innominata projection to caudate nucleus in macaque monkeys. *Brain Res.* **302,** 184-189.

Arimatsu, Y., A. Seto and T. Amano (1981) An atlas of α-bungarotoxin binding sites and structures containing acetylcholinesterase in the mouse central nervous system. *J. Comp. Neurol.* **198,** 603-631.

Ashkenazi, A., J.W. Winslow, E.G. Peralta, G.L. Peterson, M.I. Schimerlik, D.J. Capon and J. Ramachandran (1987) An M2 muscarinic receptor subtype coupled to both adenylyl cyclase and phosphoinositide turnover. *Science* **238,** 672-675.

Bayer, S.A. (1984) Neurogenesis in the rat striatum. *Int. J. Dev. Neurosci.* **2,** 163-175.

Beach, T.G. and E.G. McGeer (1984) The distribution of substance P in the primate basal ganglia: an immunohistochemical study of baboon and human brain. *Neurosci.* **13,** 29-52.

Beckstead, R.M., G.F. Wooten and J.M. Trugman (1988) Distribution of D1 and D2 dopamine receptors in the basal ganglia of the cat determined by quantitative autoradiography. *J. Comp. Neurol.* **268,** 131-145.

Ben-Barak, J., H. Gazit, I. Silman and Y. Dudai (1981) In vivo modulation of the number of muscarinic receptors in rat brain by cholinergic ligands. *Eur. J. Pharmacol.* **74,** 73-81.

Beninato, M. and R.F. Spencer (1987) A cholinergic projection from the pedunculopontine tegmental nucleus to the substantia nigra in the rat: a light and electron microscopic immunohistochemical study. *Soc. Neurosci. Abstr.* **13,** 28.

Besson, M.-J., A.M. Graybiel and M.A. Nastuk (1988) [^{3}H]-SCH23390 binding to D1 dopamine receptors in the basal ganglia of the cat and primate: delineation of striosomal compartments and pallidal and nigral subdivisions. *Neurosci.* , . in press.

Bianchi, C., S. Tangelli and L. Beani (1979) Dopamine modulation of acetylcholine release from the guinea-pig brain. *Eur. J. Pharmacol.* **58,** 235-246.

Birdsall, N.J.M., A.S.V. Burgen, C.R. Hiley and E.C. Hulme (1976) Binding of agonists and antagonists to muscarinic receptors. *J. Supramolec. Struct.* **4,** 367-371.

Birdsall, N.J.M., A.S.V. Burgen and E.C. Hulme (1978) The binding of agonists to brain muscarinic receptors. *Mol. Pharmacol.* **14,** 723-736.

Birdsall, N.J.M., E.C. Hulme and A.S.V. Burgen (1980) The character of muscarinic receptors in different regions of the rat brain. *Proc. R. Soc. Lond. B* **207,** 1-12.

Bolam, J.P., B.H. Wainer and A.D. Smith (1984) Characterization of cholinergic neurons in the rat neostriatum. A combination of choline acetyltransferase immunocytochemistry, Golgi-impregnation and electron microscopy. *Neurosci.* **12,** 711-718.

Bonner, T.I., N.J. Buckley, A.C. Young and M.R. Brann (1987) Identification of a family of muscarinic acetylcholine receptor genes. *Science* **237,** 527-532.

Bouyer, J.J., D.H. Park, T.H. Joh and V.M. Pickel (1984) Chemical and structural analysis of the relation between cortical inputs and tyrosine hydroxylase-containing terminals in rat neostriatum. *Brain Res.* **302,** 267-275.

Brand, S. (1980) A comparison of the distribution of acetylcholinesterase and muscarinic cholinergic receptors in the feline striatum. *Neurosci. Lett.* **17,** 113-117.

Brand, S. and P. Rakic (1979) Genesis of the primate neostriatum: [^{3}H]thymidine autoradiographic analysis of the time of neuron origin in the rhesus monkey. *Neurosci.* **4,** 767-778.

Brand, S. and P. Rakic (1984) Cytodifferentiation and synaptogenesis in the neostriatum of fetal and neonatal rhesus monkeys. *Anat. Embryol.* **169,** 21-34.

Braun, T., P.R. Schofield, B.D. Shivers, D.B. Pritchett and P.H. Seeburg (1987) A novel subtype of muscarinic receptor identified by homology screening. *Biochem. Biophys. Res. Comm.* **149,** 125-132.

Burgen, A.S.V., C.R. Hiley and J.M. Young (1974) The binding of [^{3}H]-propylbenzilylcholine mustard by longitudinal strips from guinea-pig small intestine. *Brit. J. Pharmacol.* **50,** 145-151.

Burgen, A.S.V., C.R. Hiley and J.M. Young (1974) The properties of muscarinic receptors in mammalian cerebral cortex. *Brit. J. Pharmacol.* **51,** 279-285.

Butcher, L.L. and L. Bilezikjian (1975) Acetycholinesterase-containing neurons in the neostriatum and substantia nigra revealed after punctate intracerebral injection of di-isopropyl fluorophosphate. *Eur. J. Pharmacol.* **37,** 115-125.

Butcher, L.L. and G.K. Hodge (1976) Postnatal development of acetycholinesterase in the caudate-putamen nucleus and substantia nigra of rats. *Brain Res.* **106,** 223-240.

Butcher, L.L. and N.J. WOolf (1982) Monoaminergic-cholinergic relationships and the chemical communication matrix of the substantia nigra and neostriatum. *Br. Res. Bull.* **9,** 475-492.

Candy, J.M., E.K. Perry, R.H. Perry, C.A. Bloxham, J. Thompson, M. Johnson, A.E. Oakley and J.A. Edwardson (1985) Evidence for the early prenatal development of cortical cholinergic afferents from the nucleus of Meynert inthe human foetus. *Neurosci. Lett.* **61,** 91-95.

Chesselet, M.-F. (1984) Presynaptic regulation of neurotransmitter release in the brain: facts and hypothesis. *Neurosci.* **12,** 347-375.

Chubb, I.W., A.J. Hodgson and G.H. White (1980) Acetylcholinesterase hydrolyses substance P. *Neurosci.* **5,** 2065-2072.

Chubb , I.W., E. Ranieri. A.J. Hodgson and G.H. White (1982) The hydrolysis of leu- and met-enkephalin by acetylcholinesterase. *Neurosci. Lett. Suppl.* **8,** S39.

Churchill, L., T.L. Pazdernik, F. Samson and S.R. Nelson (1984) Topographical disribution of down-regulated muscarinic receptors in rat brains after repeated exposure to diisopropyl phosphofluoridate. *Neurosci.* **11,** 463-472.

Clarke, P.B.S. and A. Pert (1985) Autoradiographic evidence for nicotine receptors on nigrostriatal and mesolimbic dopaminergic terminals. *Brain Res.* **348,** 355-358.

Clarke, P.B.S., C.B. Pert and A. Pert (1984) Autoradiographic distribution of nicotine receptors in rat brain. *Brain Res.* **323,** 390-395.

Clarke, P.B.S., R.D. Schwartz, S.M. Paul, C.B.Pert and A. Pert (1985) Nicotinic binding in rat brain: autoradiographic comparison of [^{3}H]acetylcholine, [^{3}H]nicotine, and [^{125}I]-α-bungarotoxin. *J. Neurosci.* **5,** 1307-1315.

Cortes, R., A. Probst and J.M. Palacios (1984) Quantitative light microscopic autoradiographic localization of cholinergic muscarinic receptors in the human brain: brainstem. *Neurosci.* **12,** 1003-1026.

Cortes, R., A. Probst, H.-J. Tobler and J.M. Palacios (1986) Muscarinic cholinergic receptor subtypes in the human brain. II. Quantitative autoradiographic studies. *Brain Res.* **362,** 239-253.

Coyle, J.T. and H.I. Yamamura (1976) Neurochemical aspects of the ontogenesis of cholinergic neurons in the rat brain. *Brain Res.* **118,** 429-440.

de la Torre, J.C. (1980) An improved approach to histofluorescence using the SPG method for tissue monoamines. *J. Neurosci. Meth.* **3,** 1-5.

deBelleroche, J. and H.F. Bradford (1978) Biochemical evidence for the presence of presynaptic receptors on dopaminergic nerve terminals. *Brain Res.* **142,** 53-68.

deBelleroche, J. and I.M. Gardiner (1982) Cholinergic action in the nucleus accumbens: modulation of dopamine and acetylcholine release. *Brit. J. Pharmacol.* **75,** 359-365.

deBelleroche, J. and I.M. Gardiner (1985) Muscarinic receptors discriminated by pirenzepine are involved in the regulation of neurotransmitter release in rat nucleus accumbens. *Brit. J. Pharmacol.* **86,** 505-508.

deBelleroche, J., Y. Lugmani and H.F.Bradford (1979) Evidence for presynaptic cholinergic receptors on dopaminergic terminals: degeneration studies with 6-hydroxydopamine. *Neurosci. Lett.* **11,** 209-213.

deBelleroche, J., I.C. Kilpatrick, N.J.M. Birdsall and E.C. Hulme (1982) Presynaptic muscarinic receptors on dopaminergic terminals in the nucleus accumbens. *Brain Res.* **234,** 327-337.

DiFiglia, M., P. Pasik and T. Pasik (1980) Early postnatal development of the monkey neostriatum: a Golgi and ultrastructural study. *J. Comp. Neurol.* **190,** 303-331.

Donkelaar, H.J. ten and P.J.W. Derderen (1979) Neurogenesis in the basal forebrain of the Chinese hamster (*Cricetulus griseus*). *Anat. Embryol.* **156,** 331-348.

Donoghue, J.P. and M. Herkenham (1983) Multiple patterns of corticostriatal projections and their relationship to opiate receptor patches in rats.. *Soc. Neurosci. Abstr.* **9,** 15.

Doucet, G., L. Descarries and S. Garcia (1986) Quantification of the dopamine innervation in adult rat neostriatum. *Neurosci.* **19,** 427-445.

Dray, A. and D.W. Straughan (1976) Synaptic mechanisms in the substantia nigra. *J. Pharm. Pharmacol.* **228,** 400-405.

Egan, T.M. and R.A. North (1986) Acetylcholine hyperpolarizes central neurones by acting on an M2 muscarinic receptor. *Nature* **319,** 405-407.

Ehlert, F.J., W.R. Roeske and H.I. Yamamura (1980) Regulation of muscarinic receptor binding by guanine nucleotides and N-ethylmaleimide. *J. Supramolec. Struct.* **14,** 149-162.

Ehlert, F.J., W.R. Roeske and H.I. Yamamura (1981) Striatal muscarinic receptors: regulation by dopaminergic agonists. *Life Sci.* **28,** 2441-2448.

Estrada, C. and D.N. Krause (1982) Muscarinic cholinergic receptor sites in cerebral blood vessels. *J. Pharm. Exp. Ther.* **221,** 85-90.

Faull, R.L.M. and J.W. Villiger (1986) Heterogeneous distribution of benzodiazepine receptors in the human striatum: a quantitative autoradiographic study comparing the pattern of receptor labelling with the distribution of acetylcholinesterase staining. *Brain Res.* **381,** 153-158.

Fibiger, H.C. (1982) The organization and some projections of cholinergic neurons of the mammalian forebrain. *Brain Res. Revs.* **4,** 327-388.

Fibiger, H.C., K. Semba and S.R. Vincent (1987) Time of origin of immunohistochemically identified interneurons in the rat striatum. *Soc. Neurosci. Abstr.* **13,** 1575.

Fishell, G. and D. van der Kooy (1987) Pattern formation in the striatum: developmental changes in the distribution of striatonigral neurons. *J. Neurosci.* **7,** 1969-1978.

Fisher, S.K. and B.W. Agranoff (1987) Receptor activation and inositol lipid hydrolysis in neural tissues. *J. Neurochem.* **48,** 999-1017.

Fisher, S.K. and R.T. Bartus (1984) Muscarinic agonists differentially stimulate inositol phosphate release from guinea-pig striatum. *Soc. Neurosci. Abstr.* **10,** 566.

Fisher, S.K. and R.T. Bartus (1985) Regional differences in the coupling of muscarinic receptors to inositol phopspholipid hydrolysis in guinea pig brain. *J. Neurochem.* **45,** 1085-1095.

Flynn, D.D. and L.T. Potter (1985) Different effects of N-ethylmaleimide on M1 and M2 muscarine receptors in rat brain. *Proc. Nat'l. Acad. Sci. USA* **82,** 580-583.

Foster, G.A., M. Schultzberg, T. Hokfelt, M. Goldstein, H.C. Hemmings, Jr., C.C. Ouimet, S.I. Walaas and P. Greengard (1987) Development of a dopamine- and cyclic adenosine 3':5'-monophosphate-regulated phosphoprotein (DARPP-32) in the prenatal rat central nervous system, and its relationship to the arrival of presumptive dopaminergic innervation. *J. Neurosci.* **7,** 1994-2018.

Freund, T.F., J.F. Powell and A.D. Smith (1984) Tyrosine hydroxylase-immunoreactive synaptic boutons in contact with identified striatonigral neurons, with particular reference to dendritic spines. *Neurosci.* **13,** 1189-1215.

Fukuda, K., T. Kubo, I. Akiba, A. Maeda, M. Mishina and S. Numa (1987) Molecular distinction between muscarinic acetylcholine receptor subtypes. *Nature* **327,** 623-625.

Geneser-Jensen, F.A. and J.W. Blackstad (1971) Distribution of acetylcholinesterase in the hippocampal region of the guinea pig. I. Entorhinal area, parasubiculum, and presubiculum. *Z. Zellforsch. Mikrosk. Anat.* **114,** 460-481.

Gerfen, C.R. (1983) Non-topographic order in the basal ganglia: evidence for a second level of organization superimposed upon the topographically ordered striato-nigral projection system. *Soc. Neurosci. Abstr.* **9,** 16.

Gerfen, C.R. (1984) Differences between the morphology and distribution of dopaminergic and non-dopaminergic nigrostriatal afferents. *Soc. Neurosci. Abstr.* **10,** 9.

Gerfen, C.R. (1985) The neostriatal mosaic. I. Compartmental organization of porjections from the striatum to the substantia in the rat. *J. Comp. Neurol.* **236,** 454-476.

Gerfen, C.R., K.G. Baimbridge and J.L. Miller (1985) The neostriatal mosaic: compartmental distribution of calcium-binding protein and parvalbumin in the basal ganglia of the rat and monkey. *Proc. Natl. Acad. Sci. USA* **82,** 8780-8784.

Gerfen, C.R., K.G. Baimbridge and J. Thibault (1987) The neostriatal mosaic: III. Biochemical and developmental dissociation of patch-matrix mesostriatal systems. *J. Neurosci.* **7,** 3935-3944.

Gerfen, C.R., M. Herkenham and J. Thibault (1987) The neostriatal mosaic: II. Patch- and matrix-directed mesostriatal dopaminergic and non-dopaminergic systems. *J. Neurosci.* **7,** 3915-3934.

Gil, D.W. and B.B. Wolfe (1985) Pirenzepine distinguishes between muscarinic receptor-mediated phosphoinositide breakdown and inibition of adenylate cyclase. *J. Pharmacol. and Exp. Ther.* **232,** 608-616.

Giorguieff, M.-F., M.L. le Floc'h, T.C. Westfall, J. Glowinski and M.-J. Besson (1976) Nicotinic effect of acetylcholine on the release of newly synthesized [^{3}H]dopamine in rat striatal slices and cat caudate nucleus. *Brain Res.* **106,** 117-131.

Giorguieff, M.-F., M.L. le Floc'h, J. Glowinski and M.-J. Besson (1977) Involvement of cholinergic presynaptic receptors of nicotinic and muscarinic types in the control of the spontaneous release of dopamine from striatal dopaminergic terminals in the rat. *J. Pharm. Exp. Ther.* **200,** 535-544.

Giorguieff-Chesselet, M.-F., M.L. Kemel, D. Wandscheer and J. Glowinski (1979) Regulation of dopamine release by presynaptic nicotinic receptors in rat striatal slices: effect of nicotine in a low concentration. *Life Sci.* **25,** 1257-1262.

Giraldo, E., R. Hammer and H. Ladinsky (1987) Distribution of muscarinic receptor subtypes in rat brain as determined in binding studies with AF-DX 116 and pirenzepine. *Life Sci.* **40,** 833-840.

Goedert, M., P.W. Mantyh, S.P. Hunt and P.C. Emson (1983) Mosaic distribution of neurotensin-like immunoreactivity in the cat striatum. *Brain Res.* **274,** 176-179.

Goedert, M., P.W. Mantyh, P.C. Emson and S.P. Hunt (1984) Inverse relationship between neurotensin receptors and neurotensin-like immunoreactivity in cat striatum. *Nature* **307,** 543-546.

Goldman, P. S. and W.J.H. Nauta (1977) An intricately patterned prefronto-caudate projection in the rhesus monkey. *J. Comp. Neurol.* **171,** 369-386.

Goldman-Rakic, P.S. (1981) Prenatal formation of cortical input and development of cytoarchitectonic compartments in the neostriatum of the rhesus monkey. *J. Neurosci.* **1,** 721-735.

Goldman-Rakic, P.S. (1982) Cytoarchitectonic heterogeneity of the primate neostriatum: subdivision into *island* and *matrix* cellular compartments. *J. Comp. Neurol.* **205,** 398-413.

Gonzales, R.A. and F.T. Crews (1985) Cholinergic- and adrenergic-stimulated inositide hydrolysis in brain: interaction, regional distribution and coupling mechanisms. *J. Neurochem.* **45,** 1076-1084.

Goodman, R.R., S.H. Snyder, M.J. Kuhar and W.S. Young III (1980) Differentiation of delta and mu opiate receptor localizations by light microscopic autoradiography. *Proc. Natl. Acad. Sci. USA* **77,** 6239-6243.

Graybiel, A.M. (1982) Correlative studies of histochemistry and fiber connections in the central nervous system. In *Cytochemical Methods in Neuroanatomy,* (Edited by Palay, S.L. and V. Chan-Palay) pp. 45-67. Alan Liss, New York.

Graybiel, A.M. (1984) Neurochemically specified subsystems in the basal ganglia. In *Ciba Foundation Symposia Vol. 107 Functions of the Basal Ganglia* pp. 114-149. Pitman, London.

Graybiel, A.M. (1984) Correspondence between the dopamine islands and striosomes in the mammalian striatum. *Neurosci.* **13,** 1157-1187.

Graybiel, A.M. and T.L. Hickey (1982) Chemospecificity of ontogenetic units in the striatum: demonstration by combining [^{3}H]-thymidine neuronography and histochemical staining. *Proc. Natl. Acad. Sci. USA* **79,** 198-202.

Graybiel, A.M. and C.W. Ragsdale (1978) Histochemically distinct compartments in the striatum of human, monkey and cat demonstrated by acetylthiocholinesterase staining. *Proc. Natl. Acad. Sci. USA* **75,** 5723-5727.

Graybiel, A.M. and C.W. Ragsdale (1979) Fiber connections of the basal ganglia. *Prog. Brain Res.* **51,** 239-283.

Graybiel, A.M. and C.W. Ragsdale (1980) Clumping of acetylcholinesterase activity in the developing striatum of the human fetus and young infant. *Proc. Natl. Acad. Sci. USA* **77,** 1214-1218.

Graybiel, A.M. and C.W. Ragsdale. (1983) Biochemical anatomy of the striatum. In *Chemical Neuroanatomy,* (Edited by Emson, P.C.) pp. 427-504. Raven Press, New York.

Graybiel, A.M., C.W. Ragsdale and S. Moon Edley (1979) Compartments in the striatum of the cat observed by retrograde cell labeling. *Exp. Br. Res.* **34,** 189-195.

Graybiel, A.M., C.W. Ragsdale, E.S. Yoneoka and R.P. Elde (1981) An immunohistochemical study of enkephalins and other neuropeptides in the striatum of the cat with evidence that the opiate peptides are arranged to form mosaic patterns in register with the striosomal compartments visible by acetylcholinesterase staining. *Neurosci.* **6,** 377-397.

Graybiel, A.M., V.M. Pickel, T.H. Joh, D.J. Reis and C.W. Ragsdale (1981) Direct demonstration of a correspondence between the dopamine islands and acetylcholinesterase patches in the developing striatum. *Proc. Natl. Acad. Sci. USA* **78,** 5871-5875.

Graybiel, A.M., M.-F. Chesselet, J.Y. Wu, F. Eckenstein and T.E. Joh (1983) The relation of striosomes in the caudate nucleus of the cat to the organization of early-developing dopaminergic fibers, GAD-positive neuropil, and CAT-positive neurons. *Soc. Neurosci. Abstr.* **9,** 14.

Graybiel, A.M., R.W. Baughman and F. Eckenstein (1987) Cholinergic neuropil of the striatum observes striosomal boundaries. *Nature* **323,** 625-628.

Graybiel, A.M., E.C. Hirsch and Y.A. Agid (1987) Differences in tyrosine hydroxylase-like immunoreactivity characterize the mesostriatal innervation of striosomes and extrastriosomal matrix at maturity. *Proc. Natl. Acad. Sci. USA* **84,** 303-307.

Greenfield, S.A. and S.G. Shaw (1982) Release of acetylcholinesterase and aminopeptidase *in vivo* following infusion of amphetamine into the substantia nigra. *Neurosci.* **7,** 2883-2893.

Greenfield, S., A. Cheramy, V. Leviel and J. Glowinski (1980) *In vivo* release of acetylcholinesterase in cat substantia nigra and caudate nucleus. *Nature* **284,** 355-357.

Greenfield, S.A., J.F. Stein, A.J. Hodgson and I.W. Chubb (1981) Depression of nigral pars compacta cell discharge by exogenous acetylcholinesterase. *Neurosci.* **6,** 2287-2295.

Gurwitz, D., Y. Kloog, V. Egozi and M. Sokolovsky (1980) Central muscarinic receptor degeneration following 6-hydroxydopamine lesion in mice. *Life Sci.* **26,** 79-84.

Guyenet, P., Y. Agid, J.-C. Beaujouan, J. Rossier and J. Glowinski (1975) Effects of dopaminergic receptor agonists and antagonists on the activity of the neostriatal cholinergic system. *Brain Res.* **84,** 227-244.

Guyenet, P., C. Euvrard, F. Javoy, A. Herbet and J. Glowinski (1977) Regional differences in the sensitivity of cholinergic neurons to dopaminergic drugs and quipazine in the rat striatum. *Brain Res.* **136,** 487-500.

Hammer, R. and A. Giachetti (1982) Muscarinic receptor subtypes: M1 and M2 biochemical and functional characterization. *Life Sci.* **31,** 2991-2998.

Hammer, R., C.P. Berrie, N.J.M. Birdsall, A.S.V. Burgen and E.C. Hulme (1980) Pirenzepine distinguishes between different subclasses of muscarinic receptors. *Nature* **283,** 90-92.

Hammer, R., E. Giraldo, G.B. Schiavi, E. Monferini and H. Ladinsky (1986) Binding profile of a novel cardioselective muscarinic receptor antagonist, AF-DX 116, to membranes of peripheral tissues and brain in the rat. *Life Sci.* **38,** 1653-1662.

Harden, T.K., L.I. Tanner, M.W. Martin, N. Nakahata, A.R. Hughes, J.R. Hepler, T. Evans, S.B. Masters and J.H. Brown (1986) Characteristics of two biochemical responses to stimulation of muscarinic cholinergic receptors. *Trends in Pharmacol. Sci. Suppl.* **2,** 14-18.

Heimer, L. and R.D. Wilson. (1975) The subcortical projections of the allocortex: similarities in the neural associations of the hippocampus, the piriform cortex, and the neocortex. In *Golgi Centennial Symposium,* (Edited by Santini, M.) pp. 177-193. Raven Press, New York.

Henderson, Z. and S.A. Greenfield (1987) Does the substantia nigra have a cholinergic innervation? *Neurosci. Lett.* **73,** 109-113.

Henn, F.A., B. Oderfeld-Nowak and R. Roskoski (1979) Receptor binding to astroglial cells. *Soc. Neurosci. Abstr.* **5,** 590.

Herkenham, M. and C.B. Pert (1981) Mosaic distribution of opiate receptors, parafascicular projections and acetylcholinesterase in rat striatum. *Nature* **291,** 415-418.

Hohmann, C.F. and F.F. Ebner (1985) Development of cholinergic markers in mouse forebrain. I. Choline acetyltransferase enzyme activity and acetylcholinesterase histochemistry. *Dev. Brain Res.* **23,** 225-241.

Hokin, L.E. (1965) Autoradiographic localization of the acetylcholine-stimulated synthesis of phosphatidylinositol in the superior cervical ganglion. *Proc. Natl. Acad. Sci. USA* **53,** 1369-1376.

Horwitz, J. and R.L. Perlman (1984) Activation of tyrosine hydroxylase n the superior cervical ganglion by nicotinic and muscarinic agonists. *J. Neurochem.* **43,** 546-552.

Hruska, R.E., R. Schwarcz, J.T. Coyle and H.I. Yamamura (1978) Alterations of muscarinic cholinergic receptors in the rat striatum after kainic acid injections. *Brain Res.* **152,** 620-625.

Hull, C.D., J.P. McAllister, M.S. Levine and A.M. Adinolfi (1981) Quantitative developmental studies of feline neostriatal spiny neurons. *Dev. Brain Res.* **1,** 309-332.

Hulme, E.C., N.J.M. Birdsall, A.S.V. Burgen and P. Mehta (1978) The binding of antagonists to brain muscarinic receptors. *Mol. Pharmacol.* **14,** 737-750.

Hunt, S. and J. Schmidt (1978) Some observations on the binding patterns of α-bungarotoxin in the central nervous system of the rat. *Brain Res.* **157,** 213-232.

Izzo, P.N. and J.P. Bolam (1988) Cholinergic synaptic input to different parts of spiny striatonigral neurons in the rat. *J. Comp. Neurol.* **269,** 219-234.

James, M.K. and L.X. Cubeddu (1987) Pharmacologic characterization and functional role of muscarinic autoreceptors in the rabbit striatum. *J. Pharm. and Exp. Ther.* **240,** 203-215.

Jiminez-Castellanos, J. and A.M. Graybiel (1985) The dopamine-containing innervation of striosomes: nigral subsystems and their striatal correspondents. *Soc. Neurosci. Abstr.* **11,** 1249.

Jiminez-Castellanos, J. and A.M. Graybiel (1986) Innervation of striosomes and extrastriosomal matrix by different subdivisions of the midbrain A8-A9-A10 dopamine-containing cell complex. *Soc. Neurosci. Abstr.* **12,** 1327.

Jiminez-Castellanos, J. and A.M. Graybiel (1987) Subdivisions of the dopamine-containing A8-A9-A10 complex identified by their differential mesostriatal innervation of striosomes and extrastriosomal matrix. *Neurosci.* **23,** 223-242.

Jiminez-Castellanos, J. and A.M. Graybiel (1987) Subdivisions of the primate substantia nigra pars compacta detected by acetylcholinesterase histochemistry. *Brain Res.* **437,** 349-354.

Johnston, J.G., S.R. Boyd and D. van der Kooy (1987) Compartmentalization of the embryonic striatum after intraocular transplantation. *Dev. Brain Res.* **33,** 310-314.

Jones, E.G., J.D. Coulter, H. Burton and R. Porter (1977) Cells of origin and terminal distribution of corticostriatal fibers arising in the sensory-motor cortex of monkeys. *J. Comp. Neurol.* **173,** 53-80.

Joyce, J.N., D.W. Sapp and J.F. Marshall (1986) Human striatal dopamine receptors are organized in compartments. *Proc. Natl. Acad. Sci. USA* **83,** 8002-8006.

Kalil, K. (1978) Patch-like termination of thalamic fibers in the putamen of the rhesus monkey: an autoradiographic study. *Brain Res.* **140,** 333-339.

Kato, G., S. Carson, M.L. Kemel, J. Glowinski and M.-F. Giorguieff (1978) Changes in striatal specific ^{3}H-atropine binding after unilateral 6-hydroxydopamine lesions of nigrostriatal dopaminergic neurones. *Life Sci.* **22,** 1607-1614.

Kelly, E.and S.R. Nahorski (1986) Specific inhibition of dopamine D-1-mediated cyclic AMP formation by dopamine D-2, muscarinic cholinergic, and opiate receptor stimulation in rat striatal slices. *J. Neurochem.* **47,** 1512-1516.

Kent, J.L., C.B. Pert and M. Herkenham (1982) Ontogeny of opiate receptors in rat forebrain: visualization by in vitro autoradiography. *Dev. Brain Res.* **2,** 487-504.

Korn, S.J., M.W. Martin and T.K. Harden (1983) N-Ethylmaleimide-induced alteration in the interaction of agonists with muscarinic cholinergic receptors of rat brain. *J. Pharm. and Exp. Ther.* **224,** 118-126.

Krause, D.N. and C. Estrada (1982) Biochemical evidence for cholinergic innervation of cerebral capillaries. *Soc. Neurosci. Abstr.* **8,** 847.

Kristt, D.A. and E.K. Kasper (1983) High density of cholinergic muscarinic receptors accompanies high intensity acetylcholinesterase-staining in layer IV of infant rat somatosensory cortex. *Dev. Brain Res.* **8,** 373-376.

Kubo, T., K. Fukuda, A. Mikami, A Maeda, H. Takahashi, M. Mishina, T. Haga, K. Haga, A. Ichiyama, K. Kangawa, M. Kojima, H. Matsuo, T. Hirose and S. Numa (1986) Cloning, sequencing and expression of complementary DNA encoding the muscarinic acetylcholine receptor. *Nature* **323,** 411-416.

Kuhar, M.J. and H.I. Yamamura (1975) Light autoradiographic localisation of cholinergic muscarinic receptors in rat brain by specific binding of a potent antagonist. *Nature* **253,** 560-561.

Kuhar, M.J. and H.I. Yamamura (1976) Localization of cholinergic muscarinic receptors in the rat brain by light microscopic radioautography. *Brain Res.* **110,** 229-243.

Kuhar, M.J., N.J.M. Birdsall, A.S.V. Burgen and E.C. Hulme (1980) Ontogeny of muscarinic receptors in rat brain. *Brain Res.* **184,** 375-383.

Kunzle, H. (1975) Bilateral projections from precentral motor cortex to the putamen and other parts of the basal ganglia. *Brain Res.* **88,** 195-210.

Kunzle, H. (1977) Projections from the primary somatosensory cortex to basal ganglia and thalamus in the monkey. *Ex. Brain Res.* **30,** 481-492.

Laduron, P. (1980) Axoplasmic transport of muscarinic receptors. *Nature* **286,** 287-288.

Large, T.H., J.J. Rauh, F.G. De Mello and W.L. Klein (1985) Two molecular weight forms of muscarinic acetylcholine receptors in the avian central nervous system: switch in predominant form during differentiation of synapses. *Proc. Natl. Acad. Sci. USA* **82,** 8785-8789.

Large, T.H., M. P. Lambert, M.A. Gremillion and W.L. Klein (1986) Parallel postnatal development of choline acetyltransferase activity and muscarinic acetylcholine receptors in the rat olfactory bulb. *J. Neurochem.* **46,** 671-680.

Lear, J.L., R.F. Ackermann, M. Kameyama and D.E. Kuhl (1982) Evaluation of [^{123}I]Isopropyliodoamphetamine as a tracer for local cerebral blood flow using direct autoradiographic comparison. *J. Cerebr. Blood Flow Metab.* **2,** 179-185.

Lehmann, J. and H.C. Fibiger (1978) Acetylcholinesterase in the substantia nigra and caudate-putamen of the rat: properties and localization in dopaminergic neurons. *J. Neurochem.* **30,** 615-624.

Lehmann, J. and S.Z. Langer (1982) Muscarinic receptors on dopamine terminals in the cat caudate nucleus: neuromodulation of [^{3}H]dopamine release in vitro by endogenous acetylcholine. *Brain Res.* **248,** 61-69.

Lehmann, J. and S.Z. Langer (1983) The striatal cholinergic interneuron: synaptic target of dopaminergic terminals? *Neurosci.* **10,** 1105-1120.

Lehmann, J., H.C. Fibiger and L.L.Butcher (1979) The localization of acetylcholinesterase in the corpus striatum and substantia nigra of the rat following kainic acid lesion of the corpus striatum: a biochemical and histochemical study. *Neurosci.* **4,** 217-225.

Levine, M.S., R.S. Fisher, C.D. Hull and N.A. Buchwald (1986) Postnatal development of identified medium-sized caudate spiny neurons in the cat. *Dev. Brain Res.* **24,** 47-62.

Lewis, M.E., H. Khachaturian and S.J. Watson (1982) Visualization of opiate receptors and opioid peptides in sequential brain sections . *Life Sci.* **31,** 1347-1350.

Lichtensteiger, W., D. Felix, R. Leinhart and F. Hefti (1976) A quantitative correlation between single unit activity and fluorescence intensity of dopamine neurons in zona compacta of substantia nigra, as demonstrated under the influence of nicotine and physostigmine. *Brain Res.* **117,** 85-103.

Liles, W.C. and N.M. Nathanson (1987) Regulation of muscarinic acetylcholine receptor number in cultured neuronal cells by chronic membrane depolarization. *J. Neurosci.* **7,** 2556-2563.

Liles, W.C., D.D. Hunter, K.E. Meier and N.M. Nathanson (1986) Activation of protein kinase C induces rapid internalization and subsequent degradation of muscarinic acetylcholine receptors in neuroblastoma cells. *J. Biol. Chem.* **261,** 5307-5313.

Lloyd, K.G., L. Davidson and O. Hornykiewicz (1975) The neurochemistry of Parkinson's disease: effect of L-dopa therapy. *J. Pharm and Exp. Ther.* **195,** 453-464.

Loopuijt, L.D., J.B. Sebens and J. Korf (1987) A mosaic-like distribution of dopamine receptors in the rat neostriatum and its relationship to striosomes. *Brain Res.* **405,** 405-408.

Lowenstein, P.R., P.A. Slesinger, H.S. Singer, L.C. Walker, M.F. Casanova, D.L. Price and J.T. Coyle (1986) Development of cholinergic and dopaminergic pre- and postsynaptic markers in the baboon and human striatum. *Soc. Neurosci. Abstr.* **16,** 1230.

Lowenstein, P.R., P.A. Slesinger, H.S. Singer, L.C. Walker, M.F. Casanova, D.L. Price and J.T. Coyle (1987) An autoradiographic study of the development of [^{3}H]-hemicholineum-3 binding sites in human and baboon basal ganglia: marker for sodium-dependent high affinity choline uptake. *Dev. Brain Res.* **34,** 291-297.

Lowry, O.H., N.J. Rosebrough, A.L. Farr and R.J. Randall (1951) Protein measurement with the Folin phenol reagent. *J. Biol. Chem.* **193,** 265-275.

Luthin, G.R. and B.B. Wolfe (1985) Characterization of [^{3}H]pirenzepine binding to muscarinic cholinergic receptors solubilized from rat brain. *J. Pharm. and Exp. Ther.* **234,** 37-44.

Lynch, G.S., P.A. Lucas and S.A. Deadwyler (1972) The demonstration of acetylcholinesterase containing neurons within the caudate nucleus of the rat. *Brain Res.* **45,** 617-621.

Mantyh, P.W., R.D. Pinnock, C.P. Downes, M. Goedert and S.P.Hunt (1984) Correlation between inositol phospholipid hydrolysis and substance P receptors in rat CNS. *Nature* **309,** 795-797.

Marchand, R. and L. Lajoie (1986) Histogenesis of the striopallidal system in the rat. Neurogenesis of its neurons. *Neurosci.* **17,** 573-590.

Marchand, C. M.-F., S.P. Hunt and J. Schmidt (1979) Putative acetylcholine receptors in hippocampus and corpus striatum of rat and mouse. *Brain Res.* **160,** 363-367.

Mash, D.C., D.D. Flynn and L.T. Potter (1985) Loss of M2 muscarine receptors in the cerebral cortex in Alzheimer's disease and experimental cholinergic denervation. *Science* **228,** 115-117.

McCormick, D.A. and D.A. Prince (1985) Two types of muscarinic response to acetylcholine in mammalian cortical neurons. *Proc. Natl. Acad. Sci. USA* **82,** 6344-6348.

McCormick, D.A. and D.A. Prince (1986) Acetylcholine induces burst firing in thalamic reticular neurones by activating a potassium conductance. *Nature* **319,** 402-405.

McCulloch, J., K. Kirkham, H. MacPherson and J. Sharkey (1983) Functional organization of the caudate nucleus defined by serial 2-deoxyglucose autoradiography and histochemistry. *J. Cerebr. Blood Flow Metab.* **3 (Suppl.),** S258-S259.

McGeer, P.L., E.G. McGeer, H.C. Fibiger and V. Wickson (1971) Neostriatal choline acetylase and cholinesterase following selective brain lesions. *Brain Res.* **35,** 308-314.

McHaffie, J.G., R.F. Spencer, M. Beninato and B.E. Stein (1986) Postnatal development of acetylcholinesterase histochemical staining pattern in the cat superior colliculus. *Soc. Neurosci. Abstr.* **12,** 1033.

Meininger, C., D.B. Rye and B.H. Wainer (1983) An atlas of cholinergic structures in the ferret brain demonstrated by immunocytochemical localization of choline acetyltransferase: cholinergic pathways VII. *Soc. Neurosci. Abstr.* **9,** 963.

Mesulam, M-M., E.J. Mufson, B.H. Wainer and A.I. Levey (1983) Central cholinergic pathways in the rat: an overview based on an alternative nomenclature (Ch1-Ch6). *Neurosci.* **10,** 1185-1201.

Mesulam, M-M., E.J. Mufson, A.I. Levey and B.H. Wainer (1984) Atlas of cholinergic neurons in the forebrain and upper brainstem of the macaque based on monoclonal choline acetyltransferase immunohistochemistry and acetylcholinesterase histochemistry. *Neurosci.* **12,** 669-686.

Meyer, E.M. and D.H. Otero (1985) Pharmacological and ionic characterizations of the muscarinic receptors modulating [^{3}H]acetylcholine release from rat cortical synaptosomes. *J. Neurosci.* **5,** 1202-1207.

Misgeld, U., M.H. Weiler and I.J. Bak (1980) Intrinsic cholinergic excitation in the rat neostriatum: nicotinic and muscarinic receptors. *Exp. Brain Res.* **39,** 401-409.

Misgeld, U., M.H. Weiler and D.K. Cheong (1982) Atropine enhances nicotinic cholinergic EPSPs in rat neostriatal slices. *Brain Res.* **253,** 317-320.

Miyoshi, R., S. Kito, M. Shimizu and H. Matsubayashi (1987) Ontogeny of muscarinic receptors in the rat brain with emphasis on the differentiation of M1- and M2-subtypes - semi-quantitative in vitro autoradiography. *Brain Res.* **420,** 302-312.

Molliver, M.E. (1982) Role of monoamines in the development of the neocortex. *Neurosci. Res. Prog. Bull.* **20,** 492-507.

Moon Edley, S. (1983) Effects of prenatal haloperidol on receptors in the developing rat striatum: opposite changes in naloxone and spiperone. *Soc. Neurosci. Abstr.* **9,** 874.

Moon Edley, S. (1984) Prenatal haloperidol alters striatal dopamine and opiate receptors. *Brain Res.* **323,** 109-113.

Moon Edley, S. and A.M. Graybiel (1983) The afferent and efferent connections of the feline nucleus tegmenti pedunculopontinus, pars compacta. *J. Comp. Neurol.* **217,** 187-215.

Moon Edley, S. and M. Herkenham (1984) Comparative development of striatal opiate receptors and dopamine revealed by autoradiography and histofluorescence. *Brain Res.* **305,** 27-42.

Morley, B.J., J.F. Lorden, G.B. Brown, G.E. Kemp and R.J. Bradley (1977) Regional distribution of nicotinic acetylcholine receptor in rat brain. *Brain Res.* **134,** 161-166.

Morris, R., M.S. Levine, E. Cherubini, N.A. Buchwald and C.D. Hull (1979) Intracellular analysis of the development of responses of caudate neurons to stimulation of cortex, thalamus and substantia nigra in the kitten. *Brain Res.* **173,** 471-487.

Moskowitz, A.S. and R.R. Goodman (1984) Light microscopic autoradiographic localization of μ and δ opioid binding sites in the mouse central nervous system. *J. Neurosci.* **4,** 1331-1342.

Munson, P.J. and D. Rodbard (1980) LIGAND: a versatile computerized approach for characterization of ligand-binding systems. *Anal. Biochem.* **107,** 220-239.

Murrin, L.C. and J.R. Ferrer (1984) Ontogeny of the rat striatum: correspondence of dopamine terminals, opiate receptors and acetylcholinesterase. *Neurosci. Lett.* **47,** 155-160.

Nastuk, M.A. and A.M. Graybiel (1983) The distribution of muscarinic binding sites in the feline striatum and its relationship to other histochemical staining patterns. *Soc. Neurosci. Abstr.* **9,** 15.

Nastuk, M.A. and A.M. Graybiel (1985) Patterns of muscarinic cholinergic binding in the striatum and their relation to dopamine islands and striosomes. *J. Comp. Neurol.* **237,** 176-194.

Nastuk, M.A. and A.M. Graybiel (1986) Autoradiography of M1 and M2 muscarinic binding in the striatum. *Trends in Pharm. Sci. Suppl.* **2,** 92-93.

Nathanson, N.M. (1987) Molecular properties of the muscarinic acetylcholine receptor. *Ann. Rev. Neurosci.* **10,** 195-236.

Newman-Gage, H. and A.M. Graybiel (1988) Expression of calcium/calmodulin-dependent protein kinase n relation to dopamine islands and synaptic maturation in the cat striatum. *J. Neurosci.* **in press.**

Nishizuka, Y. (1984) Turnover of inositol phospholipids and signal transduction. *Science* **225,** 1365-1370.

Nobin, A. and A. Bjorklund (1973) Topography of the monoamine neuron systems in the human brain as revealed in fetuses. *Acta Physiol. Scand. Suppl.* **388,** 1-40.

Nomura, Y., H. Kajiyama, Y. Nakata and T. Segawa (1979) Muscarinic cholinergic binding in striatal and mesolimbic areas of the rat: reduction by 6-hydroxydopa. *Eur. J. Pharmacol.* **58,** 125-131.

Nomura, Y., I. Yotsumoto and T. Segawa (1981) Ontogenetic development of high potassium- and acetylcholine-induced release of dopamine from striatal slices of the rat. *Dev. Brain Res.* **1,** 171-177.

North, R.A. (1986) Muscarinic receptors and membrane ion conductances. *Trends in Pharmacol. Sci. Suppl.* **2,** 19-22.

Olianas, M.C., P. Onali, N.H. Neff and E. Costa (1983) Adenylate cyclase activity of synaptic membranes from rat striatum. Inhibition by muscarinic receptor agonists. *Mol. Pharmacol.* **23,** 393-398.

Olianas, M.C., P. Onali, N.H. Neff and E. Costa (1983) Muscarinic receptors modulate dopamine-activated adenylate cyclase of rat striatum. *J. Neurochem.* **41,** 1364-1369.

Olson, L., A. Seiger and K. Fuxe (1972) Heterogeneity of striatal and limbic dopamine innervation: highly fluorescent islands in developing and adult rats. *Brain Res.* **44,** 283-288.

Olson, L., L.O. Boreus and A. Seiger (1973) Histochemical demonstration and mapping of 5-hydroxytryptamine- and catecholamine-containing neuron systems in the human fetal brain. *Z. Anat. Entwickl.-Gesch.* **139,** 259-282.

Parent, A. and L. DeBellefeuille (1983) The pallidointralaminar and pallidonigral projections in primate as studied by retrograde double-labeling method. *Brain Res.* **278,** 11-27.

Parent, A., A. Mackey and L. DeBellefeuille (1983) The subcortical afferents to caudate nucleus and putamen in primate: a fluorescence retrograde double labeling study. *Neurosci.* **10,** 1137-1150.

Pert, C.B., M.J. KUhar and S.H. Snyder (1976) Opiate receptors: autoradiographic localization in rat brain. *Proc. Natl. Acad. Sci. USA* **73,** 3729-3733.

Phelps, P.E., C.R. Houser and J.E. Vaughn (1985) Immunocytochemical localization of choline acetyltransferase within the rat neostriatum: a correlated light and electron microscopic study of cholinergic neurons and synapses. *J. Comp. Neurol.* **238,** 286-307.

Potter, L.T., D.D. Flynn, H.E. Hanchett, D.L. Kalinoski, J. Luber-Narod and D.C. Mash (1984) Independent M1 and M2 receptors: ligands, autoradiography and functions. *Trends in Pharm. Sci. Suppl.* **1,** 22-31.

Pulsinelli, W.A. and T.E. Duffy (1979) Local cerebral glucose metabolism during controlled hypoxemia in rats. *Science* **204,** 626-629.

Quirion, R. and T. Dam (1986) Ontogeny of substance P receptor binding sites in rat brain. *J. Neurosci.* **6,** 2187-2199.

Ragsdale, C.W. and A.M.Graybiel (1979) Striosomal organization of the caudate nucleus: III. Distribution of afferents from the frontal cortex of the cat. *Soc. Neurosci. Abstr.* **5,** 78.

Ragsdale, C.W. and A.M. Graybiel (1981) The fronto-striatal projection in the cat and monkey and its relationship to inhomogeneities established by acetylcholinesterase histochemistry. *Brain Res.* **208,** 269-266.

Ragsdale, C.W. and A.M. Graybiel (1984) Further observations on the striosomal organization of frontostriatal projections in cats and monkeys. *Soc. Neurosci. Abstr.* **10,** 514.

Raiteri, M. M. Marchi and G. Maura (1982) Presynaptic muscarinic receptors increase striatal dopamine release evoked by 'quasi-physiological' depolarization. *Eur. J. Pharmacol* **83,** 127-129.

Raiteri, M., R. Leardi and M. Marchi (1984) Heterogeneity of presynaptic muscarinic receptors regulating neurotransmitter release in the rat brain. *J. Pharm. and Exp. Ther.* **228,** 209-214.

Ravikumar, B.V. and P.S. Sastry (1985) Muscarinic cholinergic receptors in human foetal brain: characterization and ontogeny of [^{3}H]quinuclidinyl benzilate binding sites in frontal cortex. *J. Neurochem.* **44,** 240-246.

Ravikumar, B.V. and P.S. Sastry (1985) Cholinergic muscarinic receptors in human fetal brain: ontogeny of [^{3}H]quinuclidinyl benzilate binding sites in corpus striatum, brainstem and cerebellum. *J. Neurochem.* **45,** 1948-1950.

Richfield, E.K., D.L. Debowey, J.B. Penney and A.B. Young (1987) Basal ganglia and cerebral cortical distribution of dopamine D1- and D2-receptors in neonatal and adult cat brain. *Neurosci. Lett.* **73,** 203-208.

Rotter, A., P.M. Field and G. Raisman (1979) Muscarinic receptors in the central nervous system of the rat. III. Postnatal development of binding of [^{3}H]propylbenzilylcholine mustard. *Brain Res. Revs.* **1,** 185-205.

Rotter, A., N.J.M. Birdsall, A.S.V. Burgen, P.M. Field, E.C. Hulme and G. Raisman (1979) Muscarinic receptors in the central nervous system of the rat. I. Technique for autoradiographic localization of the binding of [^{3}H]propylbenzilylcholine mustard and its distribution in the forebrain. *Brain Res. Revs.* **1,** 141-165.

Royce, G.J. (1978) Autoradiographic evidence for a discontinuous projection to the caudate nucleus from the centromedian nucleus in the cat. *Brain Res.* **146,** 145-150.

Ruberg, M., A. Ploska, F. Javoy-Agid and Y. Agid (1982) Muscarinic binding and choline acetyltransferase activity in parkinsonian subjects with reference to dementia. *Brain Res.* **232,** 129-139.

Saelens, J.K., S. Edwards-Neale and J.P. Simke (1979) Further evidence for cholinergic thalamostriatal neurons. *J. Neurochem.* **32,** 1093-1094.

Sakurai, Y., Y. Takano, Y. Kohjimoto, K. Honda and H. Kayima (1982) Enhancement of [^{3}H]dopamine release and its [^{3}H]metabolites in rat striatum by nicotinic drugs. *Brain Res.* **242,** 99-106.

Saper, C.B. and A.D. Loewy (1982) Projections of the pedunculopontine tegmental nucleus in the rat: evidence for additional extrapyramidal circuitry. *Brain Res.* **252,** 367-372.

Satoh, K. and H.C. Fibiger (1986) Cholinergic neurons of the laterodorsal tegmental nucleus: efferent and afferent connections. *J. Comp. Neurol.* **253,** 277-302.

Scatton, B. (1982) Effect of dopamine agonists and neuroleptic agents on striatal acetylcholine transmission in the rat: evidence against dopamine receptor multiplicity. *J. Pharm and Exp. Ther.* **220,** 197-202.

Schwartz, R.D., R. McGee, Jr. amd K.J. Kellar (1982) Nicotinic cholinergic receptors labeled by [^{3}H]acetylcholine in rat brain. *Mol. Pharmacol.* **22,** 56-62.

Scremin, O.U., A.A. Rovere, A.-C. Raynaud and A. Giardini (1973) Cholinergic control of blood flow in the cerebral cortex of the rat. *Stroke* **4,** 232-239.

Segal, M., Y. Dudai and A. Amsterdam (1978) Distribution of an α-bungarotoxin-binding cholinergic nicotinic receptor in rat brain. *Brain Res.* **148**, 105-119.

Sethy, V.H. (1979) Regulation of striatal acetylcholine concentration by D2-dopamine receptors. *Eur. J. Pharmacol.* **60**, 397-398.

Spain, J.W., B.L. Roth and C.C. Coscia (1985) Differential ontogeny of multiple opioid receptors (μ, δ, and κ). *J. Neurosci.* **5**, 584-588.

Specht, L.A., V.M. Pickel, T.H. Joh and D.J. Reis (1981) Light microscopic immunocytochemical localization of tyrosine hydroxylase in prenatal rat brain. II. Late ontogeny. *J. Comp. Neurol.* **199**, 255-276.

Specht, L.A., V.M. Pickel, T.H. Joh and D.J. Reis (1981) Light-microscopic immunocytochemical localization of tyrosine hydroxylase in prenatal rat brain. I. Early ontogeny. *J. Comp. Neurol.* **199**, 233-253.

Speth, R.C., F.M. Chen, J.M. Lindstrom, R.M. Kobayashi and H.I. Yamamura (1977) Nicotinic cholinergic receptors in rat brain identified by [^{125}I]*Naja naja siamensis* α-toxin binding. *Brain Res.* **131**, 350-355.

Stoof, J.C. and J.W. Kebabian (1982) Independent in vitro regulation by D2 dopamine receptor of dopamine-stimulated efflux of cyclic AMP and potassium stimulated release of acetylcholine from rat neostriatum. *Brain Res.* **250**, 263-270.

Sugimoto, T. and T. Hattori (1984) Organization and efferent projections of nucleus tegmenti pedunculopontinus pars compacta with special reference to its cholinergic aspects. *Neurosci.* **11**, 931-946.

Tanaka, D. (1980) Development of spiny and aspiny neurons in the caudate nucleus of the dog during the first postnatal month. *J. Comp. Neurol.* **192**, 247-263.

Tempel, A., E.L. Gardner and R.S. Zukin (1984) Visualization of opiate receptor up regulation by light microscopy autoradiography. *Proc. Natl. Acad. Sci. USA* **81**, 3893-3897.

Tennyson, V.M., R.E. Barrett, G. Cohen, L. Cote, R. Heikkila and C. Mytilineou (1972) The developing neostriatum of the rabbit: correlation of fluorescence histochemistry, electron microscopy, endogenous dopamine levels, and [^{3}H]dopamine uptake. *Brain Res.* **46**, 251-285.

Tokuno, H., T. Moriizumi, M. Kudo and Y. Nakamura (1988) A morphological evidence for monosynaptic projections from the nucleus tegmenti pedunculopontinus pars compacta (TPC) to nigrostriatal projection neurons. *Neurosci. Lett.* **85,** 1-4.

Torrens, Y., J.C. Beaujouan, M.J. Besson, R. Michelot and J. Glowinski (1981) Inhibitory effects of GABA, L-glutamic acid and nicotine on the porassium-evoked release of substance P in substantia nigra slices of the rat. *Eur. J. Pharmacol.* **71,** 383-392.

van der Kooy, D. (1984) Developmental relationships between opiate receptors and dopamine in the formation of caudate-putamen patches. *Dev. Brain Res.* **14,** 300-303.

van der Kooy, D. and G. Fishell (1987) Neuronal birthdate underlies the development of striatal compartments. *Brain Res.* **401,** 155-161.

van der Kooy, D., P. Weinrich and J.I. Nagy (1986) Dopamine and opiate receptors: localization in the striatum and evidence for their axoplasmic transport in the nigrostriatal and striatonigral pathways. *Neurosci.* **19,** 139-146.

Vincent, S.R. and P.B. Reiner (1987) The immunohistochemical localization of choline acetyltransferase in the cat brain. *Brain Res. Bull.* **18,** 371-415.

Wainer, B.H., J.P. Bolam, T.F. Freund, Z. Henderson, S. Totterdell and A.D. Smith (1984) Cholinergic synapses in the rat brain: a correlated light and electron microscopic immunohistochemical study employing a monoclonal antibody against choline acetyltransferase. *Brain Res.* **308,** 69-76.

Wainer, B.H., A.I. Levey, E.J. Mufson and M.-M. Mesulam (1984) Cholinergic systems in mammalian brain identified with antibodies against choline acetyltransferase. *Neurochem. Int.* **6,** 163-182.

Walker, R.J., J.A. Kemp, H. Yajima, K. Kitagawa and G.N. Woodruff (1976) The action of substance P on mesencephalic reticular and substantia nigral neurons of the rat. *Experientia* **32,** 214-215.

Wamsley, J.K. (1983) Muscarinic cholinergic receptors undergo axonal transport in the brain. *Eur. J. Pharmacol.* **86,** 309-310.

Wamsley, J.K., M.A. Zarbin, N.J.M. Birdsall and M.J. Kuhar (1980) Muscarinic cholinergic receptors: autoradiographic localization of high and low affinity agonist binding sites. *Brain Res.* **200,** 1-12.

Wamsley, J.K., M.A. Zarbin and M.J. Kuhar (1981) Muscarinic cholinergic receptors flow in the sciatic nerve. *Brain Res.* **217,** 155-161.

Wamsley, J.K., D.R. Gehlert, W.R. Roeske and H.I. Yamamura (1984) Muscarinic antagonist binding site heterogeneity as evidenced by autoradiography after direct labeling with [^{3H}]-QNB and [^{3H}]-pirenzepine. *Life Sci.* **34,** 1395-1402.

Wassef, M., A. Berod and C. Sotelo (1981) Dopaminergic dendrites in the pars reticulata of the rat substantis nigra and their striatal input. Combined immunocytochemical localization of tyrosine hydroxylase and anterograde degeneration. *Neurosci.* **6,** 2125-2139.

Watson, M., H.I. Yamamura and W.R. Roeske (1983) A unique regulatory profile and regional distribution of [^{3}H]pirenzepine binding in the rat provide evidence for distinct M1 and M2 muscarinic receptor subtypes. *Life Sci.* **32,** 3001-3011.

Weiner, W.J. and H.L. Klawans. (1978) Cholinergic-monoaminergic interactions within the striatum: implications for choreiform disorders. In *Cholinergic-Monoaminergic Interactions in the Brain,* (Edited by Butcher, L.L.) pp. 335-362. Academic Press, New York.

Westfall, T.C. (1974) Effect of nicotine and other drugs on the release of ^{3}H-norepinephrine and ^{3}H-dopamine from rat brain slices. *Neuropharmacol.* **13,** 693-700.

Westfall, T.C. (1974) Effect of muscarinic agonists on the release of ^{3}H-norepinephrine and ^{3}H-dopamine by potassium and electrical stimulation from rat brain slices. *Life Sci.* **14,** 1641-1652.

Weston, J. and S. A. Greenfield (1986) Release of acetylcholinesterase in the rat nigrostriatal pathway: relation to receptor activation and firing rate. *Neurosci.* **17,** 1079-1088.

Wright, A.K. and G.W. Arbuthnott (1981) The pattern of innervation of the corpus striatum by the substantia nigra. *Neurosci.* **6,** 2063-2067.

Yamamura, H.I., J.K. Wamsley, P. Deshmukh and W.R. Roeske (1983) Differential light microscopic autoradiographic localization of muscarinic cholinergic receptors in the brainstem and spinal cord of the rat using [^{3}H]pirenzepine. *Eur. J. Pharmacol.* **91,** 147-149.

Yamamura, H.I., T.W. Vickroy, D.R. Gehlert, J.K. Wamsley and W.R. Roeske (1985) Autoradiographic localization of muscarinic agonist binding sites in the rat central nervous system with (+)-*cis*-[^{3}H]methyldioxolane. *Brain Res.* **325,** 340-344.

Young, J.M., C.R. Hiley and A.S.V. Burgen (1972) Homologues of benzilylcholine mustard. *J. Pharm. Pharmacol.* **24,** 950-954.

Zarbin, M.A., J.K. Wamsley and M.J. Kuhar (1982) Axonal transport of muscarinic cholinergic receptors in rat vagus nerve: high and low affinity agonist receptors move in opposite directions and differ in nucleotide sensitivity. *J. Neurosci.* **2,** 934-941.